8-2024

Landuse and Microplastic Transport in Karst Groundwater of South-Central Kentucky

Katie Norman
Western Kentucky University, katienorman077@gmail.com

LANDUSE AND MICROPLASTIC TRANSPORT IN KARST GROUNDWATER OF SOUTH-CENTRAL KENTUCKY

A Thesis submitted in partial fulfillment
Of the requirements for the degree
Master of Geoscience

Department of Earth, Environmental, & Atmospheric Sciences
Western Kentucky University
Bowling Green, Kentucky

By
Katie Norman

August, 2024

LANDUSE AND MICROPLASTIC TRANSPORT IN KARST GROUNDWATER OF SOUTH-CENTRAL KENTUCKY

Date Recommended August 13, 22024

Christopher Groves

Digitally signed by Christopher Groves
Date: 2024.08.13 11:26:52 -05'00'

Chair

Committee Member

Patricia Kambesis

Digitally signed by Patricia Kambesis
Date: 2024.08.13 22:06:37 -05'00'

Committee Member

Michael G. May

Michael May

Date: 2024 8-13-24

Committee Member

Jennifer Hammonds

Executive Director for Graduate Studies

ABSTRACT

LANDUSE AND MICROPLASTIC TRANSPORT IN KARST GROUNDWATER OF SOUTH-CENTRAL KENTUCKY

Groundwater in karst areas is susceptible to contamination from various sources of pollution. Microplastics are a prevalent source of pollution entering groundwater. This study examines karst groundwater in three areas of investigation. One point of interest is an area that is impacted by urban activities, the Lost River Groundwater Basin, which includes water drainage from the City of Bowling Green, Kentucky. Another study location is Great Onyx (GO) Spring, which is a part of the Great Onyx Groundwater Basin located in Mammoth Cave National Park, Kentucky, and that is relatively unimpacted by urban activities. The third point of interest is Biz Falls, which is located within Great Onyx Cave upstream from the spring representing a relatively pristine area in comparison to urban areas. This research sought to understand the distribution and characterization of microplastics in karst groundwater. This study utilized water grab sampling to collect two liters from each site each month from September 2023 through February 2024. Discharge, pH, water temperature, and specific conductance measurements were also conducted during sampling. This study quantified and described microplastic contamination at each site. In total Lost River Rise had a total of 278 microplastic fragments detected, whereas GO Spring and Biz Falls had a total of 286 and 260 microplastics, respectively. These results indicate that the sampled karst areas, including within a relatively pristine part of Mammoth Cave National Park, are vulnerable to microplastic pollution. Results of this study of three areas demonstrates the apparent ease with which microplastics can be transported through the environment via surface water and groundwater in karst regions.

Keywords: microplastics, karst, hydrology, transportation, pollution, landuse, contaminants

I dedicate this thesis to Mrs. Angela Page, without you I would not have a love for plastics, or any idea microplastics exist.

ACKNOWLEDGMENTS

I would not have completed this thesis without the people that surround me every day. To my family: Mom, Dad, DC, and Daisy, you all have kept me sane and let me yap just to yap. To my grandparents: Bernard and Anna Parrish, your unwavering support and being my biggest fan pushed me to even begin this journey. I adore your support and efforts to always show up to my presentations. Rylee, you have been with me throughout all the ups and downs of this journey. Thank you for letting me yap about all the specific microplastic details, thank you for going into the field, thank you for always being interested in what I have to say, I do not have enough words to express my gratitude to you. I am thrilled to end this thesis journey and begin to explore the world. Autumn, I don't even know where to begin. You have had a monumental, immeasurable impact on my life. Thank you for always making sweet treats, listening to me complain, investing so much time into helping me answer my endless questions, and bringing so much laughter to my days. I would not have completed this journey without you. Mrs. Page, this all began with you, it is crazy to think how a canoe trip turned into a thesis on microplastics. You shaped me into the student I am today, quite frankly a complete 180 from the first class of yours I took. Meghan Raines, my wonderful grad school bestie, I had such a blast doing field work with you and getting to be a reason you had to go down to the spring. Your words of wisdom will stick with me for a long, long time. Dr. Groves, thank you for taking the chance on a new topic and being a wonderful advisor. Dr. K (Pat) and Dr. May, thank you all for being such a flexible committee – you all eliminated a lot of stress. Dr. Polk, thank you for letting me bounce so many questions off you and keeping me out of delulu land. To my professors and the department, thank you for all the knowledge and opportunities you all have given me – I attribute to you all to the reason I have a big head. Will Hemenover, I have had a blast doing these last four years with you. You have made every class significantly more enjoyable, made sure I was always remembering to have fun, and did so awesome in the field. Glad to always beat you in bowling, thank you for being you. To the kettle, thank you for your constant interest and care. I can’t wait to go to Potter’s, play Wii, and Presidents again. Brittany, I don’t think I would have survived this last year without you. Your massive head took up so much space, I wasn’t sure if we both would get degrees. You brought such a joy to this experience; it was an honor to share a brain cell with you and your rain gauges. To the countless people, I did not mention by name, I am not forgetting you, thank you all for your support and completing this journey with me.

TABLE OF CONTENTS

LIST OF TABLES

LIST OF FIGURES

Chapter 1: Introduction

Approximately 71% of the Earth is covered by water (USGS, 2019). Water is a critical resource that is severely impacted by pollution. It is important to understand water quality because most times a body of water cannot be assessed without examining water quality. Water quality can be impacted by many factors, such as geology, vegetation, precipitation rates, land use and human impacts. As society continues to grow and develop, the desire and necessity for producing goods and services has increased. As a result, this has required more water consumption and has led to increased water pollution (Boyd, 2005). Water quality is important for domestic, agricultural, and industrial water suppies, as well as ecosystem and human health (Boyd, 2005). Plastics are a pollutant that are rapidly entering the waterways, which could have a major impact on water quality.

Picturing a world without plastic seems impossible; however, this was the case roughly 70 years ago (Law, 2017). Plastics have risen in popularity due to their versatility and low cost. Plastic's ability to resist degradation and durability are the same reasons that make it nearly impossible for the environment to break down (Geyer et al., 2017). Large-scale production and use of plastics did not begin until around the 1950s, and now plastic waste is generated at a rate approaching 400 million metric tons per year (Geyer et al., 2017; Chamas et al., 2020). Geyer et al., (2017) reported from 1950 through 2015 the total amount of resins and fibers manufactured was 7,800 million metric tons, with half of that value being produced in the most recent 13 years of that period. The researchers noted that if production and waste management trends continue, by 2050 roughly 12,000 million metric tons of plastic waste will end up in landfills or the natural environment. This does not take into consideration the impact COVID-19 has had on plastic production or waste, as single-use personal protection equipment was essential during this time. Since the pandemic the amount of plastic waste generated worldwide is estimated to be 1.6 million tons per day (Benson et al., 2021). Globally, roughly 129 billion face masks and 65 billion plastic gloves are used and disposed of monthly (Aragaw and Mekonnen, 2021).

The most commonly used plastics are not biodegradable, resulting in their accumulation either in landfills or the natural environment (Geyer et al., 2017). With the number of plastics entering landfills and the environment, the Great Wall of China, spanning 6000 km, by comparison could be rebuilt every 12 months in terms of volume (Chamas et al., 2020). Much of the plastic-waste pollution can be attributed to the absence of effective waste-management infrastructures. It is important to note that many developing countries are unable to afford safe disposal options or wide scale trash cleanups (Schweitzer and Noblet, 2018). A major concern is the amount of plastic waste entering the oceans. Nearly 700 species have had contact with plastic debris, 17% being threatened or near threatened species (Gall and Thompson, 2015). There is a gap in literature examining much of the specifics regarding plastic waste, such as degradation time/pathways, scale/impact of plastic debris on marine ecosystem, and most importantly long-term effects that plastic waste will have on humans, ecosystems, and the environment in general.

A “small” (but significant) implication of plastic waste is microplastics (MP). Microplastics were first observed in 1972; however, they did not receive a name until 2004 (Mai et al., 2018). Microplastics are plastic particles smaller than 5.0 mm (Masura et al., 2015). Depending on their origin, microplastics are divided into two separate categories: primary and secondary microplastics. Primary microplastics are commonly created from industrial and domestic products (Betts, 2008; Moore, 2008). Secondary microplastics are tiny plastic fragments resulting from the breakdown of larger plastic debris (Thompson et al., 2004). Another form of microplastics originates from cloth fibers, especially from ‘fast fashion’ brands. Microplastics can be observed and documented virtually everywhere from the Arctic to the Antarctic, from freshwater to oceans, from soils to sediments, and from the atmosphere to humans (Prata et al., 2019). Microplastics have been found in national parks, federally protected areas, and remote areas. Microplastics can also escape wastewater treatment plants, entering aquatic bodies of water (Sun et al., 2018). As microplastics continue to spread it is important to note that these particles are only going to get smaller unless they are removed. This is significant because through further degradation and fragmentation, microplastics can break down into smaller particles known as nanoplastics (Galloway et al., 2017). There is a wide range of processes that contribute to microplastic pollution into aquatic environments such as domestic and industrial drainage, maritime activities, agricultural runoff, and wastewater treatment plants (Figure 1) (Karbalaei et al., 2018).

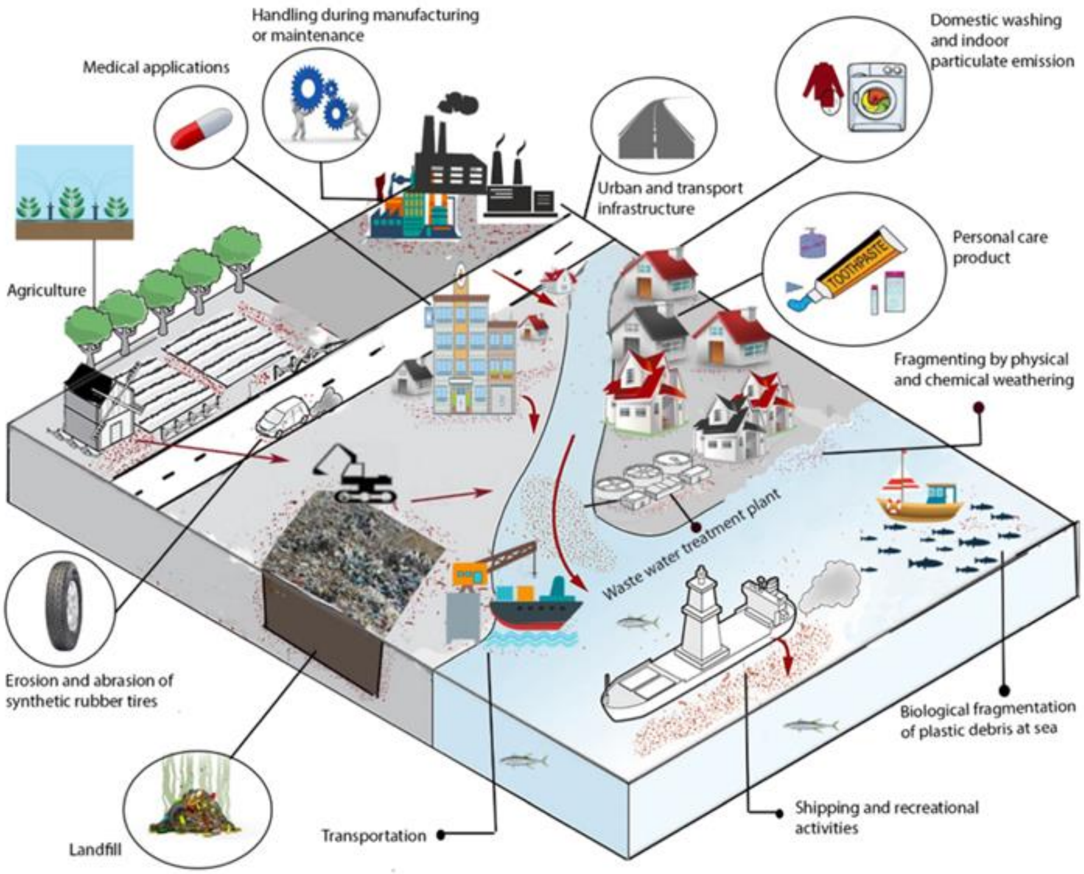

Figure 1: Sources of microplastic contamination in the environment (Source: Karbalaei et al., 2018).

Addressing the growing concentrations of microplastics is important, because they pose a health risk to organisms and humans. While the health risks are still being observed and investigated, there have been several noted effects that are a reason for concern. Microplastics can be ingested through water filtration, deposit feeding activity (organisms feeding on materials deposited in sediment such as mussels), and consumption of prey (Barboza et., al 2018). The health risks associated with microplastic consumption include ingestion of the material, as well as its ability to absorb contaminants and transfer them through food chains (Guzzetti et al., 2018). Specific characteristics such as toxic chemical components, an ability to transfer contaminants, and physical damage can negatively impact human health (Yang et al., 2022).

Another concern is microplastic presence in marine species that are consumed by humans, especially in countries with high consumption of seafood.

Overall, there is a lack of knowledge pertaining to many questions regarding microplastics. Researchers are currently pushing to expand the knowledge and depth pertaining to microplastics, their effects on the environment, and variables that affect microplastic concentrations. There is also a need to increase the amount of data available for microplastics, especially in smaller bodies of water and karst areas. As microplastic concentrations will not likely be decreasing any time soon, it is important to understand just how microplastics will reshape our environment. This study examines microplastic concentrations in karst groundwater, draining two southcentral Kentucky landscapes.

The term karst landscape describes an area of land that is underlain by soluble bedrock, containing caves, sinkholes, and sinking streams (Ford and Williams, 2007). Karst landscapes are extremely important, as karst aquifers make up about a 9.2% of the world's drinking water, accounting for approximately 678 million people (Stevanović, 2019). It is important to understand the degree of microplastic contamination in karst environments, since karst regions are extremely vulnerable to pollution. This study aims to address the knowledge gap of microplastic presence in karst regions, specifically karst regions with varying land use.

By sampling karst groundwater for microplastics, the purpose of this study is to answer the following questions:

- Are microplastics present in the karst groundwater emerging from the Lost River Rise, the outlet of the Lost River Groundwater basin?
    - What are the characteristics of microplastics found at Lost River Rise?

- Does groundwater within the relatively pristine Great Onyx Groundwater Basin, located in Mammoth Cave National Park, contain microplastics?
    - If present, what are the characteristics of microplastics within the Great Onyx Groundwater Basin?

Chapter 2: Literature Review

2.1 Water Pollution

As long as humans exist on earth, there will always be pollution. As global population increases, develops, and expands, maintaining good water quality is essential to all life. Even though most of Earth's surface is covered with water, only approximately 2.53% of the total volume is fresh water, with 1.74% being stored in Antarctic and Arctic ice sheets as well as mountain glaciers (Shiklomanov and Rodda, 2003) (Table 1).

Table 1: Water content in the hydrosphere (Source: Shiklomanov and Rodda, 2003).

Type of Water	**Fraction of total volume of hydrosphere (%)**
World Ocean	96.5
Ground water (gravity and capillary)	1.7
Predominantly fresh ground water	0.76
Soil moisture	0.001
Glaciers and permanent snow cover	1.74
Ground ice of permafrost zone	0.022
Water in lakes	0.013
Swamp water	0.0008
River stream water	0.0002
Biological water	0.0001
Water in the air	0.001
Total volume of the hydrosphere	100
Fresh water	2.53

Not only is there a limited amount of water available for human consumption, but water is vulnerable to contamination. Water quality is dependent on a wide range of factors including, but not limited to, vegetation, flow conditions, climate, precipitation, soil type, geology, and anthropogenic impact (Florescu et al., 2010; Chaudhry and Malik, 2017). Urban development, mining, oil drilling, and agriculture can also have significant impacts on water quality (Florescu et al., 2010). Water becomes polluted once it becomes impaired by a chemical, physical, or biological component that negatively interferes with the use of water or its natural function (Schweitzer and Noblet, 2018). Poor water quality has a variety of negative impacts on ecosystems and humans. As of 2021, over two billion people lived in water-stressed countries, a number expected to increase due to population growth and climate change (World Health Organization, 2023). In 2022, 2.2 billion people lacked safely managed water, which can lead to the transmission of diseases such as diarrhea, cholera, and dysentery, to name a few (World Health Organization, 2023). Trying to reduce pollution is key to maintaining water quality and overall quality of all life.

2.1.1 Types of Pollution

One of the greatest threats to water quality is from anthropogenic pollutants. Pollution is divided into two categories: point and non-point sources (Wu and Chen, 2013; Chaudhry and Malik, 2017; Schweitzer and Noblet, 2018; Arif et al., 2020). Point-source pollution has an identifiable source (Chaudhry and Malik, 2017; Schweitzer and Noblet, 2018; Arif et al., 2020). Examples of point source pollution are storm drains, sewage-treatment plants, power plants, refineries, and factories (Chaudhry and Malik, 2017; Schweitzer and Noblet, 2018; Arif et al., 2020). On the contrary, non-point source pollution (Figure 2) does not come from one identifiable source (Ongley et al., 2009; Wu and Chen, 2013; Chaudhry and Malik, 2017; Schweitzer and Noblet, 2018; Arif et al., 2020). Examples of non-point source pollution include pesticides, fertilizers, industrial waste, mobile sources (ie: trains, buses, cars), and atmospheric pollutants (Wu and Chen, 2013; Chaudhry and Malik, 2017; Schweitzer and Noblet, 2018; Arif et al., 2020).

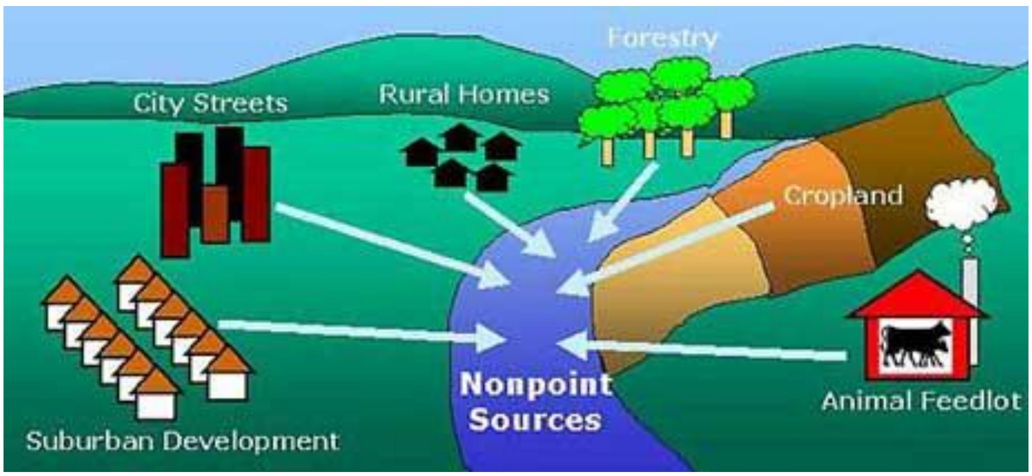

Figure 2: Examples of non-point source pollution (Source: NOAA, n.d.).

Whereas point-source pollution is quite impactful to ecosystems, non-point source pollution nonetheless is the leading cause of water pollution in America (EPA, 2003). Agricultural non-point source pollution is a major concern for water quality, especially in the United States (EPA, 2003; Ongley et al., 2009). The primary agricultural non-point source pollutants are pesticides, fertilizers, and animal wastes (EPA, 2003). Nitrogen and phosphorus are two major nutrients primarily used in agricultural that impact water quality (EPA, 2003). Not only does agricultural runoff transport these pollutants into waterways, but overloading of nitrogen and phosphorus can result in eutrophication resulting in intense plant growth and death of organisms (EPA, 2003).

In urban areas, urban storm-water runoff is a major non-point source pollutant, tying into groundwater pollution. Urban storm water runoff occurs when precipitation does not soak into the ground due to much of the area being covered in impervious surfaces resulting in pollutants such as oil, salts, lawn fertilizers, and chemicals to be carried into waterways (Chaudhry and Malik, 2017). Urban runoff pollutants can harm wildlife populations, contaminate drinking water, and make recreational areas unsuitable for use (EPA, 2023). Additionally, industrial facilities emit pollutants into the atmosphere, which can lead to the pollutants being washed out of atmosphere in the form of precipitation (NOAA, n.d.). A more recent type of pollution that is entering waterways at an alarming rate is plastic waste.

2.2 Plastics in the Environment

2.2.1 Introduction

A growing source of pollution is a result of trash, specifically plastic, being discarded and entering the waterways. As more research is conducted, it is evident that plastic pollution has a multitude of negative associations. “Plastics” gets its name from the Greek word “plastikos” and “plastos”, which mean “fit for moulding” and “moulded” respectively (Millet et al., 2018). While the first plastic was discovered in 1862, what society recognizes as modern plastic was developed around the early 1900s (Millet et al., 2018). Commercial production of plastics began around 1950 after World War II and the material’s versatility (Millet et al., 2018; Aragaw and Mekonnen, 2021). Plastics are in high demand because of their low production costs, and ability to be made into a variety of shapes through the molding process.

2.2.2 Types of Plastic

Plastics can be molded into a variety of shapes such as film, fibers, tubes, bottles, and plates with virtually any shape (Millet et al., 2018). Plastics are present in a wide array of items utilized every day, such as packing materials, cars, beauty products, kitchen products and clothing. Plastics can be grouped into two main polymer families: thermoplastics and thermosets. Thermoplastics melt when heated and harden when cooled, giving such material the ability to be reheated or reshaped (Millet et al., 2018). Thermoplastics represent almost 80% of plastics in demand (Millet et al., 2018). Thermosets are synthetic materials that undergo a chemical change when treated, meaning that they cannot be reformed or remolded (Millet et al., 2018). Plastic can be further divided into different categories based on their use such as polyethylene (PE), polypropylene (PP), polyvinyl chloride (PVC), polystyrene (PS), polyurethane (PU) and phenolic resins (Chen et al., 20200). Standard plastics, such as low-density polyethlene (LDPE), linear low-density polyethylene (LLDPE), high-density polyethylene (HDPE), polypropylene (PP), (PS), expanded polystyrene (EPS), polyethylene terephthalate (PET), are most widely used plastics accounting for more than 85% of thermoplastic demand (Millet et al., 2018) (Table 2). PP and PE polymers are used most in disposable products, such as disposable water bottles and plastic packaging (Giacovelli et al., 2018).

Table 2: Most common standard plastics, including their characteristics and applications (Source: Millet et al., 2018).

Type of Standard Plastic	Characteristics	Examples of applications
LDPE	Type of polyolefins, produced from oil and natural gas. Very versatile, resulting in a wide variety of applications.	Cling film, carrier bags, agricultural films, milk carton coatings, electrical cable coatings, heavy duty industrial bags
LLDPE	Type of polyolefins, produced from oil and natural gases. Very versatile, resulting in a wide variety of applications.	Stretch film, industrial packaging film, thin-walled containers, small/medium/heavy-duty bags
HDPE	Type of polyolefins, produced from oil and natural gases. Very versatile, resulting in a wide variety of applications.	Crates, boxes bottles (Food, detergent and cosmetic), food containers, toys, petrol tanks, industrial wrapping and film, pipes, houseware
PP	Type of polyolefins, produced from oil and natural gases. Very versatile, resulting in a wide variety of applications.	Food packaging, snack/sweet wrappers, microwave-proof containers, carpet fibers, garden furniture, medical packaging/appliances, luggage, kitchen appliances, pipes
PS	Can be solid or foamed, made from monomer styrene.	Packaging, cosmetic packs, toys, refrigerator trays
EPS	Solid foam that is light weight, durable, has insulating properties and is very processable.	Thermal insulation board in buildings, in packaging, cushioning of valuable goods, food packing
PET	Consists of polymerized units of ethylene terephthalate monomers.	Clothing fibers, food/beverage containers

2.2.3 Plastic Production

From 1950 to 2015, global production of resins and fibers increased from two million metric tons to 380 million metric tons per year, with a compound annual growth rate (CAGR) of 8.4% (Figure 3). This CAGR was roughly 2.5 times higher than the CAGR of global gross domestic products during that time frame (Geyer et al., 2017; Plastics Europe, 2017). China is a major producer of plastics, accounting for 28% of global resin and 68% of global PP&A fiber production (Geyer et al., 2017). PP&A fibers are acrylic fibers (Geyer at el., 2017), commonly used in the textile industry. There are biodegradable plastics, however these plastics currently have a global production capacity of four million metric tons (Geyer et al., 2017). Furthermore, these plastics also have much higher associated costs to produce. Globally, there has been a shift from production of durable plastics to single-use plastics (including packaging) (Geyer et al., 2017). Single-use plastics are designed to be used once before being discarded, often referred to as disposable plastics (Giacovelli, 2018). Single-use plastic products include grocery bags, water bottles, straws, cutlery, and food packaging materials (Figure 4).

In 2017, Geyer et al., conducted the first-ever global assessment of mass-produced plastics, finding that manufacturers have produced 8,300 million metric tons of virgin plastics, creating 6,300 million metric tons of plastic waste, with only 9% recycled, 12% incinerated, and the remaining 79% ending up in landfills or the environment (Geyer at al., 2017) (Figure 3). None of these mass-produced plastics can biodegrade in a meaningful way. If plastic production continues this trend, then by the end of 2050, humans will have produced 26,000 million tons of resin, 6,000 million metric tons of PP&A fibers, and 2,000 million metric tons of additives (Geyer at al., 2017). Assuming the continuance of the same trends previously described, 9,000 million metric tons of plastic waste will have been recycled, 12,000 million metric tons incinerated, and 12,000 million metric tons discarded into landfills or the natural environment (Geyer et al., 2017) (Figure 4).

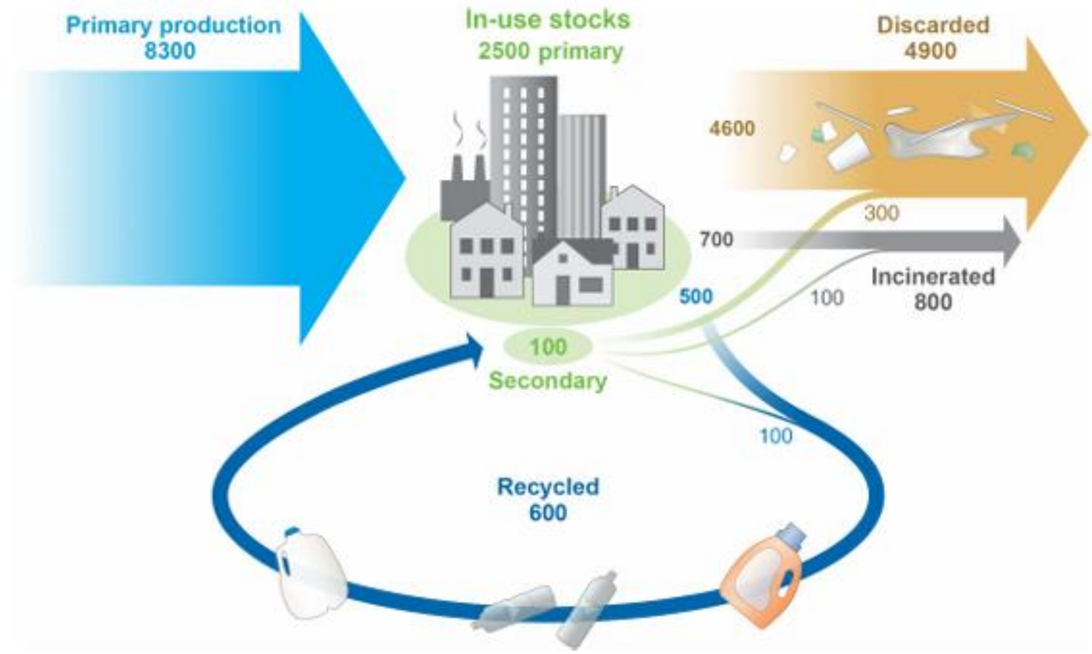

Figure 3: Global production, use, and fate for plastics (in million metric tons) (Source: Geyer et al., 2017).

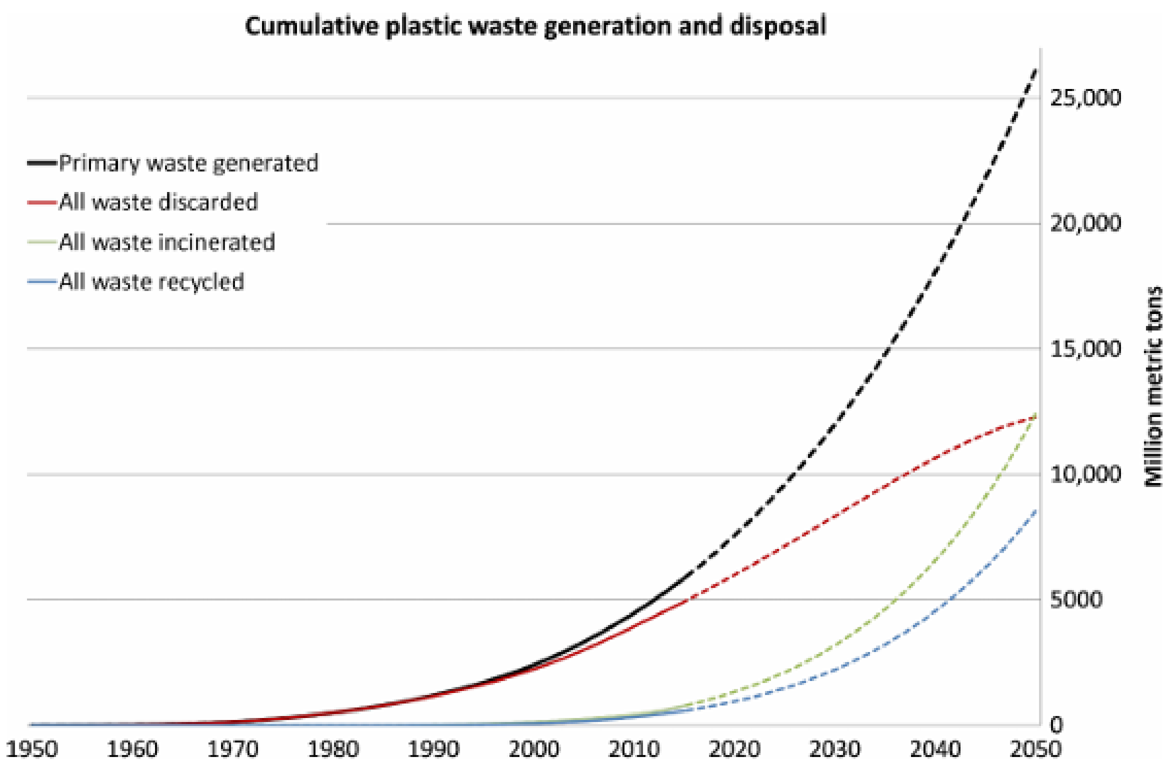

Figure 4: Cumulative plastic waste generation and disposal. Solid lines show historical data (1950-2015), and dashed lines show projected trends (to 2050) (Source: Geyer et al., 2017).

Additionally, the coronavirus disease of 2019 (COVID-19) had a major impact on plastic production levels due to the demand of single-use personal protection equipment needed. Globally, approximately 129 billion face masks and 65 billion plastic gloves are disposed of monthly (Aragaw and Mekonnen, 2021). Additionally, both the face masks and gloves are only used once before being discarded. Medical face masks are already being identified as a potential source for micro-plastic pollution in waterways (Aragaw 2020). The use and mismanagement of COVID-19 attributed medical waste is having a major contribution to plastic contamination and could exist in the environment for decades to come (Aragaw and Mekonnen, 2021).

2.2.4 Plastic Waste in the Environment

Discarded plastic contaminates a wide variety of habitats ranging from terrestrial, (including freshwater environments), to marine habitats (Thompson et al., 2009) (Figure 5). Discarded plastic has the largest effect on marine environments due to the sheer quantity entering the waterways and their effects on these ecosystems (Thompson et al., 2009). Plastic debris in the marine environment has been documented extensively, however, the quantity of plastic entering the ocean is less well known. Land-based sources of plastic debris account for 80% of the plastic debris in the marine environment (Li et al., 2016). Jambeck et al., (2015), used global solid waste, population density, and economic status to estimate the mass of land-based plastic waste entering the ocean. They found that in 2010, of 275 million metric tons of plastic waste, from 192 coastal countries, 4.8 to 12.2 million metric tons entered the ocean. If waste-management infrastructure does not improve by 2025, the cumulative quantity of plastic waste available to enter marine environments from the land is predicted to increase by an order of a magnitude (Jambeck et al., 2015).

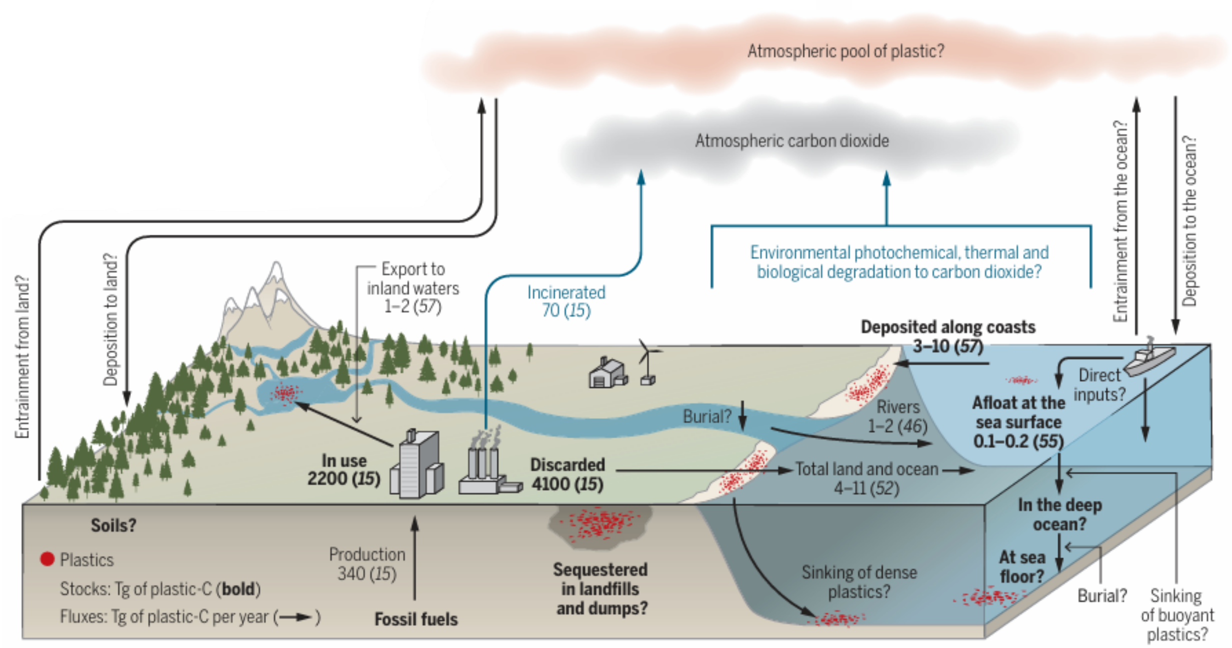

Figure 5: The 2015 global plastic-carbon cycle. Black areas demonstrate fluxes of plastics between compartments. Blue fluxes represent ways that plastics are removed (i.e. incineration to carbon dioxide or photodegradation to oligomers). Question marks represent plastic-carbon cycle terms without published estimates. Plastic mass values are the numbers shown in parentheses (Source: Stubbins et al., 2021).

Millions of tons of plastics in the ocean get concentrated into giant gyres that rotate in circular patterns because of winds and the Coriolis Effect (Schweitzer and Noblet, 2018). Currently, there are five main garbage patches located in the North Pacific, South Pacific, North Atlantic, South Atlantic, and Indian Oceans. One of the most notable such gyres is the Great Pacific Garbage Patch (Figure 6), stretching from California to Japan in the gyre of the North Pacific Subtropics Convergence Zone (Schweitzer and Noblet, 2018). As of 2018, the Great Pacific Garbage Patch is estimated to have at least 79 thousand tons of plastic floating inside an area of 1.6 million km^2 (Lebreton et al., 2018). This quantity is four to sixteen times larger than previously reported. Within the Great Pacific Garbage Patch, microplastics accounted for 8% of the total mass, but 94% of the approximately 1.8 trillion pieces floating in the sea (Lebreton et al., 2018).

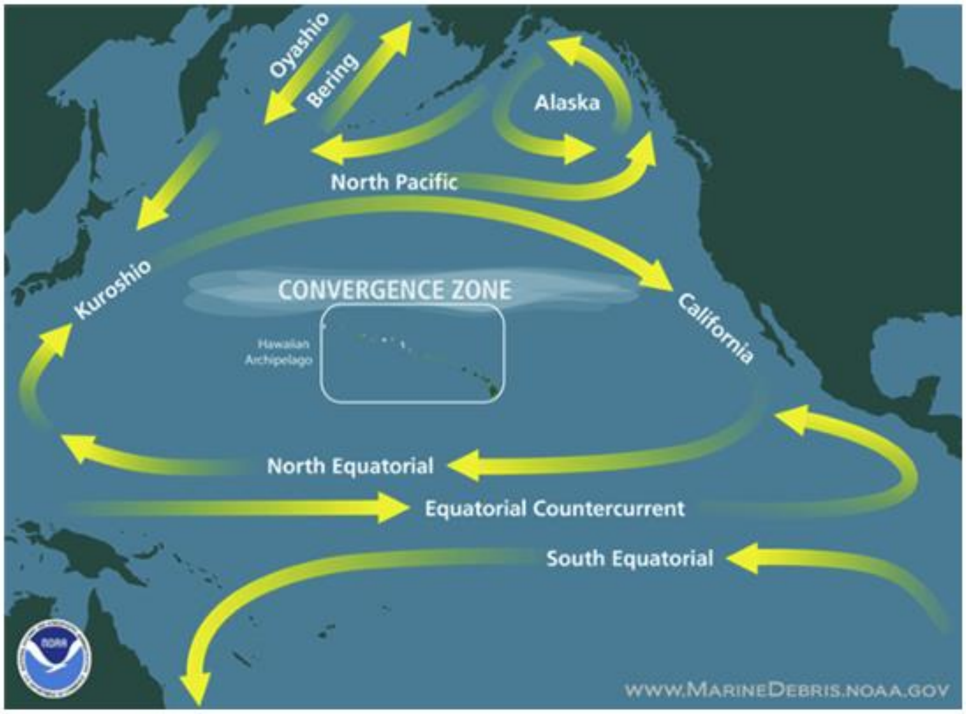

Figure 6: Great Pacific Garbage trash, Pacific Ocean gyre. (Source: Schweitzer and Noblet 2018).

2.3 Microplastics

2.3.1 Introduction

While plastic particles have been observed since 1972 (Carpenter and Smith, 1972; Mai et al., 2018), gaining the name of "microplastics" in 2004, becoming the focus for important research activity (Thompson et al., 2004). As plastic production increases and plastic waste enters the environment at an alarming rate, there is an increased interest in understanding the impacts of MPs, as the impacts remain poorly understood (Thomson et al., 2004). Despite there being no agreed-on standard size range/classification for MPs, they are most commonly defined as plastic particles measuring smaller than 5 mm in length (Betts, 2008; Arthur et al., 2009; Fendall and Sewell, 2009; Cole et al., 2011; Hidalgo-Ruiz et al., 2012; Rillig, 2012; Masura et al., 2015; Duis and Coors, 2016; GESAMP, 2016; Mai et al., 2018; Schöpel and Stamminger, 2019) (Figure 7). There is not an agreeable lower bound value for size requirements (Arthur et al., 2009). MPs can come in the form of a wide variety of shapes including pellets, microbeads, fragments, fibers, films, and foams (Crawford and Quinn, 2017).

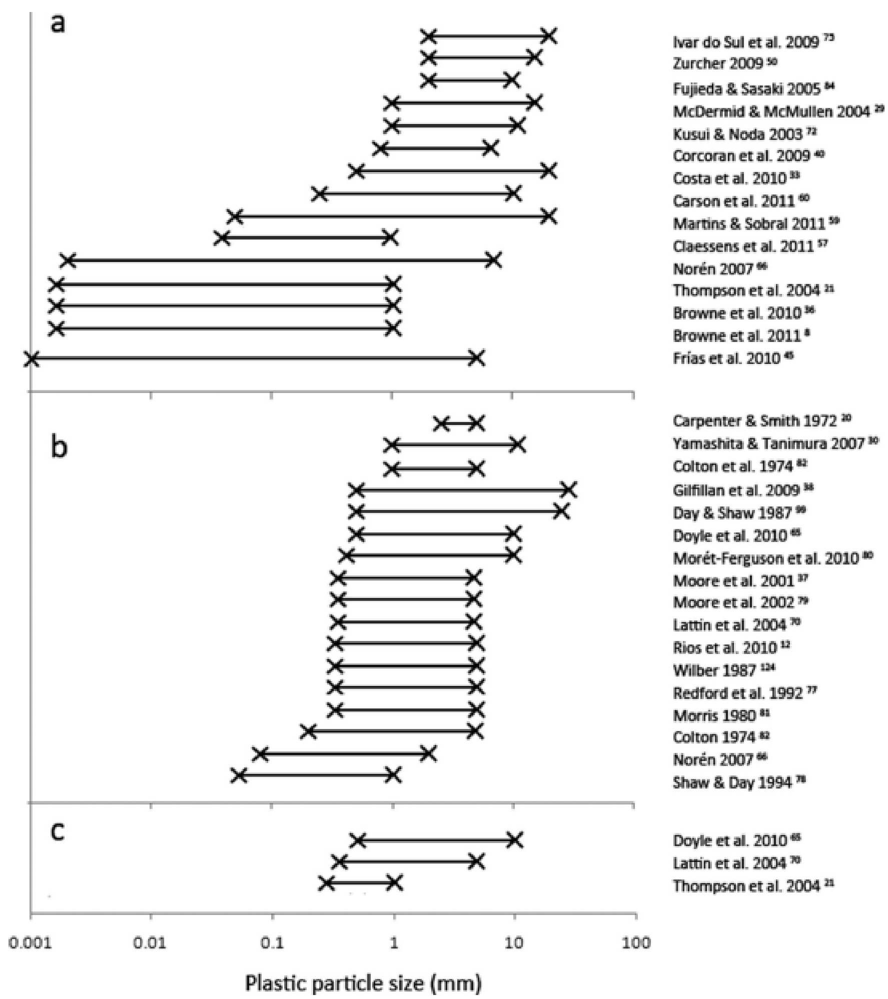

Figure 7: Size ranges for microplastic particles from (a) sediment, (b) sea surface, (c), water column studies. Note: only studies that provided lower and upper limits of microplastics and plastic pellet studies were excluded (Source: Hidalgo-Ruz et al., 2012).

2.3.2 Types of Microplastics

Potential sources of MPs have been well documented and separated into two categories: primary and secondary sources (Arthur et al., 2009; Cole et al., 2011; Hidalgo-Ruz et al., 2012; Rillig, 2012; Bråte et al., 2014; Masura et al., 2015; Duis and Coors, 2016; GESAMP, 2016; Li et al., 2016; Crawford and Quinn, 2017; de Sá et al., 2018; Mai et al., 2018; Prata et al., 2018; Schöpel and Stamminger, 2019;) (Figures 8 and 9). Primary MPs are manufactured to be microscopic in size (Cole et al., 2011). Primary MPs are commonly created from industrial and domestic products (Betts, 2008; Moore, 2008), and used in facial cleansers and cosmetics (Zitko and Hanlon, 1991), medicine drug vectors or linking plastic intracellularly with drugs (Patel et al., 2009), and air-blasting media (Gregory, 1996). Air-blasting involves blasting acrylic, melamine, or polyester microplastic scrubbers to remove rust and paint on machinery, boat hulls, or engines (Gregory, 1996). One of the most discussed primary MPs consists of scrubbers, used in facial scrubs and exfoliating hand cleansers (Li et al., 2016). Microplastic scrubbers replaced traditionally used natural ingredients, such as ground almonds, oatmeal, and pumice (Derraik, 2002). Other influential primary MPs include fibers from synthetic clothing and rope (Thompson et al., 2004; Browne et al., 2007). Browne et al., (2011) discovered that one of the most significant sources of MPs in the marine environment was fibers from washing clothes being distributed by sewage.

Secondary MPs are tiny plastic fragments resulting from the breakdown of larger plastic debris occurring both at sea and on land (Thompson et al., 2004). Fragmentation is a result of physical, biological, and chemical processes that reduce the structural integrity of the plastic over time (Browne et al., 2007). Over time, exposure to sunlight can result in photo-degradation of plastics (Cole et al., 2011). Ultraviolet (UV) radiation in sunlight causes oxidation of the polymer matrix, resulting in the bonds to split (Browne et al., 2007; Rios et al., 2007; Moore, 2008; Barnes et al., 2009; Andrady, 2011). This can also result in additives, leaching out of the plastics, which are supposed to increase durability and corrosion resistance (Talsness et al., 2009). Photooxidation is not as likely in the marine environment, but in contrast, beaches have high oxygen availability and direct exposure to sunlight resulting in plastic debris to degrade rapidly (Moore, 2008; Barnes et al., 2009; Andrady, 2011). When plastics lose their structural integrity, they are increasingly susceptible to fragmentation, resulting from abrasion, wave action and turbulence (Browne et al., 2007; Barnes et al., 2009). This process is ongoing, with fragments becoming smaller and smaller over time until they become MPs (Fendall and Sewell, 2009; Ryan et al., 2009). MPs can further degrade in size into nanoplastics, which is likely to have increasing significance in future years (Cole et al., 2011).

Figure 8: Primary microplastics example, on the left, from a personal care product. Secondary microplastics example, on the right, breakdown of larger plastic debris (Source: Bråte et al., 2014).

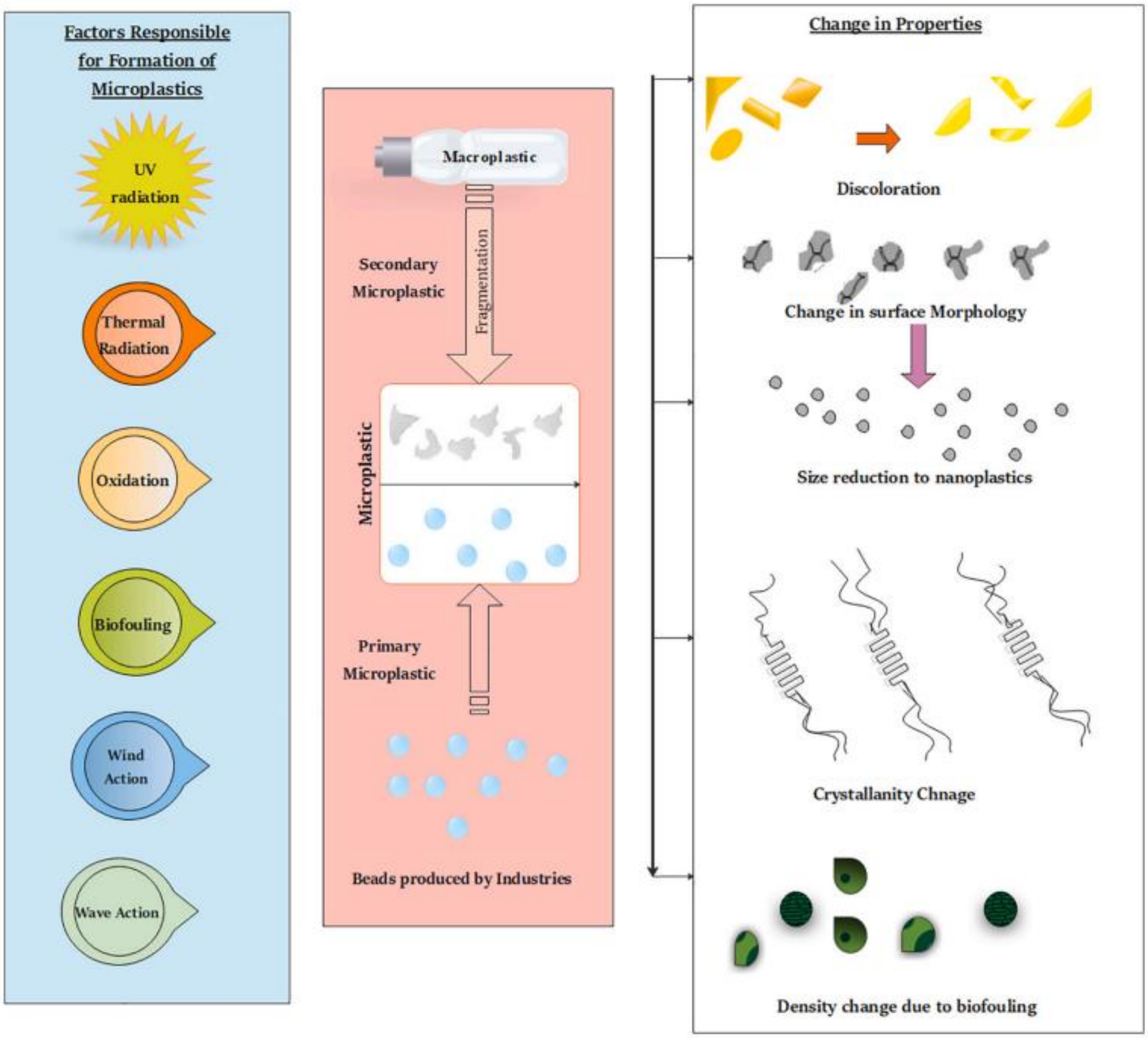

Figure 9: Microplastic degradation and results (Source: Tirkey and Upadhyay, 2021).

Even though biodegradable plastics are perhaps marketed as being a worthy replacement for traditional plastics, they can also result in MPs (Thompson et al., 2004; Cole et al., 2011). Biodegradable plastics usually consist of synthetic polymers and starch, vegetable oils or specialized chemicals that have the purpose of accelerating degradation times (Derraik, 2002; Thompson et al., 2004; Ryan et al., 2009). Biodegradable plastics will decompose if disposed of properly, in industrial composting plants under hot, humid, well-aerated conditions (Thompson, 2009; Moore, 2008). This decomposition is only partial, however, with the starch components decomposing, but an abundance of synthetic polymers being left behind (Thompson et al., 2004; Andrady, 2011). Meaning that these products are not truly biodegradable in the way that they are marketed. With the absence of terrestrial microbes in relatively cold marine environments, decomposition times of the degradable components are prolonged, resulting in an increased probability of the plastic being fouled and reducing UV permeation which the degradation process relies on (Moore 2008; Andrady, 2011). This still results in MPs being released into the marine environment once decomposition finally occurs.

2.3.3 Microplastic Sources

There is a wide range of potential sources for MPs entering the marine environment (Figure 10). Plastic debris originating from land-based sources accounts for 80% of the plastic debris in the marine environment (Andrady, 2011). These plastics can be attributed to impurely disposed user plastics occuring in cosmetics and air-blasting and plastic leachates from refuse sites (Cole et al., 2011). Industrial or densely populated areas are a main source due to littering, plastic-bag usage, and solid-waste disposal (Derraik, 2002). Other land-based sources include plastics being transported by river systems and wastewater-treatment plants to the marine environment (Browne et al., 2010; Cole et al., 2011). Extreme weather events, such as hurricanes or flooding, increase movement of land-based debris to the sea (Barnes et al., 2009). Globally, the entire fishing fleet uses plastic gear, inevitably some being lost or discarded, with 18% of marine plastic debris being attributed to the fishing industry (Watson et al., 2006; Andrady et al., 2011). Another source of plastic debris occurs from the manufacture of plastic products that use granules and small resin pellets (Cole et al., 2011). These materials can enter the marine environment from accidental spillage during transport, inappropriate use as packing materials, and direct outflow from processing plants (Cole et al., 2011).

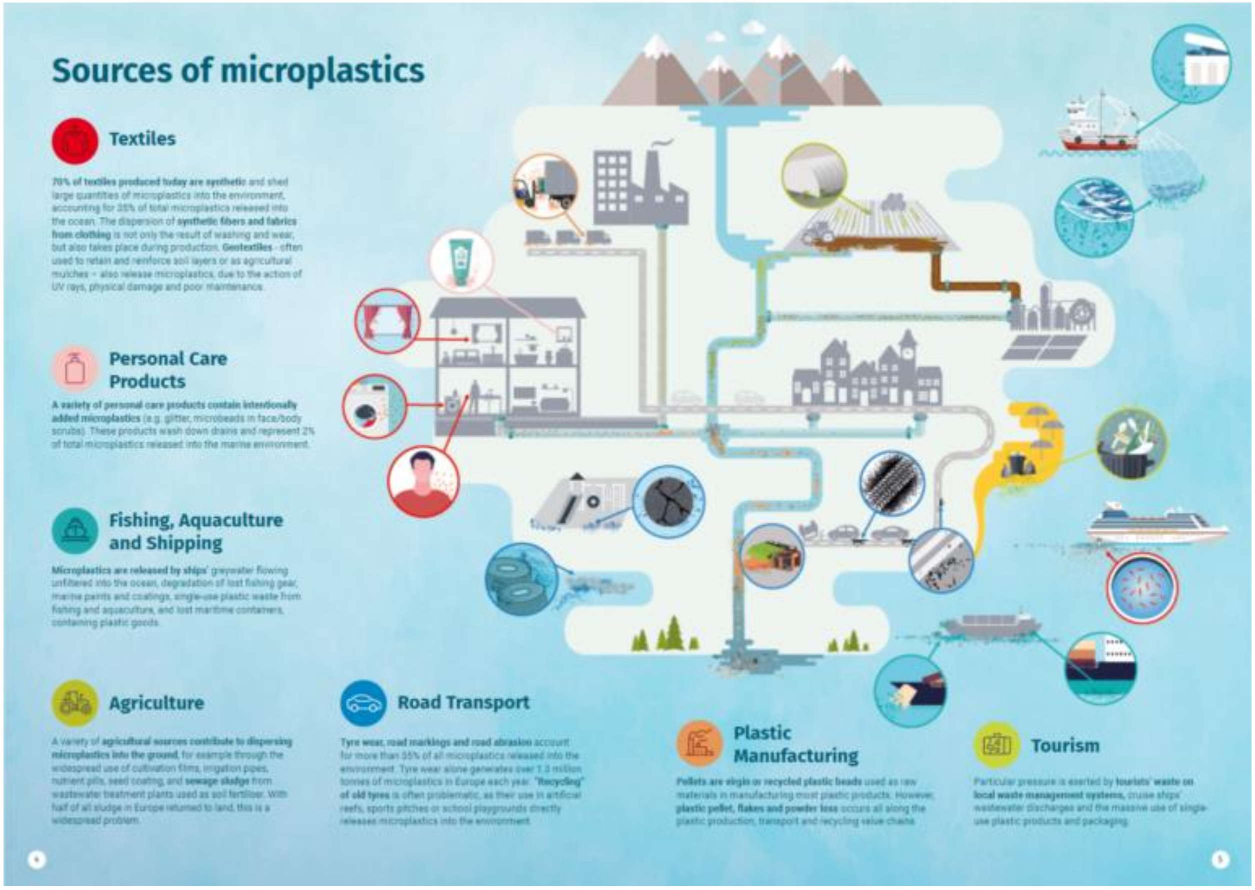

Figure 10: Microplastic sources into the ecosystem (Source: Seas at Risk, 2022).

2.3.4. Abundance of MPs

MPs have been detected in virtually all environments. The occurrence of MPs has mostly been investigated in the marine environment due to the detection of unexpectedly high levels in oceanic convergence zones (Duis and Coors, 2016). Globally, MP abundance is estimated to be anywhere between five and fifty trillion particles, with a mass between 32,000 to 236,000 metric tons (van Sebille et al., 2015). High concentrations of MPs are observable near industrial centers, metropolitan areas, and enclosed/semi-enclosed seas and in gyres (Duis and Coors, 2016). MPs have also been documented in what are considered some of the most remote marine environments (GESAMP, 2016), such as the Arctic (Lusher et al., 2015), in Arctic Sea ice (Obbard et al., 2014) and in the Southern Ocean (Barnes et al., 2010). About half of floating MPs in the open ocean are in the subtropical gyres of North and South Atlantic, North and South Pacific, and the Indian Ocean, with concentrations having the potential to be a million times higher in comparison to other regions. There is a lesser understanding of how MPs occur below the ocean surface (GESAMP, 2016).

2.3.5 Degradation Times

Plastic debris typically degrades in two ways: biodegradation and photodegradation (Li et al., 2016). Degradation occurs at a slow rate depending on the availability of bacteria, light, and oxygen (Koelmans et al., 2022). There is little information available on specific fragmentation and degradation rates of MPs (Duis and Coors, 2016). Extrapolated persistence data (Figure 11) has been used to estimate half-lives of plastics, which ranges from 58 years for bottles to 12,000 years for pipes (Chamas et al., 2020). Using calibration of experimental weathering data and modeling of fragmentation, fragments at the ocean surface and beaches have an average 176-year lifespan. The production of plastic only began around 70 years ago, implying the formation of MPs is quite rapid (Koelmans et al., 2022). In 2016, Koelman et al., calculated that in the ocean, approximately 50% of plastics had been there for more than 13 years, 80% more than 4 years, and 90% more than 2 years. As a result, it can be inferred that present-day plastics are still in the early stages of degradation based off estimated half-lives and timescales of 100 to 1,000 years (Koelmans et al., 2022).

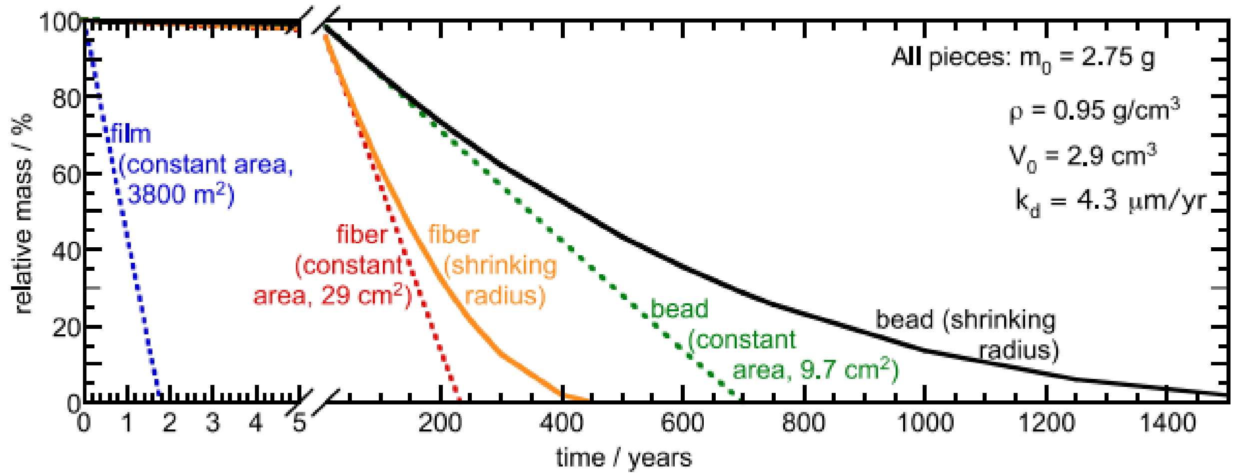

Figure 11: Predicted degradation profiles for HDPE and SSDR (pieces with the same mass and density), but different shapes (film, fiber, bead). The dashed lines represent extrapolations assuming constant surface area, while the solid lines represent a shrinking radius model (surface area decreasing over time) (Source: Chamas et al., 2020).

2.3.6 Implications of Microplastic Contamination

Even though MPs are widespread globally, the impact MPs have on organisms in the marine environment have only recently emerged (Cole et al., 2011) (Figure 12). MP's small size make them a threat to a wide range of marine organisms (Derraik, 2002; Thompson et al., 2004; Barnes et al., 2009; Fendall and Sewall, 2009). If ingested, MPs can pose a physical hazard to organisms (Fendall and Sewell, 2009), such as blockage of the intestinal tract, inhibition of gastric enzyme secretion, reduced feeding stimuli, decreased steroid hormone levels, delays in ovulation, and failure to reproduce (Azzarello and Vleet, 1987; Ryan, 1988; Spears et al., 1995; McCauley and Bjorndal, 1999; Derraik, 2002; Wright et al., 2013). Seabirds are extremely vulnerable to plastic ingestion as they rarely regurgitate undigested hard material, meaning that MPs are a new and increasing problem associated with plastic ingestion (Li et al., 2016).

A review by Li et al., (2016) found that MP particles have been detected in fish species originating in the Mediterranean Sea (Romeo et al., 2015), North Pacific Ocean (Boerger et al., 2010; Jantz et al., 2013), South Atlantic Ocean (Possatto et al., 2011; Dantas et al., 2012), and North Sea. Predation activities are a common way fish ingest plastic (Li et al., 2016). Tuna chase or find their prey in shallow waters, hence ingesting plastic particles during feeding since these waters have abundant buoyant plastic debris (Romeo et al., 2015; Li et al., 2016). Other species affected by ingestion include sea turtles and at least 48 cetacean species (i.e. whales and dolphins) (Li et al., 2016). Once ingested, MPs can be transported through the digestive tract until excretion, and accumulate in the gut, digestive gland, gills, or the liver (Lu et al., 2016; Riberio et al., 2017; Koelmans et al., 2022).

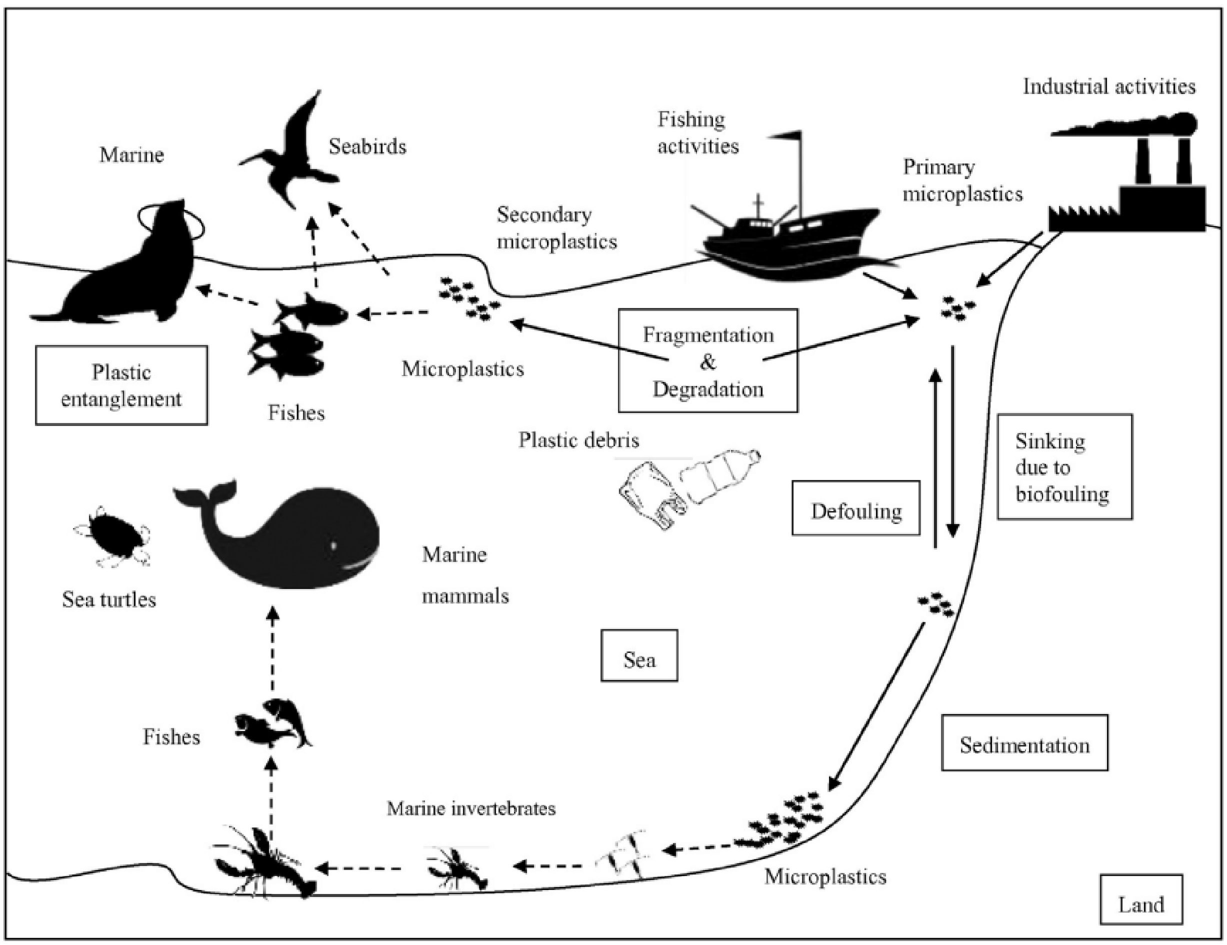

Figure 12: Potential pathways of plastic debris and biological interactions. Dotted arrows represent plastic ingestion, while solid arrows represent transportation (Source: Li et al., 2016).

In addition to physical impacts, ingestion can also have chemical effects (Li et al., 2016). A review by Li et al., (2016) indicated multiple studies have found plastic debris to be a vector for the absorption or transportation of waterborne chemical pollutants from invertebrates to higher trophic levels (Gregory, 1996; Teuten et al., 2009), including polychlorinated biphenyls (PCBs) (Zarfl and Matthies, 2010), polycyclic aromatic hydrocarbons (PAHs) (Teuten et al., 2009), and organochlorine pesticides such as DDT (Ivar do Sul and Costa, 2014). These pollutants are persistent organic pollutants (POPs), which remain persistent in the environment for extended time, bioaccumulative, toxic, hydrophobic, and have a long-range transport potential (Zarfl and Matthies, 2010). MPs have such an affinity for carrying POPs due to plastics being composed of highly hydrophobic materials (Ivar do Sul and Costa, 2014). Concentrations of PCBs held by MPs are one million-fold higher than PCB concentrations in surrounding water (Betts, 2008). Multiple studies have correlated a positive relationship between quantity of plastics ingested and concentration of PCBs (Li et al., 2016). A high concentration of POPs (i.e. PCBs) can cause endocrine disruption, teratogenicity and toxicity of the liver and kidney (Yogui and Sericano, 2009; Muirhead et al., 2016).

Low concentrations of plastic additives, such as brominated flame retardants, phthalates, and the constituent monomer bisphenol A, can have harmful effects on mollusks, crustaceans, fish and amphibians (Oehlmann et al., 2009; Li et al., 2016). The purpose of plastic additives is to reduce the chemical affinity between molecules or used as monomers in polycarbonate plastic, but they are unstable in plastic resulting in leaching into the environment (Staples et al., 1997; Li et al., 2016). Plastic additives have been found in the bodies of organisms, released once ingested, resulting in a high concentration of additives to be able to disrupt biological processes (Lithner et al., 2011; Engler, 2012; Li et al., 2016). Plastic additive studies primarily were conducted on fish, with little research on how plastic additives affect marine seabirds or mammals (Li et al., 2016).

The presence of MPs in marine species for human consumption should be of concern in regard to the potential effects of MPs on human health, especially in countries with high intake of seafood (Barboza et al., 2018). Information on occurrence of MPs in seafood products, exposure levels, and potential health effects for humans is largely unknown and still being studied (Barboza et al., 2018). Although MPs in the human body are being studied initially, MPs have been seen in the human stool (Schwabl et al., 2019) and the placenta (Ragusa et al., 2020).

In addition to health implications, MPs can also contribute to the dispersal of invasive species, species that cause harmful algal blooms, microorganisms, and pathogens (Duis and Coors, 2016). MPs have the potential to be a more effective invasive species dispersal mechanism than ship hulls or ballast water (Barnes, 2005). MPs have been implicated in the northward range extension of the large barnacle *Perforatus perforates* (Rees and Southward, 2008) and provide substrate for bryozoans, barnacles, polychaete worms, hydroids, and mollusks (Moore, 2008). Additionally, once MPs are present in marine environments, it is virtually impossible to remove them without also disrupting ecosystem function by removing planktonic biomass (Bråte et al., 2014).

2.3.7 MP Water-Sampling Methods

There is no standard sampling method for MPs in water or sediment. For water samples, there is no standard or specific depth required for sampling. The medium chosen for collecting water depends on the size of the body and amount of water to be collected. A large portion of studies and reviews focus on sampling large bodies of water or beaches. MP distribution in the water column is dependent on a multitude of properties including shape, density, size, and environmental conditions. Quantity and quality of MPs are highly dependent on sampling location and depth. Distribution of MPs in the water column can change depending on fresh or salt water, typically MPs will be deeper in the water column in freshwater (Prata et al., 2019).

There are a several ways to sample MPs by using nets, sieves, pumps, or glass containers (Mai et al., 2018; Prata et al., 2019). One of the most common methods for sampling the sea is using a neuston tow (Barrows et al., 2017). Neuston plankton nets sample a large volume of water by collecting plastic pieces as they sieve through the water (Barrows et al., 2017). Using glass bottles and metal sieves are ideal to reduce the chance of contamination but are commonly associated with being able to collect limited amounts of water (Prata et al., 2019). MPs must be separated from water samples in order to be analyzed which can occur in two ways: 1) a reduction step that allows one to reduce sample volume (i.e. use of nets during collection) or 2) a separation step typically through filtration and/or density separation (Prata et al., 2019). Water samples contain biological materials, and a digestion step, usually hydrogen peroxide (H_2O_2) is used to remove organic material and is highly recommended but not required (Prata et al., 2019). Visual inspection is conducted for identification and quantification of MPs, and this is followed by chemical characterization. A stereoscope or a microscope can be used for visual inspection, allowing MPs to be classified by size, color, and shape. Chemical characterization of MPs by Fourier transform infrared spectroscopy (FTIR), Raman spectroscopy, or a Scanning electron microscope (SEM) is highly recommended to confirm MPs (Prata et al., 2019).

2.4 Karst

Karst landscapes are areas of land that are underlain by soluble bedrock, containing caves, sink holes, and sinking steams. Karst is produced when rock solubility is combined with rock structure and lithology (Ford and Williams, 2007). Karst regions can be observed on every continent except Antarctica, and account for 15.2% of the world's ice-free land surfaces (Goldscheider et al., 2020). Karst regions are significant as karst aquifers hold fresh water and are home to underground ecosystems. Karst landscape appearances vary, with prominence of features being dependent on the local hydrogeological factors (Veni et al., 2001). Subsurface karst features include caves and conduits where bedrock has dissolved away (Palmer, 2012). Above ground, on the surface, karst features include sinkholes and sinking streams (Veni et al., 2001). Karst areas are very fragile environments that have been impacted by human activities since the industrial revolution (Parise et al., 2008). Globally, 1.18 billion people (16.5% of the global population) live on karst, making it important to understand (Goldscheider et al., 2019).

2.4.1 Water Pollution in Karst

Karst landscapes are extremely important, as 678 million people, 9.2% of the global population, rely on aquifers for drinking water (Stevanović, 2019). The largest consumer of karst aquifers is China with approximately 150 million citizens relying on such aquifers (Zektser and Everett, 2004), followed by approximately 50 million people in the USA in rural areas (Karst Water Institute, 2016). Karst aquifers act as a reservoir of water, able to transport water to springs or wells underground via natural dissolution processes that result in fractures (Veni et al., 2001). Karst aquifers allow for large volumes of water to be stored underground, which is advantageous in arid climates due to high evaporation rates (Veni et al., 2001).

Karst landscapes are extremely vulnerable to hazards and pollution. Karst regions are especially vulnerable to the rapid rate and ease with which contaminants enter the aquifer. Contamination is common for karst aquifers in both rural and urban areas. Urban contamination includes oil, grease, solid trash, human wastes, chemical waste, septic tank effluent, and other forms of runoff (Veni et al., 2001). In rural areas, fertilizers, pesticides, and herbicides contaminate karst aquifers (Veni et al., 2001). In rural karst areas contamination of wells or springs is especially dangerous due to health risks associated with drinking untreated water.

2.4.2 Microplastics in Karst

Karst caves are extremely fragile ecosystems with a significant scientific value in fauna and speleothems (Balestra and Bellopede, 2021). As previously described, karst aquifers are an important source of drinking water. MP pollution in caves and karst aquifers is poorly understood (Panno et al., 2019; Balestra and Bellopede, 2021). It is important to understand how MP impacts caves and karst aquifers, as both are easily impacted by anthropogenic factors.

2.4.3 Literature Gap

As MP contamination increases, there are many information gaps that need to be examined. There needs to be a standardized method for sampling and analyzing MPs, to allow for a comparison of results between studies. Current methods likely result in bias and underestimating of smaller MPs. There are also no methods to characterize MP by source location, however using FT-IR is a promising method to characterize MPs by polymer type. More research needs to be conducted on MP interactions within food chains, and their effects on organisms. There is little information on leaching rates of plastics in water. There is also limited information on MP contamination in caves and karst aquifers. The aim of this study is to examine MP contamination in karst regions, characterize MP particles, and to aid in understanding MP detection.

Chapter 3: Study Area

3.1 Introduction

There are three areas of interest within southern Kentucky: Lost River Rise, GO Spring, and Biz Falls. An important location to study is Bowling Green, Kentucky. Bowling Green (Figure 13) is a city in south-central Kentucky that is rapidly developing. In 2010, Bowling Green had a population of 58,067 and as of 2020 the population grew to 72,294 (U.S.A. Census, 2020). Bowling Green is the fastest growing, and third largest, city in Kentucky, following Louisville and Lexington. It is home to Western Kentucky University, the National Corvette Museum, and multiple major manufacturing plants, such as Fruit of the Loom and General Motors. Bowling Green covers about 103.6 km^2 (U.S.A. Census, 2020). On average, Bowling Green receives 127.3 centimeters (cm) of precipitation per year and has an average temperature of 15.1 °C. Land use within the city of Bowling Green is mostly urban, developed space, with residential and commercial use. Bowling Green is underlain by a karst landscape, which is extremely vulnerable to water pollution. This area is important to study due to the karst landscape's ability to allow for the fast movement of water within karst systems and the storage of water in aquifers. Bowling Green also represents an urbanized area that theoretically should have MPs present in the groundwater.

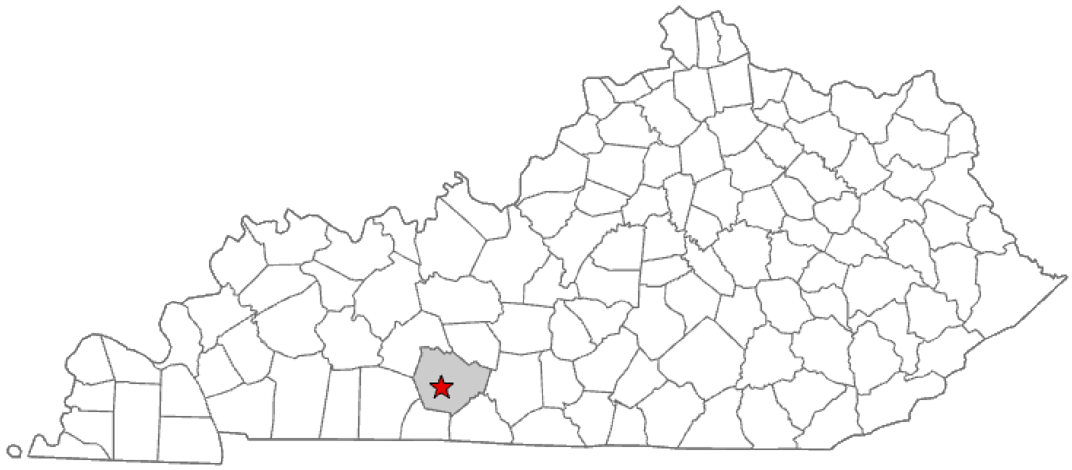

Figure 13: Map of Bowling Green, Warren County, Kentucky (Source: Created by Author).

3.2 Lost River Groundwater Basin

Bowling Green, Kentucky is built over the Lost River Cave System. Lost River Cave represents the primary drainage system for the Lost River Groundwater Basin (Figure 14). The headwaters of Lost River originate about 19 km south of the Bowling Green city limits, near Woodburn, composed of several surface streams that converge into a single river system (Jackson, 2017). As the stream reaches Bowling Green, it reemerges at the surface four times at multiple blue holes within the Lost River Valley, before disappearing into Lost River Cave (Jackson, 2017). At Blue Hole #4, Lost River emerges on the surface and flows for approximately 120 meters before draining into Lost River Cave. Roughly 61 meters from the entrance of Lost River Cave is a three-meter-high epikarst-fed waterfall that drains directly to the water table (Jackson, 2017). This waterfall is accessible year-round, functioning as a tourist site. The stream continues northward until it resurges at Lost River Rise in Lampkin Park. The final discharge point, the Lost River Rise, represents roughly 152 km^2 of urban and agricultural landscape runoff (Jackson, 2017).

The annual average discharge at the Lost River Rise is approximately 0.35 m^3/s. The Lost River Basin lies within the Pennyroyal Sinkhole Plain, which is composed of Mississippian-aged St. Louis and Ste. Genevieve limestones, as well as Girkin Limestone (Crawford, 1989). This groundwater basin has a multitude of karst features such as sinkholes, sinking streams, springs and caves. Both formations are thick-bedded and can look very similar to one another. An important distinction is that the Ste. Genevieve limestone is largely oolitic, while the St. Louis is not (Creech, 2019). Even though Bowling Green comprises a large portion of the Lost River Groundwater Basin, over 50% of the basin is agricultural, but the main portion of the cave is under the urbanized part of the city itself (Lawler, 2023).

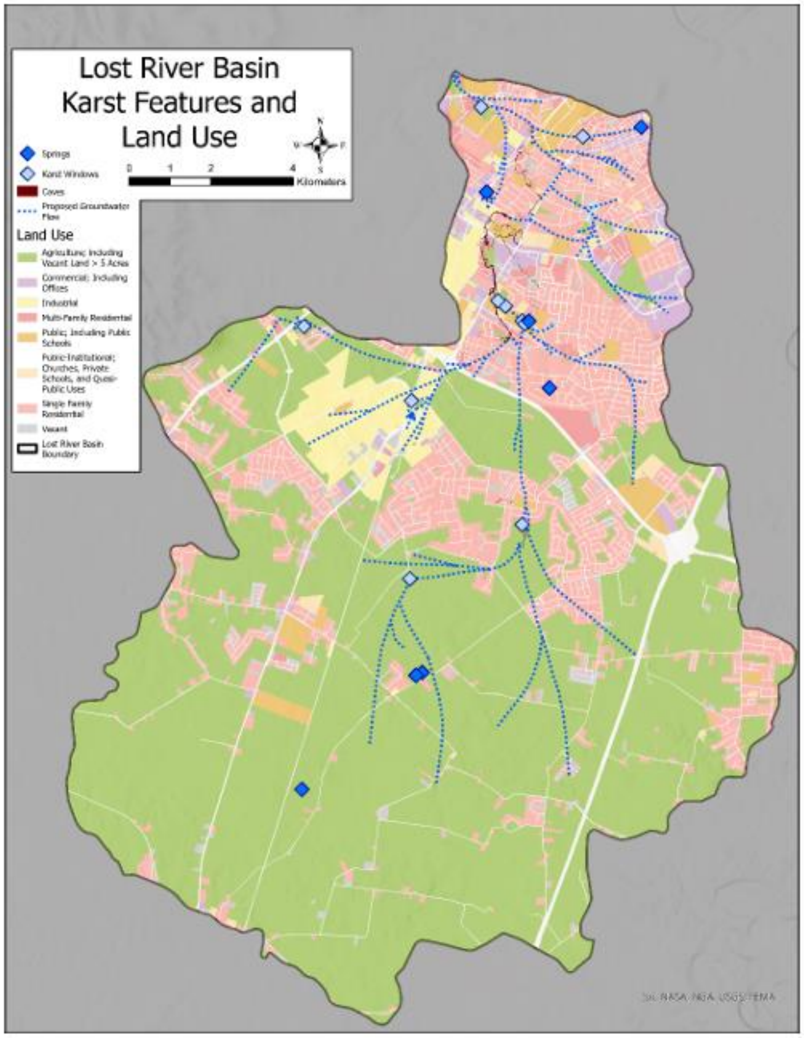

Figure 14: Lost River Groundwater Basin Map (Source: Lawler, 2023).

3.3 Great Onyx Groundwater Basin

Great Onyx Cave is within part of Mammoth Cave National Park (MACA) located in south-central Kentucky. MACA is home to 52,830 acres of karst terrain, including the world's most extensive known cave system (Soto and Pate, 2016; Groves et al., 2021). MACA has been designated as a World Heritage Site and an International Biosphere Reserve by the United Nations, due to the unique karst landscape (Bledsoe et al., 2021). MACA lies within the central

Kentucky karst limestone belt, including St. Louis Limestone, Ste. Genevieve Formation, and the Girkin Formation, all Mississippian age limestone (Palmer, 1995, 2017).

The Great Onyx Groundwater Basin is the main sampling location for the study area. Several dye traces have been conducted to delineate the Great Onyx Groundwater Basin (Soto and Pate, 2016). Great Onyx Spring is the main discharge point of the basin, flowing into the Green River through a spring run. Great Onyx Spring has a recharge area of approximately four-square kilometers (Figure 15) (Williams, 2021). Great Onyx Groundwater Basin has an average annual temperature of 14.6°C and an average annual rainfall of 130 centimeters (Climate-Data.org, n.d.).

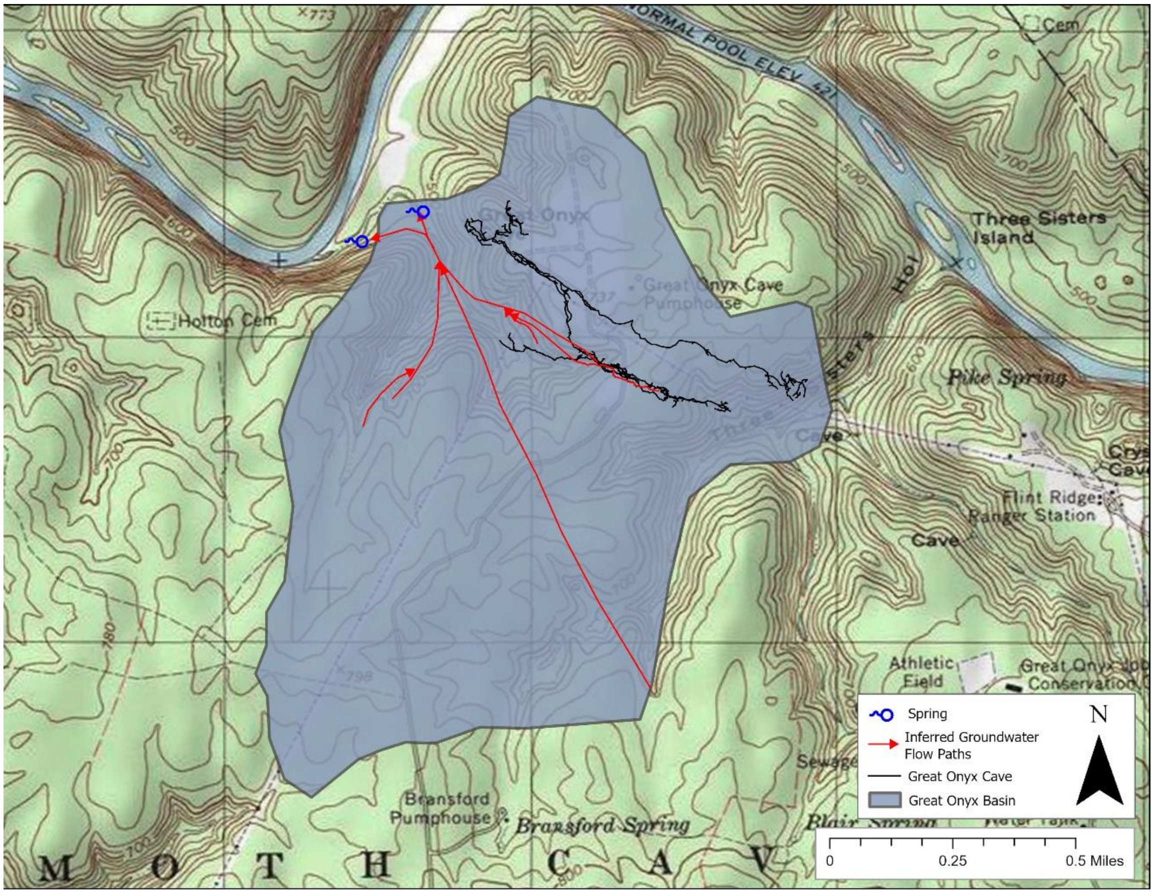

Figure 15: Inferred groundwater flow paths within Great Onyx Groundwater basin determined by dye traces. Map modified from National Park Service Map by Rick Toomey (Source: Bledsoe, 2023).

Great Onyx Groundwater Basin essentially serves as a relatively pristine landscape, the last direct land use in 1961 before the park acquired ownership of the cave and property (Duckeck, 2021). Prior to when MACA began protecting the land, there were two small tourist hotels and scattered farmsteads that occupied the land. The road leading into the basin is secured by gated access, requiring a key and permit to enter. The cave itself, approximately three kilometers from the gate, requires a National Park Service (NPS) permit to enter during times other than tours. There is a tour route that does run through 1.6 km of the cave, with a maximum of 38 tickets available for each tour, plus one to two NPS Rangers (National Park Service, 2024).

Since 2014, there have been about 35,000 Great Onyx tours, resulting in approximately a ten-year average of approximately 3,500 people per year (Merideth, 2024).

3.4 Great Onyx Cave - Biz Falls

Great Onyx Cave is located within the Great Onyx Groundwater Basin (Figure 14), composed of approximately 7.4 kilometers of passages. Edwards and Cox Avenues are the two main, nearly horizontal upper-level passages formed in the Girkin and Ste. Genevieve limestones in Great Onyx Cave (Raines, 2023) (Figure 16). Cascade River flows through these upper levels, up and over a large waterfall, then falling approximately 25 meters to the lower-level cave. At this point, the stream merges with another to form the Lucykovah River which flows to Great Onyx Spring, and flows to the Green River (Williams, 2021).

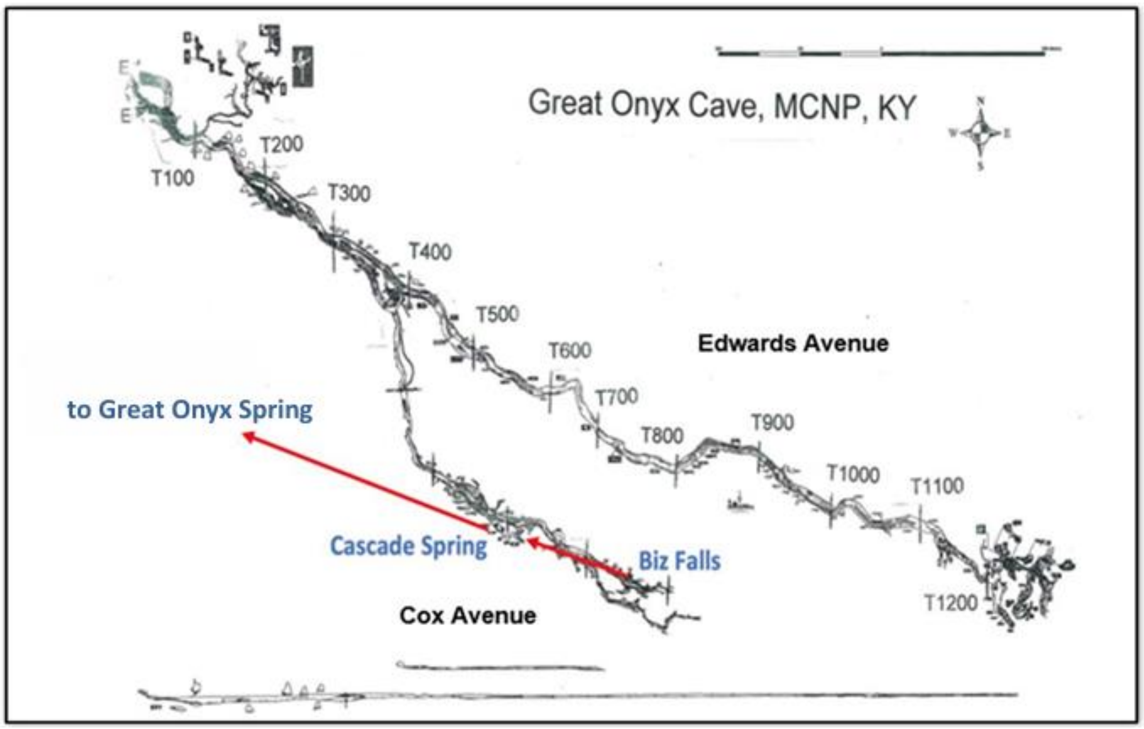

Figure 16: Edwards and Cox Avenue: mapped passages of Great Onyx Cave. Red lines demonstrate inferred water pathways from dye-tracing, showing the connection of Biz Falls to Cascade River to Great Onyx Spring. Map modified from Cave Research Foundation, NPS (Source: Williams, 2021).

Biz Falls, the focus of this study site, is a small waterfall where Cascade River begins at the base of the waterfall. This site is composed of a small waterfall that sinks into a rocky streambed. This site is home to a plastic barrel used for conducting discharge method; all sampling was done upstream from this barrel. Above this point in the cave is remote, wooded area, without any direct anthropogenic use. The tour route does not run through this passage of the cave.

Chapter 4: Methodology

4.1 Overview

The purpose of this study was to examine and categorize MPs in the Lost River Groundwater Basin, Bowling Green Kentucky and Great Onyx Groundwater Basin, Mammoth Cave National Park, Kentucky. Under an approved NPS research permit, field techniques utilized collecting grab samples and discharge measurements. Laboratory procedures consisted of filtering using a Buchner funnel and vacuum flask, organic digestion step, and visual analysis of MPs. Methodology was adapted from an extensive literature review, with significant influence from Balestra and Bellopede, (2021) and Panno et al., (2019), as studies specifically dealt with karst regions.

When designing this study determining site selection was a key step. The goal of this study was to examine microplastic concentrations in karst groundwater with varying land use. Lost River Rise was selected because it is the final discharge point for the Lost River Groundwater Basin. Lost River Rise represents roughly 152 km^2 of urban and agricultural landscape runoff (Jackson 2017). Since it represents such a large area of runoff and is heavily impacted by anthropogenic use, Lost River Rise is likely impacted by microplastic contamination. Great Onyx Groundwater Basin was selected because it is inside Mammoth Cave National Park, specifically a relatively undeveloped area. Great Onyx Spring is the main discharge point of the basin, which is important because it could show the potential impact that tours and research use have on an otherwise pristine area. In addition, to MPs being deposited via precipitation into the cave system, anthropogenic use can deposit MPs as well. Biz Falls was selected for two reasons 1) in-cave it is off the tour route, upstream from Great Onyx Spring.

This means that the only way microplastics would enter this point in the cave is from research use or rainfall above the cave. 2) the land area above Biz Falls is undeveloped, remote, backcountry forest, assumed to be not impacted by any anthropogenic use. These sites represent groundwater that is heavily impacted by anthropogenic use and groundwater that should not be relatively impacted by anthropogenic use.

4.2 Sample Collection

4.2.1 Grab Sampling

Grab sampling was conducted monthly from September 2023 through February 2024, with an additional sample collected representing a precipitation event. For each sampling event, the same clothes were worn almost each time and recorded to examine any potential cross-contamination. Monthly sampling events did not occur on the same day of every month but were selected based on convenience. Grab sampling was conducted at each site on the same day for all sites to ensure similar atmospheric conditions. One liter (L) glass bottles were pre-rinsed before being taken into the field using acetone. The acetone was originally in a plastic bottle before being transferred to a glass jar for storage. Before collecting samples, the glass bottles were triple rinsed in situ with sample water. The bottles were then filled and capped underwater with no air space, when conditions permitted, to prevent atmospheric contamination. Two liters in total were collected at each site. At Biz Falls a plastic barrel is used for measuring discharge so to ensure no risk of contamination from the barrel, samples were collected upstream from a small waterfall resulting in the inability to cap the samples underwater. Samples were transported back to the laboratory and were kept out of sunlight until analysis. A field blank was conducted at Lost River Rise at every sampling event, using distilled water created in the laboratory (distilled water filtration apparatus was all glass and metal) to assess for any potential contamination. Assuming safe, accessible flow conditions, samples were collected at the same spot every month. General water quality measures including pH, water temperature (°C), and specific conductivity (SpC) (µS/cm) were also collected during grab sampling using a YSI Pro 1030 handheld meter. The YSI Pro 1030 was calibrated prior to each sampling for pH and SpC using 4.01, 7.00, and 10.00 buffer solutions and 1,000 µS/cm standard for SpC in accordance with the manufacturer's manual (YSI, 2009).

4.3 Laboratory Process

All surfaces and materials were rinsed with distilled water prior to use. Before working with any samples, a QAQC air blank, a 47 mm Whatman gridded filter was placed into an aluminum weigh dish, to record any potential atmospheric contamination. Total processing time and individual sample processing time were recorded, to note exposure time per sample. Type of clothing worn during laboratory process were also recorded.

A vacuum filtration process (Figure 17) was utilized to separate MPs from the sample water collected. The filtration apparatus was set up consisting of a filter flask, a filter funnel, 47 mm Whatman gridded filter, and a vacuum pump. A rubber stopper is inserted into a 2,000 mL flask, before the Buchner funnel is placed into the hole in the center of the rubber stopper. A 250 mL glass funnel is clamped to the Buchner funnel, which can be removed easily to change the 47 mm Whatman gridded filter that sits on top of the Buchner Funnel. Rubber tubing connected to the vacuum pump is then connected to the side nozzle of the flask (Figure 18). The rubber stopper and tubing were below the filter paper and did not come into contact with sample water. A petri dish was constantly covering the funnel when not actively pouring a sample to reduce possible atmospheric contamination.

Each sample bottle was given a unique lab name to correspond to the filter(s) associated with it. Samples were inverted several times before filtration to equally distribute/suspend any potential MPs throughout the sample. To ensure a proper seal, a small amount of sample water was placed into the funnel and the vacuum pump started. Once the seal was established, a known, recorded amount was poured into the funnel, repeating this step until all the sample had been filtered. For turbid or slow-filtering samples, samples were to be split across multiple filters. On occasions where there was no change observed in sample volume after 1-2 hours, filtration was stopped, and filters were swapped according to standard practices used in membrane filtration for concentrations of bacteria (Source Molecular Corporation, 2019). Equipment was triple rinsed between samples with 50 ml of distilled water. A lab blank, totaling 2L of distilled water, was processed every filtration day to account for any potential contamination.

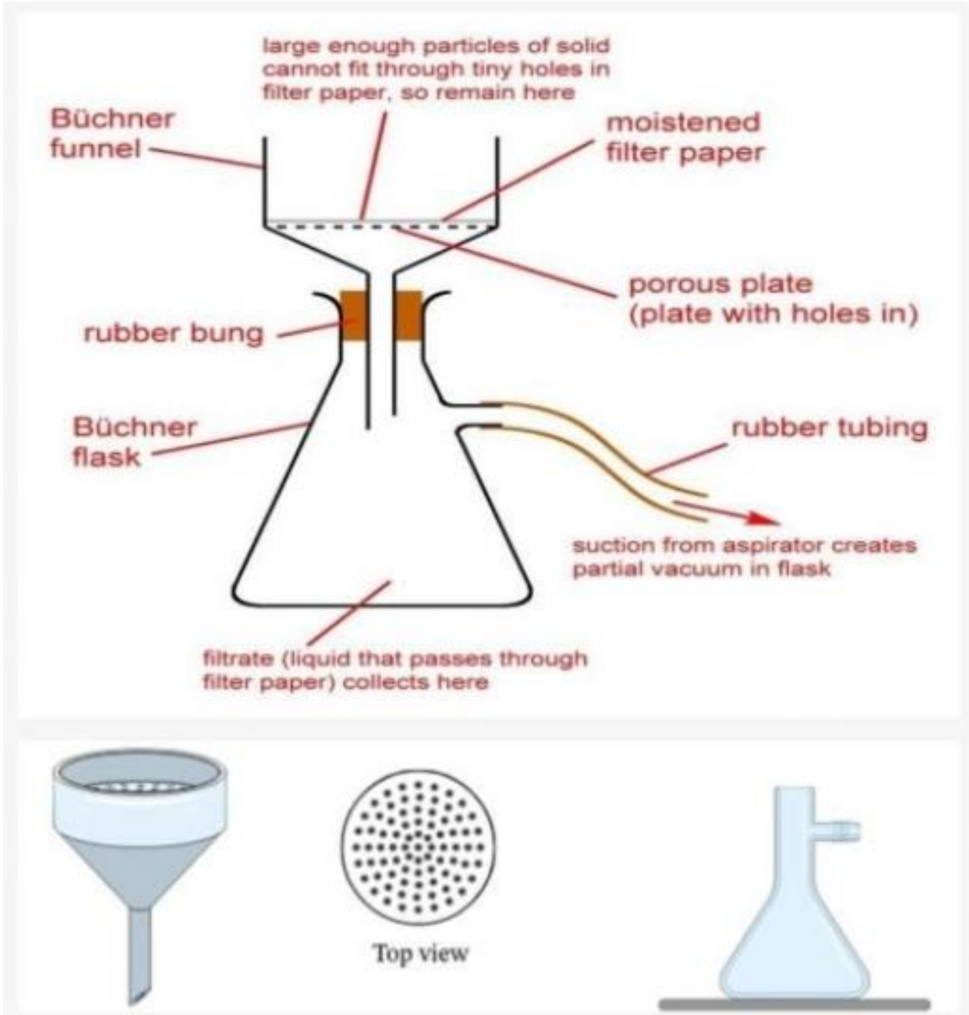

Figure 17: Vacuum filtration process (Source: Hawach Scientific, n.d.).

Figure 18: Laboratory filtration set up (Source: Author).

After filtration was complete, the funnel was unclamped and, placed onto a paper towel, before moving the filter paper into an aluminum dish. This step was completed as fast as possible, without tearing the filter paper. The aluminum dish was immediately covered with an aluminum cover and labeled with the corresponding lab identification. Samples were placed into the oven to dry at 50°C for 40 minutes. This drying time resulted in filters being able to properly dry but did not result in the filter papers curling up from being in the oven too long. Once samples were dry, organic matter was removed through the application of 0.5 ml of 15%

hydrogen peroxide and left to react for 30 minutes before being dried again for 40 minutes at 50°C. A portion of samples were treated with 30% hydrogen peroxide prior to availability of 15% hydrogen peroxide. No differences were observed, however, using 30% can cause MPs to break down into smaller particles. The organic digestion step is not a required standardized step, with most studies using either 15% or 30% hydrogen peroxide. Samples were stored until visual analysis.

4.4 Laboratory Analysis

Before analysis a QA/QC air blank, as previously described, was placed on the work bench to account for any potential atmospheric contamination. Filters were examined at 45X and 100X magnification under a Nikon Eclipse E200 compound microscope (Figure 19). Filters were uncovered during examination due to the objective lens almost touching the filter due to the stage height required for focus. Visual identification was used to count MPs according to strict criteria: no cellular or organic structures present and filters had equal thickness throughout (Hidalgo-Ruz et al., 2012; Crawford and Quinn, 2016; Balestra and Bellopede, 2022). Each particle was examined under 100x to confirm MP identification. Using an iPad, a picture of each filter was taken, and the locations of MPs were recorded on the squares of their respective filter. Each MP was photographed for future reference and to double-check identification. All counted MPs were described using a standardized size and color sorting system (SCS) for categorizing MPs (Crawford and Quinn, 2016) (Figure 20). Questionable particles were subject to the hot needle test (Barrows et al., 2017), if the composition was still questionable, the piece was not considered plastic to avoid misidentification.

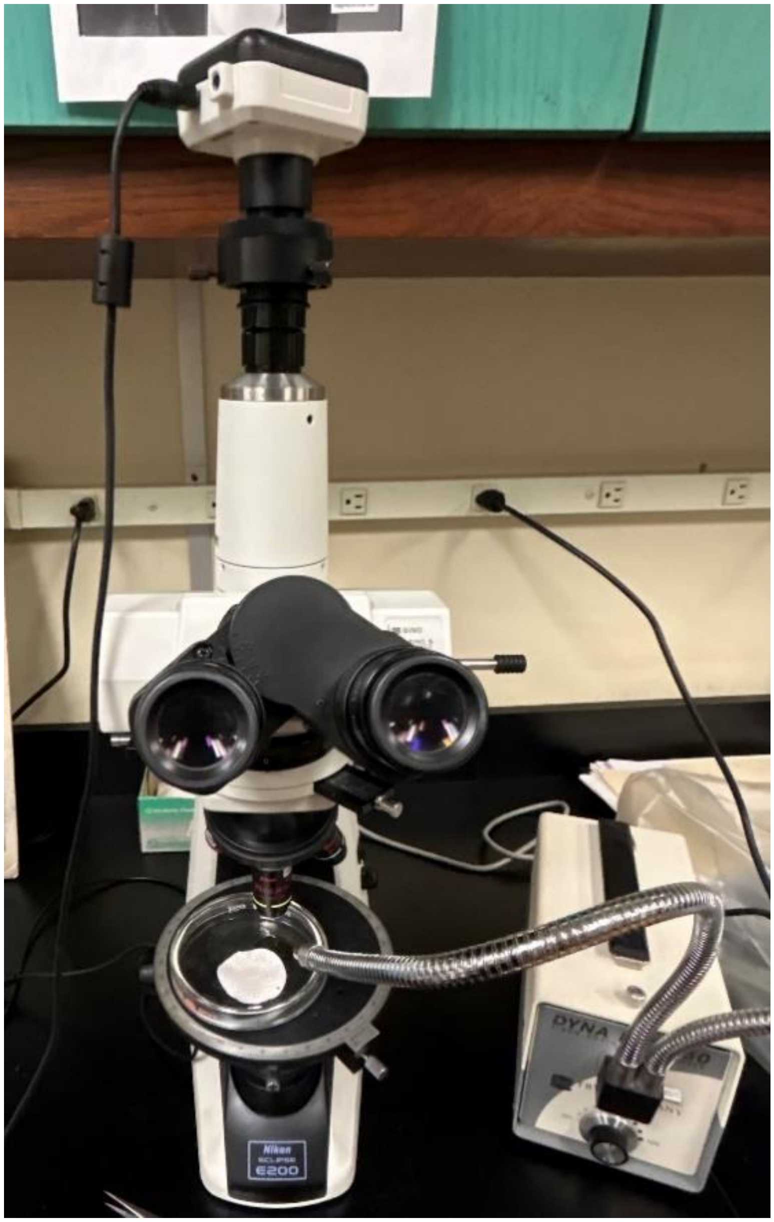

Figure 19: Microscope used for identification (Source: Author).

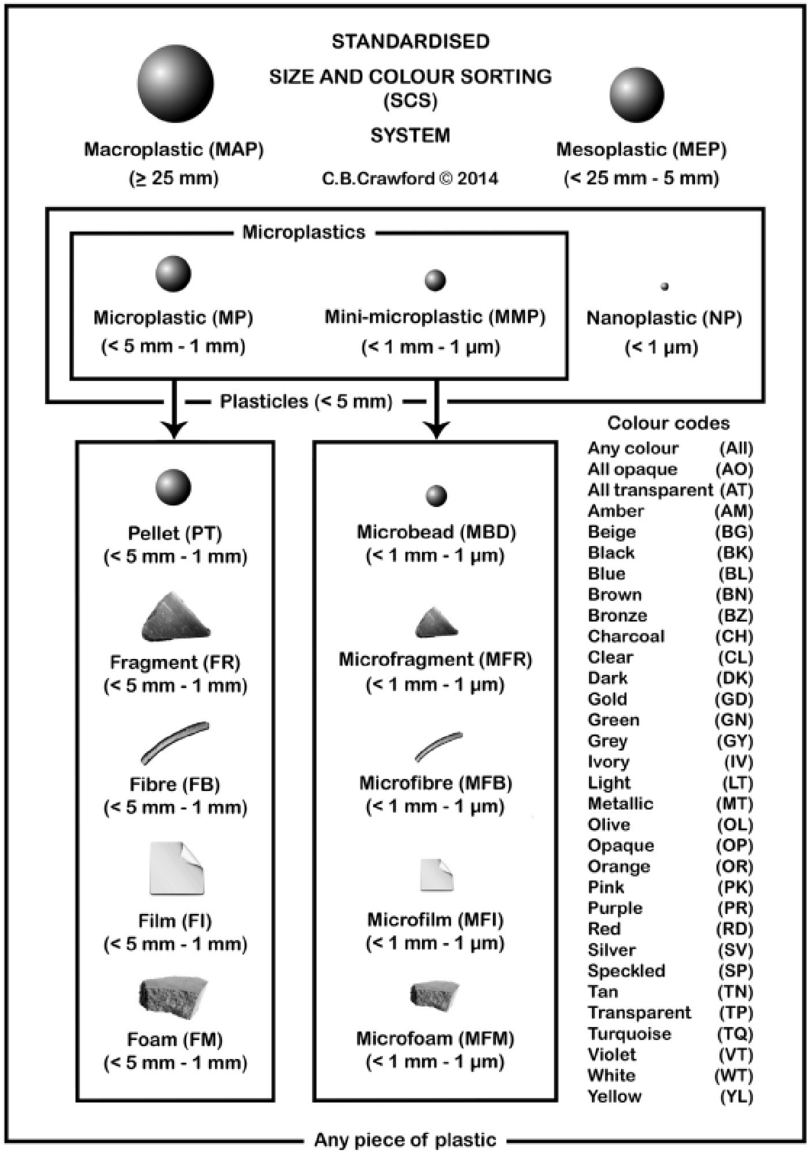

Figure 20: Standardized size and color sorting system used for MP identification (Source: Crawford and Quinn, 2016).

4.5 LRR Rain Event

On October 19, 2023, 0.58 inches of rain was recorded at Lost River Rise. An additional sampling event took place the next day with goal of capturing how rain could affect microplastic concentrations. This sampling event was done in addition to the monthly sampling event.

4.6 Field Blanks

Field blanks were conducted at Lost River Rise, to examine potential contamination during the sample processing event, by pouring one liter of distilled water into a clean jar. This process was done twice, for a total of two liters. The distilled water apparatus used to make the distilled water used in the field blanks was found to not be free of microplastics. However, since the sample water itself does not come into contact with distilled water, these microplastic values were not subtracted out from the sample. Instead, a separate graph and analysis was conducted detailing the characteristics and abundance of microplastics in the distilled water used for field blanks.

4.7 QA/QC Blank Subtraction

While collecting grab samples, a 47 mm Whatman gridded filter was placed into an aluminum weigh dish, to account for any atmospheric contamination, and covered once sampling was complete. The identified MPs from air blanks were subtracted from the corresponding sample total based on color, shape, and size.

4.8 Data Processing

All data were compiled and maintained in Excel and organized by site/date. In each site/date Excel sheet microplastics were then noted based on their size, shape, and color. Quantitative analysis to sum the counts of shape, size, color, and overall amount was performed using Excel. All tables were made using Excel. All graphs were made using Origin software.

4.9 Contamination Avoidance

Many steps were taken in an attempt to reduce contamination. One step taken was to always record clothing worn when sampling or processing samples. When possible, the same clothes were worn during every monthly sampling event. A white laboratory coat was worn when filtering samples or examining filters under a microscope. Bottles were pre-rinsed with acetone to try to eliminate microplastics that could have been in the bottle. When sampling, filtering samples, or examining filters under a microscope, a weigh tray with a filter was exposed to account for any atmospheric contamination. When filtering samples, a Petri dish was placed over the funnel to prevent atmospheric exposure. Filters were kept covered until being placed under a microscope. Due to the stage height of the microscope, filters could not be covered while using 100x. A filter to account for atmospheric contamination was left to capture atmospheric contamination. The time of atmospheric exposure per filter was recorded. Of all filters analyzed, on average, the atmospheric exposure time per filter resulted in less than one particle per hour. Therefore, this value was not subtracted from samples and was deemed to be insignificant. Any time a sample was not being processed or examined, it was immediately covered and stored in a drawer.

Chapter 5: Results

5.1 Overview

Microplastics were detected at all sites, during every sampling event. In total LRR had a total of 278 MPs detected, while GO Spring and Biz Falls had a total of 286 and 260 MPs, respectively. Shapes identified included: fibers (Figure 21), fragments (Figure 22), films (Figure 23), and pellets (Figure 24). Across all sites the most prominent shape seen were fibers. Lost River Rise had a total of 238 fibers, Great Onyx Spring and Biz Falls had 261 fibers and 234 fibers, respectively. Clear and blue were the dominant colors for all sites. Clear and blue MPs accounted for 83.45% of all MPs at LRR, 84.97% at GO Spring, and 88.08% at Biz Falls. Size of MPs was split into two categories: MPs and Mini-MPs. The size classification for MPs was < 5 mm to 1 mm. The size classification for Mini-MPs was 1 mm to 1 μm. Mini-MPs (MMPs) had a higher occurrence at all sites in comparison to MPs. Lost River Rise, GO Spring, and Biz Falls had a total of 249, 256, and 241 mini-MPs, respectively.

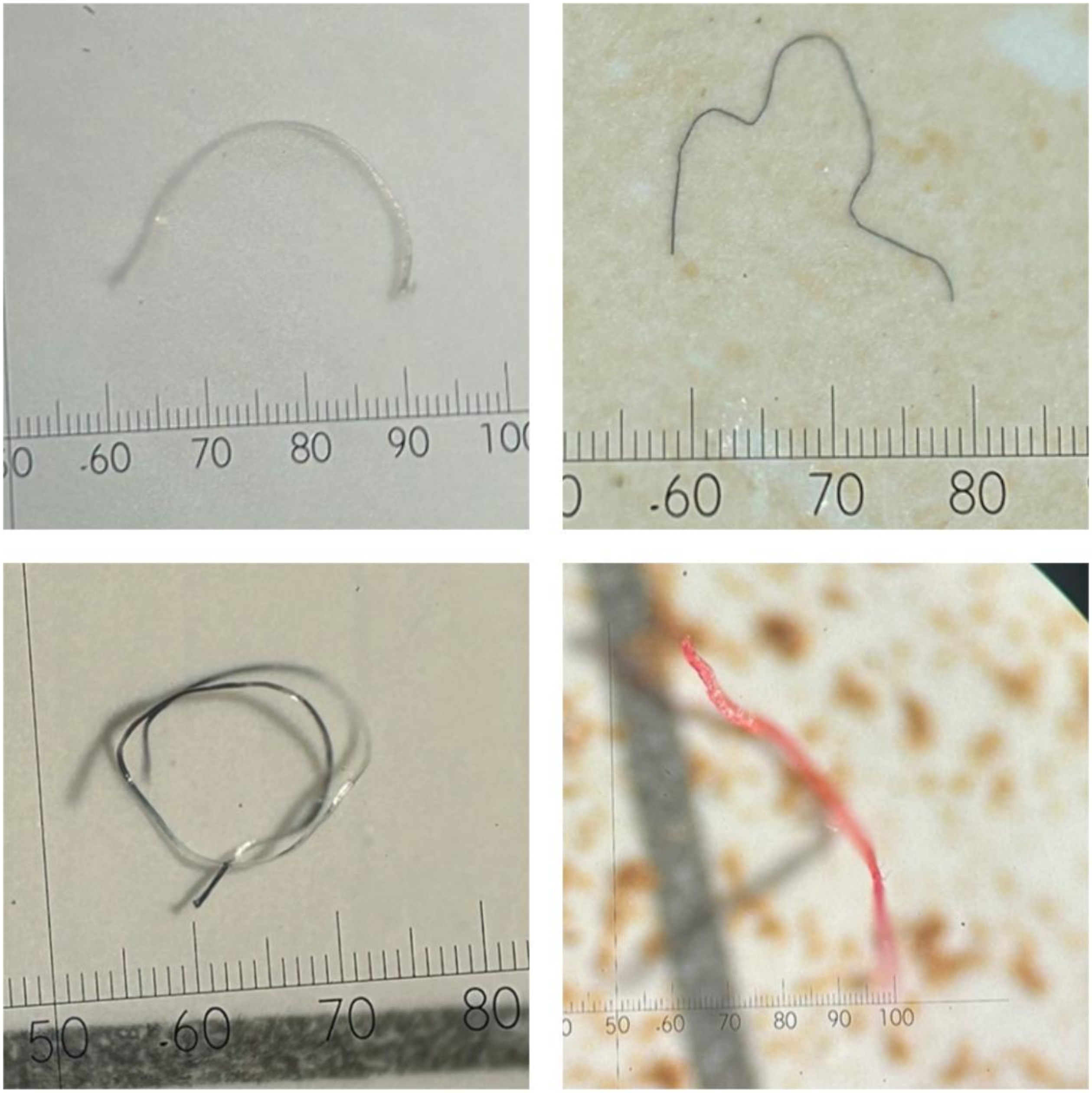

Figure 21: Examples of fibers (Source: created by Author).

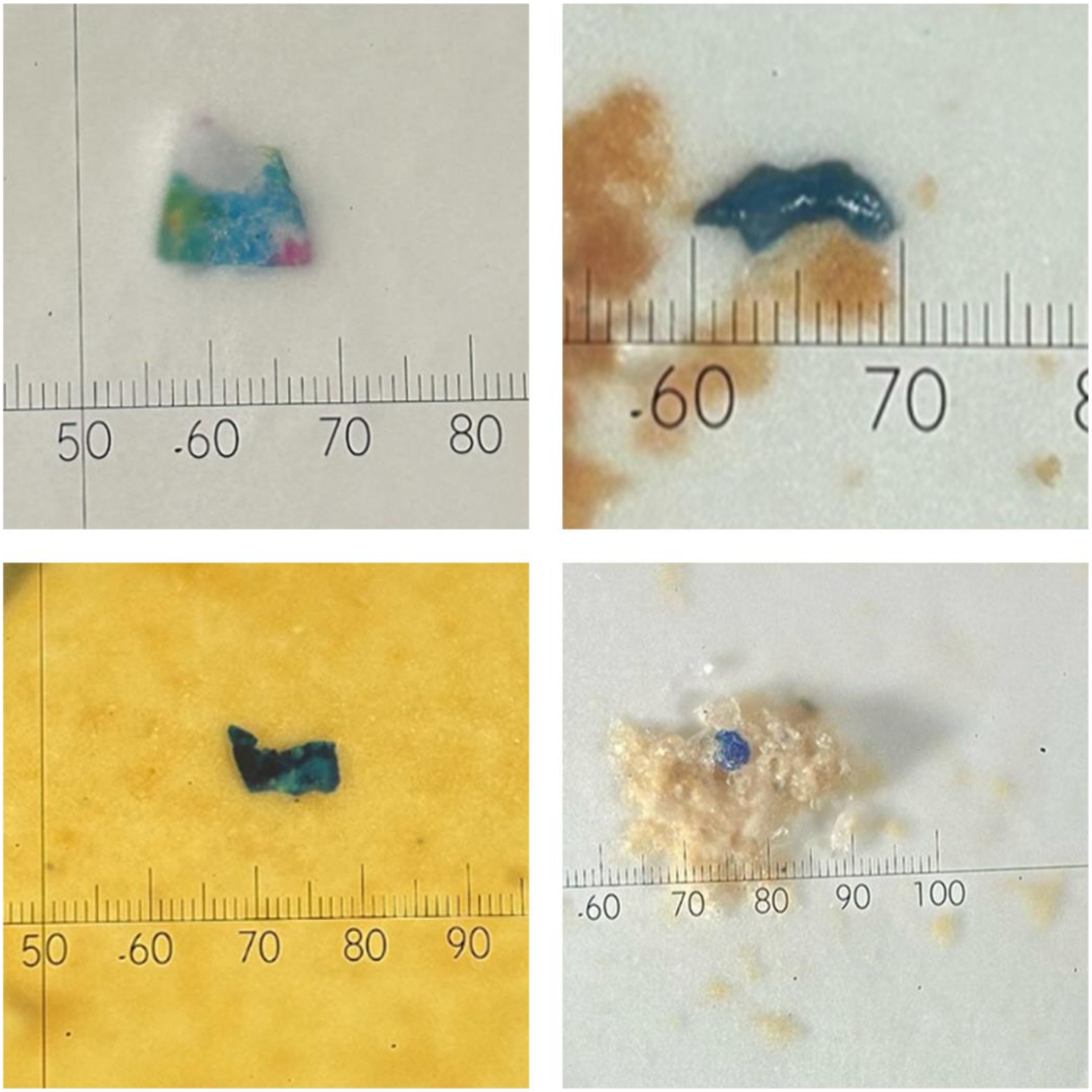

Figure 22: Examples of fragments (Source: created by Author).

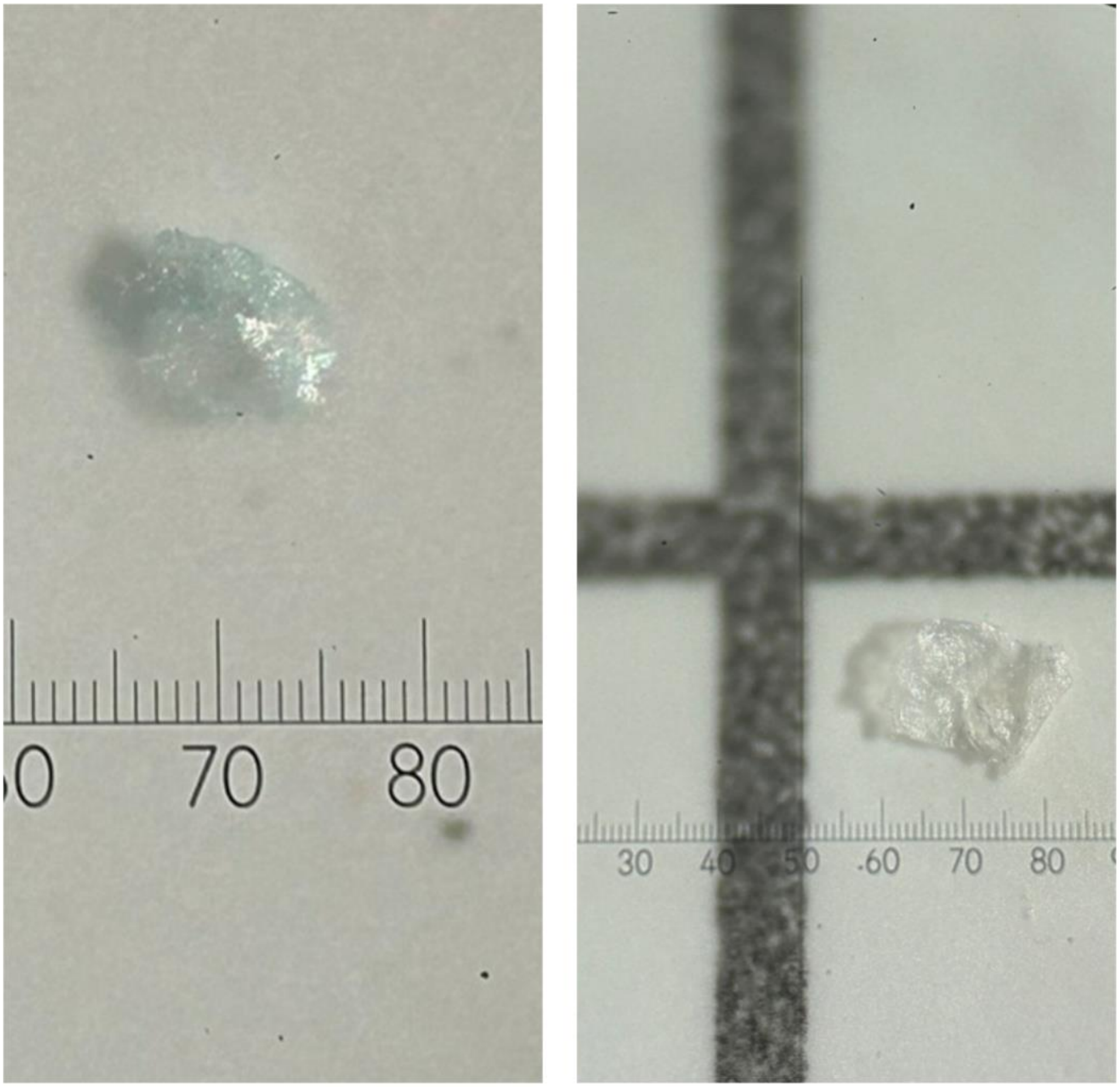

Figure 23: Examples of films (Source: created by Author).

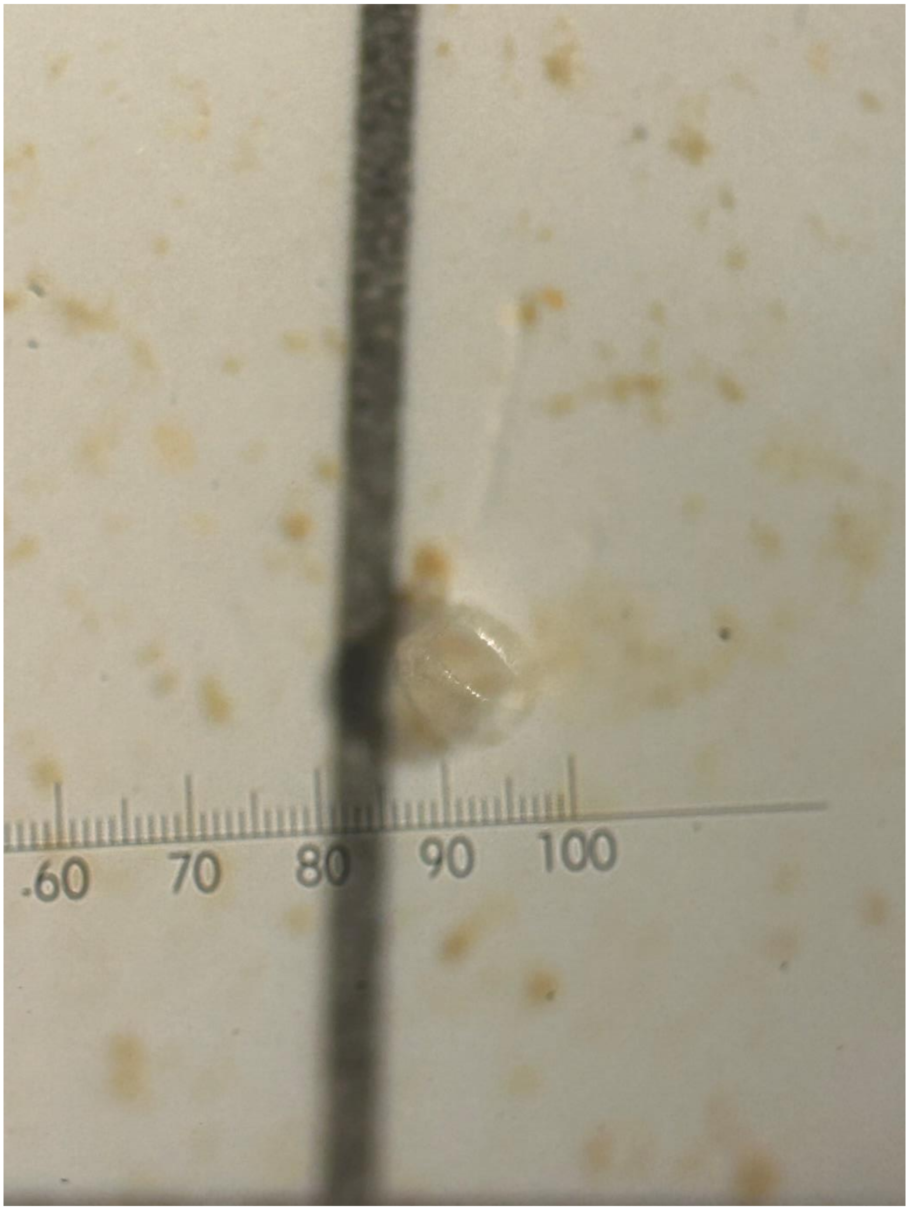

Figure 24: Examples of pellets (Source: created by Author).

5.2 *Lost River Rise MP*

MPs detected for the LRR are provided in Figure 25 and Tables 3-6. Shapes identified included fibers (FB), films (FI), fragments (FR), and pellets (PT). Colors identified included: clear (CL), blue (BL), pink (PK), red (RD), green (GN), grey (GY), black (BK), purple (PR), and multicolor (MC). Microplastics identified fell within the mini-MP and MP size range. Monthly differences are displayed in Figure 15 based on shape, color and size.

September had the highest number of MPs detected with 90 total particles detected. In September fibers and fragments accounted for 97.78% of MPs detected. Clear and blue particles accounted for 78.89% of MPs, followed by black and pink particles accounting for 13.33%. Mini MPs accounted for 92.22% of the sample. More specifically, out of the 80 fibers identified clear fibers accounted for 50%, followed by blue accounting for 30%. Out of the eight fragments identified, blue fragments made up 62.50% of the sample. 83 mini-MPs were identified, with 87.95% being fibers, 9.65% fragments, and 2.41% being films. Moreover, clear and blue accounted for 77.11% of mini-MPs. For the seven identified MPs, five were clear.

October had a total of 57 MPs identified. Fibers were the main shape detected during this sampling month, accounting for 91.23%. Clear and blue were the main colors identified, accounting for 87.72%. Mini MPs account for almost all MPs seen, accounting for 98.25%. Out of the 52 fibers identified 75% were clear, with the next most identified color being blue accounting for 13.46%. Out of the three fragments identified, two were blue and one was red. Out of the 52 fibers identified 51 fell within the mini-MP size range.

November had the lowest number of MPs detected with 20 particles detected. Out of the 20 particles detected, 13 were fibers, five were fragments, one was a film, and one was a pellet. Clear and blue accounted for 90% of MPs detected. 17 of the 20 particles fell into the mini-MPs size range, while three were in the MPs size range. Out of the 13 fibers, eight were clear, four were blue and one was multi-color. Out of the five fragments, four were blue. 10 of the 13 fibers fell within the mini-MP size range. For all mini-MPs, 47.06% were blue, while 41.18% were clear.

December had a total of 42 MPs identified. Out of the 42 MPs identified, 36 were fibers and 6 were fragments. Blue and clear accounted for 80.95% of all MPs, with the next most common color being multi-colored accounting for 11.90%. Out of the 42 MPs identified, 76.19% fell within the mini-MP size range and 23.81% fell within the MP size range. More specifically, out of the 36 fibers the most predominant color identified was clear, followed by blue and multi-color. For fragments identified, five out of six identified were blue. Out of the 32 MMP identified 26 were fibers and six were fragments. The most identified color in relation to mini-MPs was clear followed by blue. The 10 MPs that fell into the MP size range were all fibers. The most predominant color in relation to the MP size range was clear, then multi-color and blue.

January had a total of 32 MPs identified. Fibers made up 24 of the 32 identified MPs, while fragments made up the remaining eight. Clear was the leading color accounting for 46.88%, followed by blue (34.38%), green (6.25%), black (6.25%), grey (3.13%), and multi-color (3.13%). Mini-MPs were the predominant size range, identified 31 times, while the MP size range was identified once. Of the fibers identified, 15 were clear, five were blue, two were black, one was multi-colored, and one was grey. For the fragments identified six were blue and 2 were green. For the MMP size range, 23 identified MMPs were fibers, while eight were fragments. The one MP identified was a fiber. The predominant color in the MMP size range was clear (48.39%), followed by blue (32.26), green (6.45%), black (6.45%), multi-color (3.23%), grey (3.23). The one MP was blue.

February had a total of 37 MPs identified, 33 of which were fibers and four were fragments. The most frequent color identified was clear (67.57%), followed by blue (21.62%), multi-color (5.41%), black (2.70%), and purple (2.70%). Particles falling into the mini-MPs size range were identified more than the MP size range, with 30 MMPs being identified and 7 MPs. Out of the 33 fibers identified, 25 were clear, five were blue, one was multi-colored, one was black, and one was purple. For the 4 four fragments identified, three were blue and one was multi-colored. Among the 30 MMPs identified, 26 were fibers and four were fragments. All 7 MPs identified were fibers. The predominant color for particles falling within the MMP size range were clear (66.67%), blue (20%), multi-color (6.67%), black (3.33%), purple (3.33%). The most frequent color for MPs was clear accounting for 71.43%, followed by blue accounting for 28.57%.

In total, LRR had a total of 278 MPs identified, 238 being fibers, 34 being fragments, four being films, and two being pellets. Clear was the most prominent color accounting for 56.47% of MPs identified, followed by blue (26.98%), multi-color (5.76%), black (3.96%), pink (2.16%), red (1.80%), green (1.80%), purple (0.72%), and grey (0.36%). Mini-MPs were the predominant size range accounting for 89.57%, while MP accounted for 10.43%. Out of the 238 fibers identified, 151 were clear, 50 were blue, 14 were multi-colored, 11 were black, six were pink, four were red, one was grey, and one was pink. Out of the 34 fragments identified, 25 were blue, five were green, two were multi-colored, one was purple, and one was red. All four films identified were clear. Both pellets identified were clear. Out of the 249 mini-MPs observed, 209 were fibers, 34 were fragments, four were films, and two were pellets. Out of the 29 MPs identified, all 29 were fibers. The most dominant color in the MMP size range was clear (54.62%), followed by blue (27.71%), multi-color (5.62%), black (4.42%), pink (2.41%), red (2.01%), green (2.01%), purple (0.80%), and grey (0.40%). The most frequent color identified in the MP size range was clear (68.97%), followed by blue (20.69%), then multi-colored (10.34%).

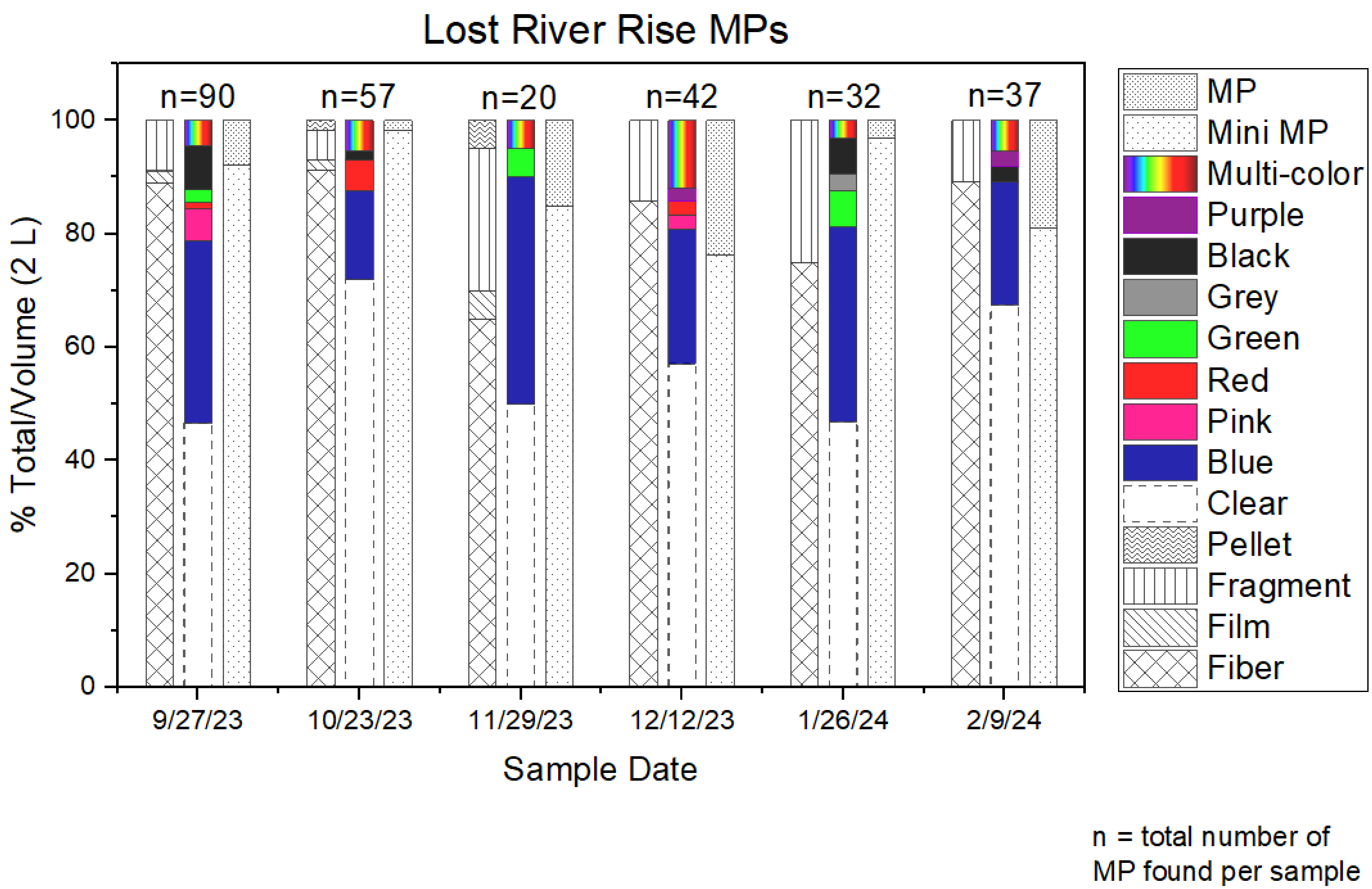

Figure 25: Lost River Rise monthly MPs differences grouped by shape, color, and size (Source: created by Author).

Table 3: Total MP Results from Lost River Rise. All results are per two liters (Source: Created by Author).

Site/Date	Fiber	Film	Fragment	Pellet	Clear	Blue	Pink	Red	Green	Grey	Black	Purple	Multi-color	Mini MP	MP	Total
LRR 9/27/23	80	2	8	0	42	29	5	1	2	0	7	0	4	83	7	90
LRR 9/27/23 %	88.89	2.22	8.89	0.00	46.67	32.22	5.56	1.11	2.22	0.00	7.78	0.00	4.44	92.22	7.78	
LRR 10/23/23	52	1	3	1	41	9	0	3	0	0	1	0	3	56	1	57
LRR 10/23/23 %	91.23	1.75	5.26	1.75	71.93	15.79	0.00	5.26	0.00	0.00	1.75	0.00	5.26	98.25	1.75	
LRR 11/29/23	13	1	5	1	10	8	0	0	1	0	0	0	1	17	3	20
LRR 11/29/23 %	65.00	5.00	25.00	5.00	50.00	40.00	0.00	0.00	5.00	0.00	0.00	0.00	5.00	85.00	15.00	
LRR 12/12/23	36	0	6	0	24	10	1	1	0	0	0	1	5	32	10	42
LRR 12/12/23 %	85.71	0.00	14.29	0.00	57.14	23.81	2.38	2.38	0.00	0.00	0.00	2.38	11.90	76.19	23.81	
LRR 1/26/24	24	0	8	0	15	11	0	0	2	1	2	0	1	31	1	32
LRR 1/26/24 %	75.00	0.00	25.00	0.00	46.88	34.38	0.00	0.00	6.25	3.13	6.25	0.00	3.13	96.88	3.13	
LRR 2/9/24	33	0	4	0	25	8	0	0	0	0	1	1	2	30	7	37
LRR 2/9/24 %	89.19	0.00	10.81	0.00	67.57	21.62	0.00	0.00	0.00	0.00	2.70	2.70	5.41	81.08	18.92	

Table 4: Breakdown of color and shape for Lost River Rise. All results are per two liters (Source: Created by Author).

Site/Date	CL FB	MC FB	BL FB	BK FB	PK FB	RD FB	GY FB	PR FB	BL FR	MC FR	RD FR	GN FR	PR FR	CL FI	CL PT	Total
LRR 9/27/23	40	3	24	7	5	1	0	0	5	1	0	2	0	2	0	90
LRR 9/27/23 %	50	3.75	30	8.75	6.25	1.25	0	0	62.50	12.50	0.00	25.00	0.00	100	0	
LRR 10/23/23	39	3	7	1	0	2	0	0	2	0	1	0	0	1	1	57
LRR 10/23/23 %	75.00	5.77	13.46	1.92	0.00	3.85	0.00	0.00	66.67	0.00	33.33	0.00	0.00	100.00	100.00	
LRR 11/29/23	8	1	4	0	0	0	0	0	4	0	0	1	0	1	1	20
LRR 11/29/23 %	61.54	7.69	30.77	0.00	0.00	0.00	0.00	0.00	80.00	0.00	0.00	20.00	0.00	100.00	100.00	
LRR 12/12/23	24	5	5	0	1	1	0	0	5	0	0	0	1	0	0	42
LRR 12/12/23 %	66.67	13.89	13.89	0.00	2.78	2.78	0.00	0.00	83.33	0.00	0.00	0.00	16.67	0.00	0	
LRR 1/26/24	15	1	5	2	0	0	1	0	6	0	0	2	0	0	0	32
LRR 1/26/24 %	62.50	4.17	20.83	8.33	0.00	0.00	4.17	0.00	75.00	0.00	0.00	25.00	0.00	0.00	0	
LRR 2/9/24	25	1	5	1	0	0	0	1	3	1	0	0	0	0	0	37
LRR 2/9/24 %	75.76	3.03	15.15	3.03	0.00	0.00	0.00	3.03	75.00	25.00	0.00	0.00	0.00	0	0	

Table 5: Breakdown of shape and size for Lost River Rise. All results are per two liters (Source: Created by Author).

Site/Date	FB MMP	FR MMP	FI MMP	PT MMP	FB MP	Total
LRR 9/27/23	73	8	2	0	7	90
LRR 9/27/23 %	87.95	9.64	2.41	0.00	100.00	
LRR 10/23/23	51	3	1	1	1	57
LRR 10/23/23 %	91.07	5.36	1.79	1.79	100.00	
LRR 11/29/23	10	5	1	1	3	20
LRR 11/29/23 %	58.82	29.41	5.88	5.88	100.00	
LRR 12/12/23	26	6	0	0	10	42
LRR 12/12/23 %	81.25	18.75	0.00	0.00	100.00	
LRR 1/26/24	23	8	0	0	1	32
LRR 1/26/24 %	74.19	25.81	0.00	0.00	100.00	
LRR 2/9/24	26	4	0	0	7	37
LRR 2/9/24 %	86.67	13.33	0.00	0.00	100.00	

Table 6: Breakdown of color and size for Lost River Rise. All results are per two liters (Source: Created by Author).

Site/Date	CL MMP	MC MMP	BL MMP	PK MMP	RD MMP	GN MMP	BK MMP	GY MMP	PR MMP	CL MP	MC MP	BL MP	Total
LRR 9/27/23	36	4	28	5	1	2	7	0	0	5	1	1	90
LRR 9/27/23 %	43.37	4.82	33.73	6.02	1.20	2.41	8.43	0.00	0.00	71.43	14.29	14.29	
LRR 10/23/23	40	3	9	0	3	0	1	0	0	1	0	0	57
LRR 10/23/23 %	71.43	5.36	16.07	0.00	5.36	0.00	1.79	0.00	0.00	100.00	0.00	0.00	
LRR 11/29/23	7	1	8	0	0	1	0	0	0	3	0	0	20
LRR 11/29/23 %	41.18	5.88	47.06	0.00	0.00	5.88	0.00	0.00	0.00	100.00	0.00	0.00	
LRR 12/12/23	18	3	8	1	1	0	0	0	1	6	2	2	42
LRR 12/12/23 %	56.25	9.38	25.00	3.13	3.13	0.00	0.00	0.00	3.13	60.00	20.00	20.00	
LRR 1/26/24	15	1	10	0	0	2	2	1	0	0	0	1	32
LRR 1/26/24 %	48.39	3.23	32.26	0.00	0.00	6.45	6.45	3.23	0.00	0.00	0.00	100.00	
LRR 2/9/24	20	2	6	0	0	0	1	0	1	5	0	2	37
LRR 2/9/24 %	66.67	6.67	20.00	0.00	0.00	0.00	3.33	0.00	3.33	71.43	0.00	28.57	

5.2.1 Lost River Rise Rain Event

MPs detected for the LRR rain event are provided in Tables 7-10. Shapes identified included: fibers, films, and fragments. Colors identified included: clear, blue, red, green, grey, black, and multicolor. Microplastics identified fell within the mini-MP and MP size range. MP characteristics are displayed in Figure 26 grouped by shape, color and size. In total 53 particles were identified, with 42 being fibers, five being films, and six being fragments. The most frequent color identified was clear, followed by black, green, multi-color, grey, blue, and red. Out of the 53 particles identified. 49 fell into the mini-MP size range, and four fell within the MP size range. Of the fibers identified 34 were clear, five were black, two were multi-color, and one was red. Out of the 6 fragments identified, 4 were green, one was grey, and one was blue. All five films identified were clear. Of the mini-MPs identified 39 were fibers, six were fragments, and four were films. All particles falling within the MP size ranger were fibers. The most common color of mini-MP sized particles was clear accounting for 75.51%, followed by green (8.16%), black (8.16%), multi-color (4.08%), blue (2.04%), and grey (2.04%). The most identified color for MP sized particles was clear accounting for 50%, followed by red (25%) and black (25%).

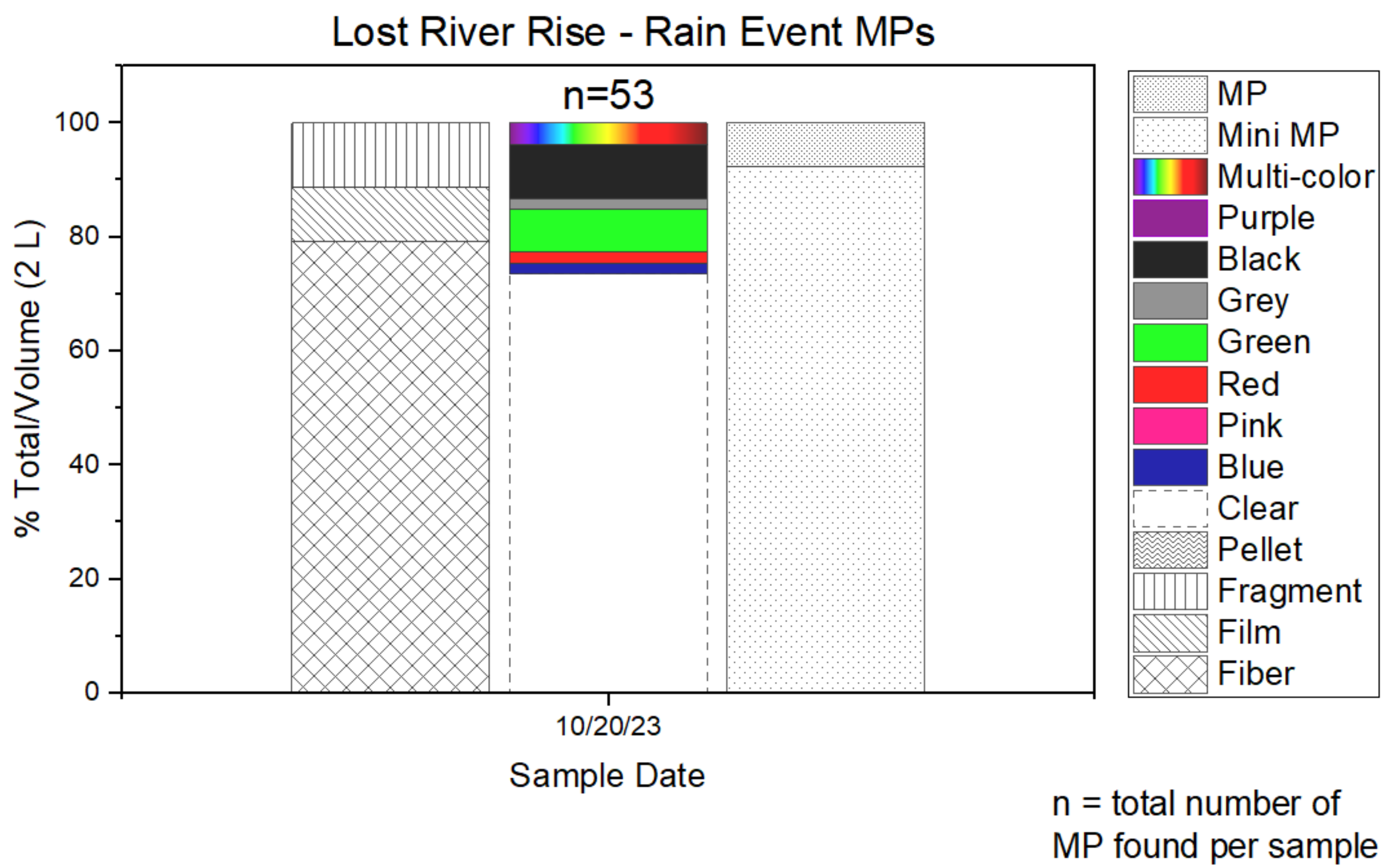

Figure 26: Lost River Rise rain event MPs characteristics differences grouped by shape, color, and size (Source: created by author).

Table 7: Total MP Results from Lost River Rise Rain Event. All results are per two liters (Source: Created by Author).

Site/Date	Fiber	Film	Fragment	Clear	Blue	Red	Green	Grey	Black	Multi-color	Mini MP	MP	Total
LRR 10/20/24	42	5	6	39	1	1	4	1	5	2	49	4	53
LRR 10/20 %	79.25	9.43	11.32	73.58	1.89	1.89	7.55	1.89	9.43	3.77	92.45	7.55	

Table 8: Breakdown of color and shape for Lost River Rise Rain Event. All results are per two liters (Source: Created by Author).

Site/Date	CL FB	MC FB	BK FB	RD FB	BL FR	GN FR	GY FR	CL FI	Total
LRR 10/20/24	34	2	5	1	1	4	1	5	53
LRR 10/20 %	80.95	4.76	11.90	2.38	16.67	66.67	16.67	100.00	

Table 9: Breakdown of shape and size for Lost River Rise Rain Event. All results are per two liters (Source: Created by Author).

Site/Date	FB MMP	FR MMP	FI MMP	FB MP	Total
LRR 10/20/24	39	6	4	4	53
LRR 10/20 %	79.59	12.24	8.16	100.00	

Table 10: Breakdown of color and size for Lost River Rise Rain Event. All results are per two liters (Source: Created by Author).

Site/Date	CL MMP	MC MMP	BL MMP	GN MMP	BK MMP	GY MMP	CL MP	RD MP	BK MP	Total
LRR 10/20/24	37	2	1	4	4	1	2	1	1	53
LRR 10/20 %	75.51	4.08	2.04	8.16	8.16	2.04	50.00	25.00	25.00	

5.3 Great Onyx Spring MP

MPs detected for GO Spring are provided in Tables 11-14. Shapes identified included: fibers, films, fragments, and pellets. Colors identified: clear, blue, pink, red, green, grey, black, orange, and multi-color. MPs identified fell within the MMP and MP size range. Monthly differences are displayed in Figure 27 based on shape, color, and size.

September had a total of 48 MPs, including 44 fibers, three fragments, and one pellet. Colors identified blue, red, grey, and black. Of the 48 MPs identified, 44 fell within the MMP size range, and four fell within the MP size range. Out of the 44 fibers identified, the most predominant color identified was clear accounting for 72.72%, followed by blue (15.91%), black (4.55%), red (4.55%), grey (2.27%). Three fibers were identified, with two being blue, and one being clear. The one pellet seen was clear. The predominant shapes for the mini-MP size range were fibers (90.91%), fragments (6.82%), pellets (2.27%). All particles in the MP size range were fibers. The most frequent color identified in the MMP size range was clear (70.45%), blue (20.45%), black (4.55%), grey (2.27%), red (2.27%). The highest frequency of color in the MMP size range was clear (75%), followed by red (25%).

October had a total of 54 MP detected, of these, 47 were fibers, three fragments, and four films. Colors observed were clear, blue, green, black, orange, and multi-color. Of the 54 MPs detected, 49 fell within the mini-MP size range and the remaining five fell within the MP size range. Moreover, the most frequent fiber color observed was clear (61.7%), followed by green (14.89%), blue (12.77%), multi-color (6.38%), black (2.13%), and orange (2.13%). Green accounted for two fragments identified, with the other being blue. All four films identified were clear. Out of the 49 MMPs identified, fibers comprised of 85.71%, fragments representing

6.12%, and films representing 8.16%. All five MPs identified were fibers. The most frequent color seen in the MMP size range was clear representing 63.27%, followed by green (18.37), blue (12.24%), multi-color (2.04%), black (2.04%), and orange (2.04%). The most frequent MP color was clear and multi-color, both representing 40%, followed by blue representing 20%.

November had a total of 52 MPs detected, 49 of which were fibers, and three were fragments. Colors identified included clear, blue, grey, and black. 49 particles fell within the mini-MP size range and three fell within the MP size range. The most common color identified for fibers was clear (83.67%), followed by blue (12.24%), back (2.04%), and grey (2.04%). There were two blue and one clear fragment identified. 46 of the 49 fibers fell within the MMP size range, as well as three fibers. All three particles within the MP size range were fibers. The predominant color identified in the mini-MP size range was clear (81.63%), then blue (14.29%), grey (2.04%), and black (2.04%). The most common color identified in the MP size range was clear (66.67), followed by blue (33.33).

December had a total of 20 MPs identified, 18 being fibers and two being fragments. Colors identified included clear, blue, and multi-color. All particles identified were in the mini-MP size range. Of the 18 fibers observed 14 were clear, 3 blue, and one multi-color. Both fragments were blue. As previously stated, all fibers and fragments identified were in the mini-MP size range.

January had a total of 58 MPs identified, 49 being fibers and nine being fragments. Colors identified included clear, blue, pink, red, black, and multi-color. Of the 58 MPs identified, 46 fell within the MMP size range and 12 within the MP size range. The most frequently identified color in relation to fibers was clear (48.98%), followed by blue (30.61%), multi-color (8.16%), pink (6.12%), black (4.08%), and red (2.04%). The most predominant color observed in relation to fragments was blue (88.89%), followed by red (11.11%). Fibers represented 82.61% of particles in the MMP size range, while fragments represented 17.39%. All particles in the MP size range were fibers. The predominant color associated with particles in the MMP size range was clear (45.65%), followed by blue (36.96%), multi-color (6.52%), pink (4.35%), red (4.35%), and black (2.17%). Blue was the predominant color seen associated with particles in the MP size range representing 50%, followed by clear (33.33%), pink (8.33%), and black (8.33%).

February had a total of 57 particles identified, all of which were fibers. Colors identified included clear, blue, pink, black, and multi-color. Out of the 57 particles identified, 51 fell within the MMP size range, and six fell within the MP size range. Clear was the most frequent color identified representing 64.91%, followed by blue (17.54%), pink (12.28%), multi-color (3.51%), and black (1.75%). In relation to particles falling within the MMP size range, clear was the most frequent color representing 68.63%, followed by blue (15.69%), pink (11.76%), and multi-colored (3.92%). Clear and blue were the predominant colors seen in the MP size range, both accounting for 33.33%, followed by pink and black both representing 16.67%.

Overall, Great Onyx Spring had a total of 286 particles identified, composed of 261 fibers, four films, 20 fragments, and one pellet. Colors observed were clear, blue, pink, red, green, grey, black, orange, and multi-color. Clear was the most identified color representing 64.34%, followed by blue (20.63%), pink (3.50%), multi-color (3.50%), green (3.15%), black (2.45%), red (1.40%), grey (0.70%), and orange (0.35%). Out of the 286 particles identified, 256 fell within the MMP size range, and 30 fell within the MP size range. Of the fibers identified. clear was the most frequent color identified accounting for 67.82%, followed by blue (16.86%), pink (3.83%), multi-color (3.83%), black (2.68%), green (2.68%), red (1.15%), grey (0.77%), and orange (0.38%). Blue was the most identified color in relation to fragments representing

75%, followed by clear (10.0%), green (10.0%), and red (5.0%). All films and pellets identified were clear. Of the particles identified in the mini-MP size range 90.63% were fibers, 7.42% were fragments, 1.56% were films, and 0.39% were pellets. All particles identified in the MP size range were fibers. The most frequent color identified in relation to particles identified in the MMP size range were clear (67.19%), followed by blue (19.14%), green (3.52%), pink (3.13%), multi-color (2.73%), black (1.95%), red (1.17%), grey (0.78%), and orange (0.39%). The predominant color identified in relation to particles identified in the MP size range was clear (43.33%), followed by blue (33.33%), multi-color (6.67%), pink (6.67%), black (6.67%), and red (3.33%).

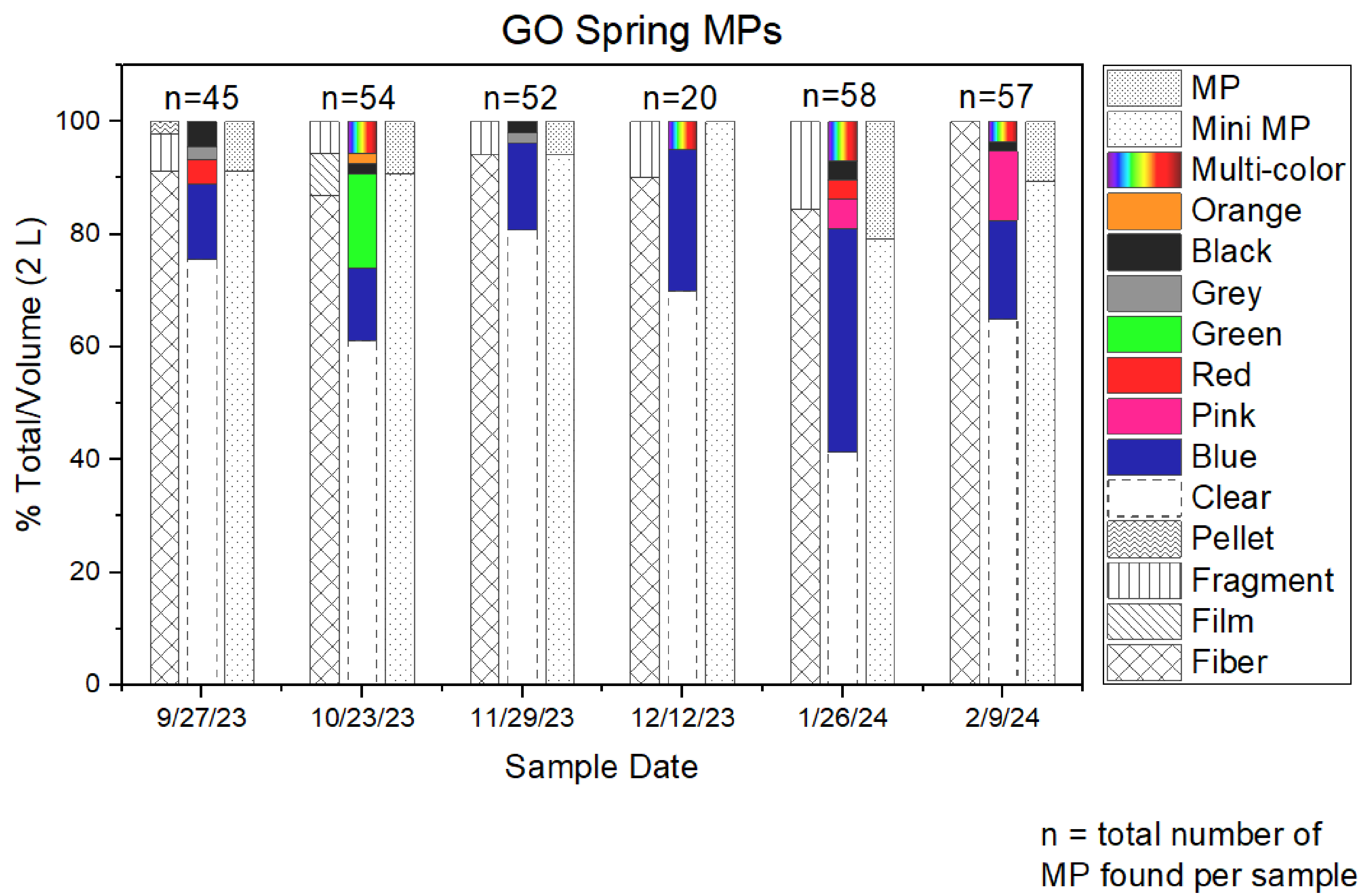

Figure 27: Great Onyx Spring MPs characteristics differences grouped by shape, color, and size (Source: created by Author).

Table 11: Total MP Results from GO Spring. All results are per two liters (Source: Created by Author).

Site/Date	Fiber	Film	Fragment	Pellet	Clear	Blue	Pink	Red	Green	Grey	Black	Orange	Multi-color	Mini MP	MP	Total
GO 9/27/2023	41	0	3	1	34	6	0	2	0	1	2	0	0	41	4	45
GO 9/27/23 %	91.11	0.00	6.67	2.22	75.56	13.33	0.00	4.44	0.00	2.22	4.44	0.00	0.00	91.11	8.89	
GO 10/23/23	47	4	3	0	33	7	0	0	9	0	1	1	3	49	5	54
GO 10/23/23 %	87.04	7.41	5.56	0.00	61.11	12.96	0.00	0.00	16.67	0.00	1.85	1.85	5.56	90.74	9.26	
GO 11/29/23	49	0	3	0	42	8	0	0	0	1	1	0	0	49	3	52
GO 11/29/23 %	94.23	0.00	5.77	0.00	80.77	15.38	0.00	0.00	0.00	1.92	1.92	0.00	0.00	94.23	5.77	
GO 12/12/23	18	0	2	0	14	5	0	0	0	0	0	0	1	20	0	20
GO 12/12/23 %	90.00	0.00	10.00	0.00	70.00	25.00	0.00	0.00	0.00	0.00	0.00	0.00	5.00	100.00	0.00	
GO 1/26/24	49	0	9	0	24	23	3	2	0	0	2	0	4	46	12	58
GO 1/26/24 %	84.48	0.00	15.52	0.00	41.38	39.66	5.17	3.45	0.00	0.00	3.45	0.00	6.90	79.31	20.69	
GO 2/9/24	57	0	0	0	37	10	7	0	0	0	1	0	2	51	6	57
GO 2/9/24 %	100.00	0.00	0.00	0.00	64.91	17.54	12.28	0.00	0.00	0.00	1.75	0.00	3.51	89.47	10.53	

Table 12: Breakdown of color and shape for GO Spring. All results are per two liters (Source: Created by Author).

Site/Date	CL FB	BL FB	BK FB	PK FB	RD FB	MC FB	GY FB	GN FB	OR FB	CL FR	BL FR	RD FR	GN FR	CL FI	PT CL	Total
GO 9/27/2023	32	4	2	0	2	0	1	0	0	1	2	0	0	0	1	45
GO 9/27/23 %	78.05	9.76	4.88	0.00	4.88	0.00	2.44	0.00	0.00	33.33	66.67	0.00	0.00	0	100.0	
GO 10/23/23	29	6	1	0	0	3	0	7	1	0	1	0	2	4	0	54
GO 10/23/23 %	61.70	12.77	2.13	0.00	0.00	6.38	0.00	14.89	2.13	0.00	33.33	0.00	66.67	100.0	0.0	
GO 11/29/23	41	6	1	0	0	0	1	0	0	1	2	0	0	0	0	52
GO 11/29/23 %	83.67	12.24	2.04	0.00	0.00	0.00	2.04	0.00	0.00	33.33	66.67	0.00	0.00	0.00	0.00	
GO 12/12/23	14	3	0	0	0	1	0	0	0	0	2	0	0	0	0	20
GO 12/12/23 %	77.78	16.67	0.00	0.00	0.00	5.56	0.00	0.00	0.00	0.00	100.00	0.00	0.00	0.00	0.00	
GO 1/26/24	24	15	2	3	1	4	0	0	0	0	8	1	0	0	0	58
GO 1/26/24 %	48.98	30.61	4.08	6.12	2.04	8.16	0.00	0.00	0.00	0.00	88.89	11.11	0.00	0.00	0.00	
GO 2/9/24	37	10	1	7	0	2	0	0	0	0	0	0	0	0	0	57
GO 2/9/24 %	64.91	17.54	1.75	12.28	0.00	3.51	0.00	0.00	0.00	0.00	0.00	0.00	0.00	0.00	0.00	

Table 13: Breakdown of shape and size for GO Spring. All results are per two liters (Source: Created by Author).

Site/Date	FB MMP	FR MMP	FI MMP	PT MMP	FB MP	Total
GO 9/27/2023	37	3	0	1	4	45
GO 9/27/23 %	90.24	7.32	0.00	2.44	100.00	
GO 10/23/23	42	3	4	0	5	54
GO 10/23/23 %	85.71	6.12	8.16	0.00	100.00	
GO 11/29/23	46	3	0	0	3	52
GO 11/29/23 %	93.88	6.12	0.00	0.00	100.00	
GO 12/12/23	18	2	0	0	0	20
GO 12/12/23 %	90.00	10.00	0.00	0.00	0.00	
GO 1/26/24	38	8	0	0	12	58
GO 1/26/24 %	82.61	17.39	0.00	0.00	100.00	
GO 2/9/24	51	0	0	0	6	57
GO 2/9/24 %	100.00	0.00	0.00	0.00	100.00	

Table 14: Breakdown of color and size for GO Spring. All results per two liters (Source: Created by Author).

Site/Date	CL MMP	MC MMP	BL MMP	GY MMP	PK MMP	RD MMP	BK MMP	GN MMP	OR MMP	CL MP	RD MP	BL MP	MC MP	PK MP	BK MP	Total
GO 9/27/2024	31	0	6	1	0	1	2	0	0	3	1	0	0	0	0	45
GO 9/27 %	75.61	0.00	14.63	2.44	0.00	2.44	4.88	0.00	0.00	75.00	25.00	0.00	0.00	0.00	0.00	
GO 10/23/24	31	1	6	0	0	0	1	9	1	2	0	1	2	0	0	54
GO 10/23 %	63.27	2.04	12.24	0.00	0.00	0.00	2.04	18.37	2.04	40.00	0.00	20.00	40.00	0.00	0.00	
GO 11/29	40	0	7	1	0	0	1	0	0	2	0	1	0	0	0	52
GO 11/29 %	81.63	0.00	14.29	2.04	0.00	0.00	2.04	0.00	0.00	66.67	0.00	33.33	0.00	0.00	0.00	
GO 12/12	14	1	5	0	0	0	0	0	0	0	0	0	0	0	0	20
GO 12/12 %	70.00	5.00	25.00	0.00	0.00	0.00	0.00	0.00	0.00	0.00	0.00	0.00	0.00	0.00	0.00	
GO 1/26	21	3	17	0	2	2	1	0	0	4	0	6	0	1	1	58
GO 1/26%	45.65	6.52	36.96	0.00	4.35	4.35	2.17	0.00	0.00	33.33	0.00	50.00	0.00	8.33	8.33	
GO 2/9	35	2	8	0	6	0	0	0	0	2	0	2	0	1	1	57
GO 2/9%	68.63	3.92	15.69	0.00	11.76	0.00	0.00	0.00	0.00	33.33	0.00	33.33	0.00	16.67	16.67	

5.4 Biz Falls MP

MPs detected for Biz Falls are provided in Tables 15-18. Shapes identified included: fibers, films, and fragments. Colors identified: clear, blue, pink, red, green, brown, grey, black, and multi-color. MPs identified fell within the mini-MP and MP size range. Monthly differences are displayed in Figure 28 based on shape, color, and size.

September had a total of 58 particles identified, 57 being fibers and one being a fragment. The most frequent color identified was clear representing 79.31% of particles, followed by blue (10.34%), black (5.17%), pink (3.45%), and brown (1.72%). Of the 58 particles identified, 56 fell into the MMP size range and two fell within the MP size range. Of the fibers identified, clear was the predominant color (80.70%), followed by blue (10.53%), black (5.26%), pink (1.75%), and brown (1.75%). The one fragment identified was pink. Out of the 56 particles that fell within the MMP size range 55 were fibers and 1 was a fragment. Both particles within the MP size range were fibers. For particles that fell within the MMP size range, the most frequent color identified was clear (78.57%), followed by blue (10.71%), black (5.36%), pink (3.57%), and brown (1.79%). Both particles within the MP size range were clear.

October had a total of 51 particles identified, composed of 48 fibers, one film, and two fragments. The most abundant color observed was clear (72.55%), followed by blue (19.61%), pink (1.96%), red (1.96%), black (1.96%), and multi-color (1.96%). Of the 51 particles identified 48 were in the MMP size range and three were in the MP size range. Of the fibers identified, clear was the predominant color representing 77.08%, followed by blue (18.75%), black (2.08%), and pink (2.08%). Blue and red were the colors of the two fragments detected. The film observed was multi-color. Of the particles within the MMP size range, 93.75% were fibers, 4.17% were fragments, and 2.08% were films. All particles that fell within the MP size range were fibers. The predominant color seen in particles within the MMP size range was clear (70.83%), followed by blue (20.83%), multi-color (2.08%), black (2.08%), pink (2.08), and red (2.08%). The three particles within the MP size range were clear.

November had a total of 34 particles identified, of which 26 were fibers and eight were fragments. The predominant color observed was clear representing 50%, followed by blue (35.29%), grey (8.82%), red (2.94%), and multi-color (2.94%). Of the 34 particles identified, 32 fell within the mini-MP size range and two fell within the MP size range. Of the fibers identified, clear (61.54%) was the most observed color, followed by blue (26.92%), grey (7.69%), and multi-color (3.85%). For fragments detected, blue (62.50%) was the most observed color, followed by clear (12.50%), red (12.50%), and grey (12.50%). Of the 32 particles within the mini-MP size range, 24 were fibers and eight were fibers. Both particles that fell within the MP size range were fibers. Of the 32 particles within the mini-MP size range, the predominant color was clear (56.25%), followed by blue (34.38%), and grey (9.38%). Blue and red represented the two particles observed within the MP size range.

December had a total of 16 particles identified, composed of 15 fibers and one fragment. Clear was the predominant color observed accounting for 87.50% of the sample, followed by red (6.25%), and black (6.25%). All particles identified fell within the MMP size range. Of the fibers identified clear was the most abundant color representing 93.33%, followed by black (6.67%). The one fragment identified was red.

January had a total of 45 particles identified, composed of 40 fibers and five fragments. Clear was the predominant color seen accounting for 66.67% of all particles, followed by blue (22.22%), pink (6.67%), green (2.22%), and black (2.22%). Of the 45 particles identified, 40 fell within the MMP size range, five fell within the MP size range. Of the fibers observed, clear was the most frequent color seen accounting for 75%, followed by blue (15%), pink (7.5%), and black (2.5%). Of the fragments identified 80% were blue and 20% were green. For the particles falling within the MMP size range 87.50% were fibers and 12.5% fragments. All particles within the MP size range were fibers. Of the particles within the mini-MP size range, the most frequent color was clear (65.0%), followed by blue (25.0%), pink (5.0%), black (2.5%), and green (2.5%). The most frequent color observed within the MP size range was clear (80.0%), followed by pink (20.0%).

February had 56 particles identified, of which 48 were fibers and 8 were fragments. The most frequent color identified was clear (64.29%), followed by blue (19.64%), multi-color (7.14), green (3.57%), black (3.57%), and grey (1.79%). Of the 56 particles identified, 49 fell within the MMP size range and 7 fell within the MP size range. Of the fibers identified, the most frequent color was clear (68.75%), blue (18.75%), black (4.17%), multi-color (4.17%), green (2.08%), and grey (2.08%). Of the fragments identified, clear was the most abundant accounting for 37.5%, followed by blue (25.0%), multi-color (25.0%), and green (12.50%). Of the particles within the MMP size range, 83.67% were fibers, while 16.33% were fragments. All the particles within the MP size range were fibers. Within the mini-MP size range, clear was the most frequent color observed accounting for 63.27%, followed by blue (20.41%), multi-color (6.12%), black (4.08%), green (4.08%), and grey (2.04%). Within the MP size range, clear was the most abundant color observed representing 71.43%, followed by blue (14.29%), and multi-color (14.29%).

Overall, 260 particles were observed, of which 234 were fibers, 25 were fragments, and one was a film. Colors identified included clear, blue, pink, red, green, brown, grey, black, and multi-color. Of all particles identified, clear was the most abundant color accounting for 69.23%, followed by blue (18.85%), black (3.08%), pink (2.31%), multi-color (2.31%), grey (1.54%), red (1.15%), green (1.15%), and brown (0.38%). Of the 260 particles identified, 92.69% fell within the MMP size range and 7.31% within the MP size range. Of all fibers identified, clear (75.21%) was the most abundant color seen, followed by blue (15.81), black (3.42%), pink (2.14%), grey (1.28%), multi-color (1.28%), green (0.43%), and brown (0.43%). Of all fragments identified, blue (48.0%), was the most abundant color observed, followed by clear (16.0%), red (12.0%), multi-color (8.0%), green (8.0%), grey (4.0%), and pink (4.0%). The one film identified was multi-color. Of all particles falling within the MMP size range, 89.21% were fibers, 10.37% were fragments, and 0.41% were films. All particles within the MP size range were fibers. Within the MMP size range the most abundant color observed was clear (69.29%), followed by blue (19.50%), black (3.32%), pink (2.07%), multi-color (1.66%), grey (1.66%), green (1.24%), red (0.83%), and brown (0.41%). Within the MP size range, the most observed color was clear (73.68%), blue (10.53%), pink (10.53%), and multi-color (5.26%).

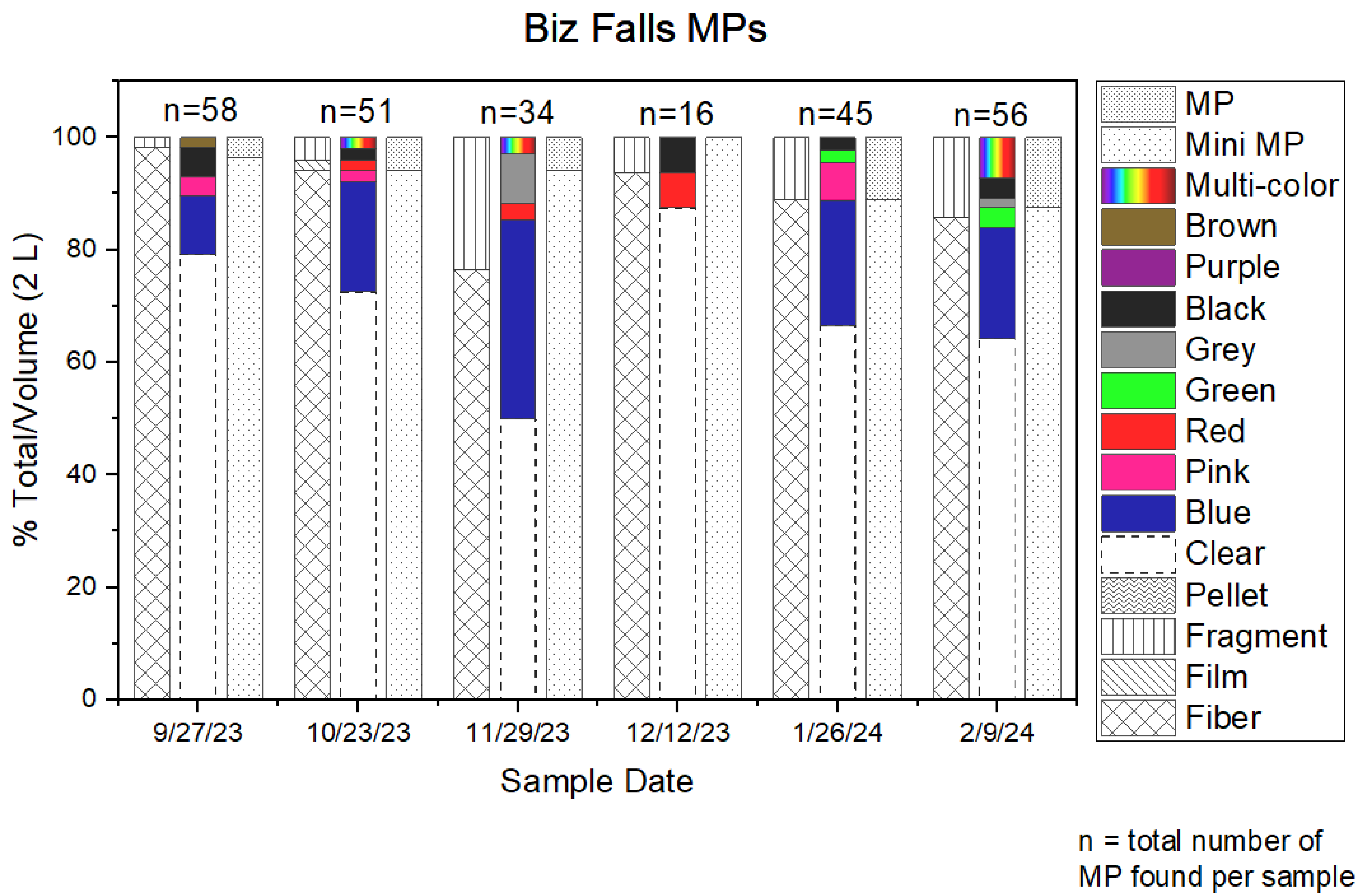

Figure 29: Biz Falls rain event MPs characteristics differences grouped by shape, color, and size (Source: created by author).

Table 15: Total MP Results from Biz Falls. All results are per two liters (Source: Created by Author).

Site/Date	Fiber	Film	Fragment	Clear	Blue	Pink	Red	Green	Brown	Grey	Black	Multi-color	Mini MP	MP	Total
BZF 9/27/2023	57	0	1	46	6	2	0	0	1	0	3	0	56	2	58
BZF 9/27/23 %	98.28	0.00	1.72	79.31	10.34	3.45	0.00	0.00	1.72	0.00	5.17	0.00	96.55	3.45	
BZF 10/23/23	48	1	2	37	10	1	1	0	0	0	1	1	48	3	51
BZF 10/23/23 %	94.12	1.96	3.92	72.55	19.61	1.96	1.96	0.00	0.00	0.00	1.96	1.96	94.12	5.88	
BZF 11/29/23	26	0	8	17	12	0	1	0	0	3	0	1	32	2	34
BZF 11/29/23 %	76.47	0.00	23.53	50.00	35.29	0.00	2.94	0.00	0.00	8.82	0.00	2.94	94.12	5.88	
BZF 12/12/23	15	0	1	14	0	0	1	0	0	0	1	0	16	0	16
BZF 12/12/23 %	93.75	0.00	6.25	87.50	0.00	0.00	6.25	0.00	0.00	0.00	6.25	0.00	100.00	0.00	
BZF 1/26/24	40	0	5	30	10	3	0	1	0	0	1	0	40	5	45
BZF 1/26/24 %	88.89	0.00	11.11	66.67	22.22	6.67	0.00	2.22	0.00	0.00	2.22	0.00	88.89	11.11	
BZF 2/9/24	48	0	8	36	11	0	0	2	0	1	2	4	49	7	56
BZF 2/9/24 %	85.71	0.00	14.29	64.29	19.64	0.00	0.00	3.57	0.00	1.79	3.57	7.14	87.50	12.50	

Table 16: Breakdown of color and shape for Biz Falls. All results are per two liters (Source: Created by Author).

Site/Date	CL FB	BL FB	BK FB	PK FB	RD FB	GN FB	GY FB	BN FB	MC FB	CL FR	BL FR	MC FR	RD FR	GN FR	GY FR	PK FR	MC FI
BZF 9/27/2023	46	6	3	1	0	0	0	1	0	0	0	0	0	0	0	1	0
BZF 9/27/23 %	80.70	10.53	5.26	1.75	0.00	0.00	0.00	1.75	0.00	0.00	0.00	0.00	0.00	0.00	0.00	100.00	0.00
BZF 10/23/23	37	9	1	1	0	0	0	0	0	0	1	0	1	0	0	0	1
BZF 10/23/23 %	77.08	18.75	2.08	2.08	0.00	0.00	0.00	0.00	0.00	0.00	50.00	0.00	50.00	0.00	0.00	0.00	100.00
BZF 11/29/23	16	7	0	0	0	0	2	0	1	1	5	0	1	0	1	0	0
BZF 11/29/23 %	61.54	26.92	0.00	0.00	0.00	0.00	7.69	0.00	3.85	12.50	62.50	0.00	12.50	0.00	12.50	0.00	0
BZF 12/12/23	14	0	1	0	0	0	0	0	0	0	0	0	1	0	0	0	0
BZF 12/12/23 %	93.33	0.00	6.67	0.00	0.00	0.00	0.00	0.00	0.00	0.00	0.00	0.00	100.00	0.00	0.00	0.00	0
BZF 1/26/24	30	6	1	3	0	0	0	0	0	0	4	0	0	1	0	0	0
BZF 1/26/24 %	75.00	15.00	2.50	7.50	0.00	0.00	0.00	0.00	0.00	0.00	80.00	0.00	0.00	20.00	0.00	0.00	0.00
BZF 2/9/24	33	9	2	0	0	1	1	0	2	3	2	2	0	1	0	0	0
BZF 2/9/24 %	68.75	18.75	4.17	0.00	0.00	2.08	2.08	0.00	4.17	37.50	25.00	25.00	0.00	12.50	0.00	0.00	0

Table 17: Breakdown of shape and size for Biz Falls. All results are per two liters (Source: Created by Author).

Site/Date	FB MMP	FR MMP	FI MMP	FB MP
BZF 9/27/2023	55	1	0	2
BZF 9/27/23 %	98.21	1.79	0.00	100.00
BZF 10/23/23	45	2	1	3
BZF 10/23/23 %	93.75	4.17	2.08	100.00
BZF 11/29/23	24	8	0	2
BZF 11/29/23 %	75.00	25.00	0.00	100.00
BZF 12/12/23	15	1	0	0
BZF 12/12/23 %	93.75	6.25	0.00	0.00
BZF 1/26/24	35	5	0	5
BZF 1/26/24 %	87.50	12.50	0.00	100.00
BZF 2/9/24	41	8	0	7
BZF 2/9/24 %	83.67	16.33	0.00	100.00

Table 18: Breakdown of color and size for Biz Falls. All results are per two liters (Source: Created by Author).

Site/Date	CL MMP	MC MMP	BL MMP	BK MMP	PK MMP	RD MMP	BN MMP	GN MMP	GY MMP	CL MP	BL MP	PK MP	MC MP
BZF 9/27/2023	44	0	6	3	2	0	1	0	0	2	0	0	0
BZF 9/27/23 %	78.57	0.00	10.71	5.36	3.57	0.00	1.79	0.00	0.00	100.00	0.00	0.00	0.00
BZF 10/23/23	34	1	10	1	1	1	0	0	0	3	0	0	0
BZF 10/23/23 %	70.83	2.08	20.83	2.08	2.08	2.08	0.00	0.00	0.00	100.00	0.00	0.00	0.00
BZF 11/29/23	18	0	11	0	0	0	0	0	3	0	1	1	0
BZF 11/29/23 %	56.25	0.00	34.38	0.00	0.00	0.00	0.00	0.00	9.38	0.00	50.00	50.00	0.00
BZF 12/12/23	14	0	0	1	0	1	0	0	0	0	0	0	0
BZF 12/12/23 %	87.50	0.00	0.00	6.25	0.00	6.25	0.00	0.00	0.00	0.00	0.00	0.00	0.00
BZF 1/26/24	26	0	10	1	2	0	0	1	0	4	0	1	0
BZF 1/26/24 %	65.00	0.00	25.00	2.50	5.00	0.00	0.00	2.50	0.00	80.00	0.00	20.00	0.00
BZF 2/9/24	31	3	10	2	0	0	0	2	1	5	1	0	1
BZF 2/9/24 %	63.27	6.12	20.41	4.08	0.00	0.00	0.00	4.08	2.04	71.43	14.29	0.00	14.29

5.5 Field Blanks MP

MPs detected for field blanks are provided in Tables 19-22. Shapes identified included: fibers, films, and fragments. Colors identified: clear, blue, pink, red, green, grey, black, purple, and multi-color. MPs identified fell within the MMP and MP size range. Monthly differences are displayed in Figure 30 based on shape, color, and size.

September had a total of 41 particles identified, composed of 36 fibers, 4 fragments, and 1 film. The predominant color observed was clear (46.34%), followed by blue (24.39%), multi-color (12.20%), black (9.76%), red (2.44%), green (2.44%), grey (2.44%). Of the particles identified, 85.37% fell within the MMP size range and 14.63% fell within the MP size range. Of the fibers observed, 47.22% were clear, 27.78% were blue, 11.11% were black, 11.11% were multi-color, 2.78% were grey. Of the 4 fragments identified, one was red, one was multi-color, one was clear, and one was green. The film identified was clear. Of the particles within the MMP size range 85.71% were fibers, 11.43% were fragments, and 2.86% were films. All particles within the MP size range were fibers. The most abundant color within the MMP size range was clear (40.0%), blue (28.57%), multi-color (11.43%), black (11.43%), red (2.86%), grey (2.86%), and green (2.86%). The predominant color seen in the MP size range was clear (83.33%), followed by multi-color (16.67%).

October 20th had a total of 25 particles identified, of which 24 were fibers, and one was a film. The most frequent color identified was clear (56.0%), followed by blue (28.0%), multi-color (8.0%) grey (4.0%), and black (4.0%). Of the particles identified 72.0% fell within the MMP size range and 28.0% fell within the MP size range. Of the fibers identified, the most common color observed was clear (58.33%), blue (25.0%), multi-color (8.33%), black (4.17%), grey (4.17%). The one film identified was clear. Within the MMP size range 94.44% were fibers, and 5.56% were films. All particles within the MP size range were fibers. Within the MMP size range, the most abundant color observed was clear (66.67%), blue (11.11%), multi-color (11.11%), black (5.56%), and grey (5.56%). Within the MP size range, the most frequent color identified was blue (71.43%) and clear (28.57%).

October 23rd had a total of 13 particles identified, composing of 12 fibers and one fragment. The predominant color identified was blue (46.15%), followed by clear (15.38%), red (15.38%), pink (7.69%), black (7.69%), and multi-color (7.69%). For the particles identified, 76.92% fell within the MMP size range and 23.08% fell within the MP size range. Of the fibers observed, the most frequent color identified was blue (50.0%), clear (16.67%), black (8.33%), multi-color (8.33%), pink (8.33%), and red (8.33%). The one fragment identified was red. Within the MMP size range, fibers accounted for 90.0% and fragments accounted for 10.0%. All particles within the MP size range were fibers. Within the MMP size range, the most identified color was blue (40.0%), followed by red (20.0%), clear (10.0%), multi-color (10.0%), pink (10.0%), and black (10.0%). The most frequently identified color within the MP size range was blue (66.67%), followed by clear (33.33%).

November had a total of 31 particles identified, composed of 28 fibers and 3 fragments. The most frequent color identified was blue (48.39%), followed by clear (29.03%), multi-color (6.45%), pink (3.23%), red (3.23%), grey (3.23%), black (3.23%), and purple (3.23%). Of the 31 particles identified, 80.65% fell within the MMP size range and 19.35% fell within the MP size range. Of the fibers detected, the most frequent color identified was blue (42.86%), followed by clear (32.14%), multi-color (7.14%), black (3.57%), grey (3.57%), pink (3.57%), red (3.57%), and purple (3.57%). All the fragments identified were blue. Of all particles within the MMP size range, 88.0% were fibers and 12.0% were fragments. All particles within the MP size range were fibers. Within the MMP size range, the most abundant color seen was blue (44.0%), followed by clear (32.0%), multi-color (8.0%), pink (4.0%), black (4.0%), red (4.0%), and purple (4.0%). Within the MP size range, blue (66.67%) was the most frequent color seen, followed by clear (16.67%), and grey (16.67%).

December had a total of 11 particles identified, of which 10 were fibers and one was a fragment. The most frequent color seen was blue (36.36%), followed by clear (18.18%), pink (18.18%), multi-color (18.18%), and red (9.09%). Of the 11 particles identified, 90.91% fell within the MMP size range and 9.09% fell within the MP size range. Of the fibers identified, blue was the most frequent color identified accounting for 40.0%, followed by clear (20.0%), multi-color (20.0%), and pink (20.0%). The one fragment identified was red. Within the MMP size range, 90.0% of particles were fibers and 10.0% were fragments. All particles within the MP size range were fibers. Within the MMP size range, the most abundant color seen was blue (30.0%), clear (20.0%), multi-color (20.0%), pink (20.0%), and red (10.0%). The one MP particle was blue.

January had a total of 19 particles identified, composed of 17 fibers and two fragments. The predominant color observed was clear (52.63%), blue (21.05%), pink (10.53%), red (5.26%), black (5.26%), multi-color (5.26%). Of the particles identified, 89.47% fell within the MMP size range and 10.53% fell within the MP size range. Within the fibers identified, clear was the most frequent color observed accounting for 58.82%, followed by blue (17.65%), pink (11.76%), black (5.88%), and multi-color (5.88%). Of the two fragments identified, one was blue, and one was red. Within the MMP size range, 88.24% were fibers and 11.76% were fragments. All particles within the MP size range were fibers. Within the MMP size range, the most frequent color identified was clear (52.94%), followed by blue (23.53%), multi-color (5.88%), pink (5.88%), black (5.88%), and red (5.88%). The two particles within the MP size range were clear and pink.

February had a total of 28 particles identified, of which 27 were fibers and one was a fragment. The most frequent color identified was clear (50.0%), followed by blue (25.0%), pink (7.14%), purple (7.14%), red (3.57%), green (3.57%), and black (3.57%). Of the 28 particles identified, 75.0% fell within the MMP size range and 25.0% fell within the MP size range. Of the fibers identified, the most abundant color observed was clear (51.85%), followed by blue (25.93%), pink (7.41%), purple (7.41%), black (3.70%), red (3.70%). The one fragment identified was green. Within the MMP size range, 95.24% were fibers and 4.76% were fragments. All seven particles within the MP size range were fibers. Within the MMP size range, 61.90% were clear, 14.29% were blue, 9.52% were pink, 4.76% were black, 4.76% were green, and 4.76% were purple. Within the MP size range, the predominant color identified was blue (57.14%), followed by clear (14.29%), red (14.29%), and purple (14.29%).

Overall, a total of 168 particles were identified, of which 154 were fibers, 12 were fragments, and 2 were films. The predominant color seen was clear (41.67%), followed by blue (31.55%), multi-color (7.74%), black (5.36%), pink (4.76%), red (4.17%), grey (1.79%), purple (1.76%), and green (1.19%). Of the 168 particles identified, 80.95% fell within the MMP size range and 19.05% fell within the MP size range. Of the fibers identified, the most frequent color seen was clear (44.16%), followed by blue (31.17%), multi-color (7.79%), black (5.84%), pink (5.19%), grey (1.95%), red (1.95%), and purple (1.95%). Blue and red were the most frequent colors seen within fibers, each accounting for 33.33%, followed by green (16.67%), multi-color (8.33%), and clear (8.33%). Both films identified were clear. Within the MMP size range, 89.71% were fibers, followed by 8.82% being fragments, and 1.47% being films. All 32 particles within the MP size range were fibers. Within the MMP size range the most frequent color observed was clear (43.38%), followed by blue (27.21%), multi-color (8.82%), black (6.62%), pink (5.15%), red (4.41%), grey (1.47%), green (1.47%), and purple (1.47%). The most frequent color seen within the MP size range was blue (50.0%), clear (34.38%), multi-color (3.13%), grey (3.13%), pink (3.13%), red (3.13%), and purple (3.13%).

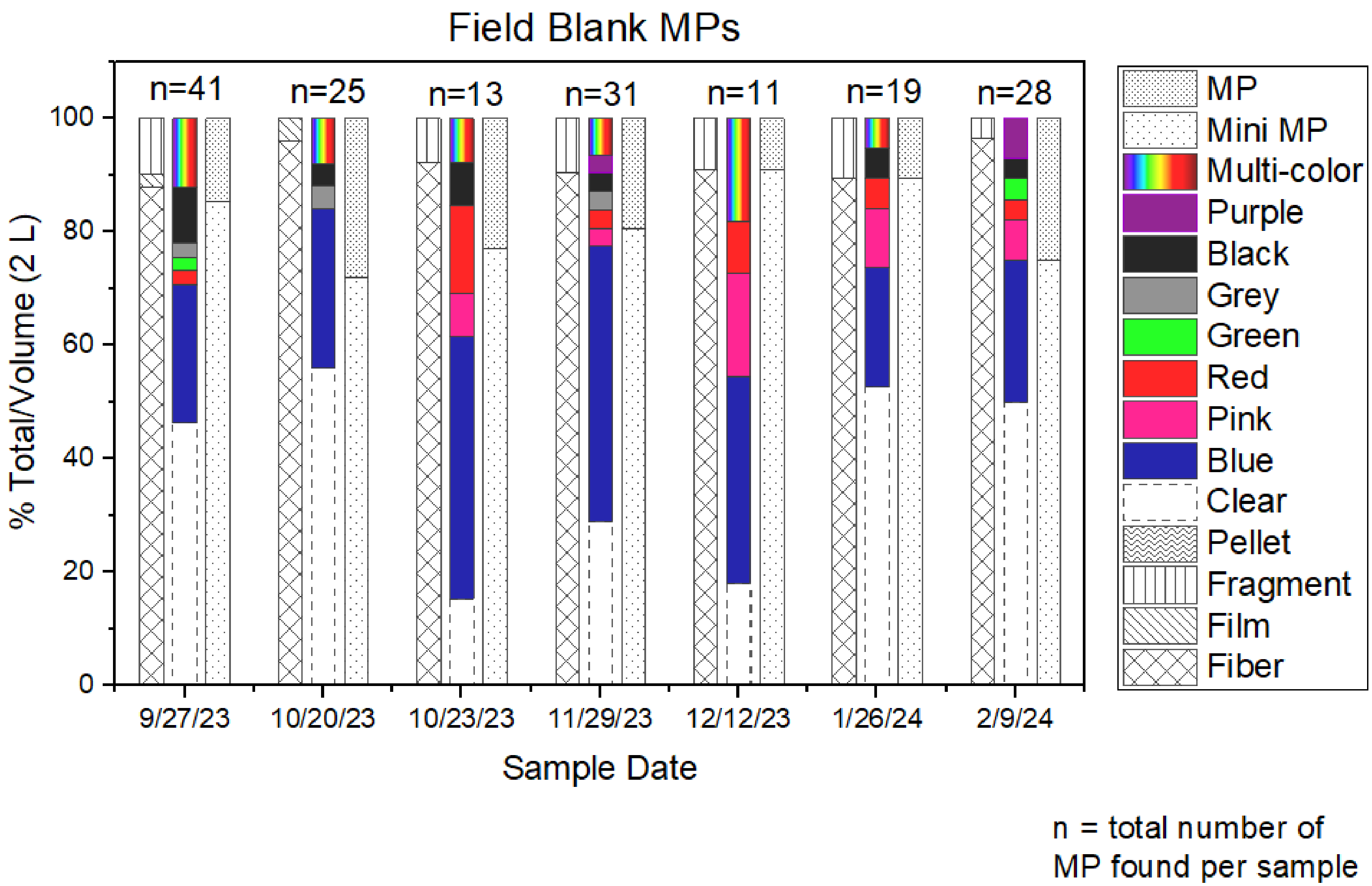

Figure 30: Field Blank MPs characteristics differences grouped by shape, color, and size (Source: created by Author).

Table 19: Total MP Results from Field Blanks. All results are per two liters (Source: Created by Author).

Site/Date	Fiber	Film	Fragment	Clear	Blue	Pink	Red	Green	Grey	Black	Purple	Multi-color	Mini MP	MP	Total
FB 9/27/23	36	1	4	19	10	0	1	1	1	4	0	5	35	6	41
FB 9/27/23 %	87.80	2.44	9.76	46.34	24.39	0.00	2.44	2.44	2.44	9.76	0.00	12.20	85.37	14.63	
FB 10/20/23	24	1	0	14	7	0	0	0	1	1	0	2	18	7	25
FB 10/20/23 %	96.00	4.00	0.00	56.00	28.00	0.00	0.00	0.00	4.00	4.00	0.00	8.00	72.00	28.00	
FB 10/23/23	12	0	1	2	6	1	2	0	0	1	0	1	10	3	13
FB 10/23/23 %	92.31	0.00	7.69	15.38	46.15	7.69	15.38	0.00	0.00	7.69	0.00	7.69	76.92	23.08	
FB 11/29/23	28	0	3	9	15	1	1	0	1	1	1	2	25	6	31
FB 11/29/23 %	90.32	0.00	9.68	29.03	48.39	3.23	3.23	0.00	3.23	3.23	3.23	6.45	80.65	19.35	
FB 12/12/23	10	0	1	2	4	2	1	0	0	0	0	2	10	1	11
FB 12/12/23 %	90.91	0.00	9.09	18.18	36.36	18.18	9.09	0.00	0.00	0.00	0.00	18.18	90.91	9.09	
FB 1/26/24	17	0	2	10	4	2	1	0	0	1	0	1	17	2	19
FB 1/26/24 %	89.47	0.00	10.53	52.63	21.05	10.53	5.26	0.00	0.00	5.26	0.00	5.26	89.47	10.53	
FB 2/9/24	27	0	1	14	7	2	1	1	0	1	2	0	21	7	28
FB 2/9/24 %	96.43	0.00	3.57	50.00	25.00	7.14	3.57	3.57	0.00	3.57	7.14	0.00	75.00	25.00	

Table 20: Breakdown of color and shape for Field Blanks. All results are per two liters (Source: Created by Author).

Site/Date	CL FB	BL FB	BK FB	GY FB	BN FB	MC FB	PK FB	RD FB	PR FB	BL FR	RD FR	MC FR	CL FR	GN FR	CL FI
FB 9/27/23	17	10	4	1	0	4	0	0	0	0	1	1	1	1	1
FB 9/27/23 %	47.22	27.78	11.11	2.78	0.00	11.11	0.00	0.00	0.00	0.00	25.00	25.00	25.00	25.00	100.00
FB 10/20/23	14	6	1	1	0	2	0	0	0	0	0	0	0	0	1
FB 10/20/23 %	58.33	25.00	4.17	4.17	0.00	8.33	0.00	0.00	0.00	0.00	0.00	0.00	0.00	0.00	100.00
FB 10/23/23	2	6	1	0	0	1	1	1	0	0	1	0	0	0	0
FB 10/23/23 %	16.67	50.00	8.33	0.00	0.00	8.33	8.33	8.33	0.00	0.00	100.00	0.00	0.00	0.00	0.00
FB 11/29/23	9	12	1	1	0	2	1	1	1	3	0	0	0	0	0
FB 11/29/23 %	32.14	42.86	3.57	3.57	0.00	7.14	3.57	3.57	3.57	100.00	0.00	0.00	0.00	0.00	0
FB 12/12/23	2	4	0	0	0	2	2	0	0	0	1	0	0	0	0
FB 12/12/23 %	20.00	40.00	0.00	0.00	0.00	20.00	20.00	0.00	0.00	0.00	100.00	0.00	0.00	0.00	0
FB 1/26/24	10	3	1	0	0	1	2	0	0	1	1	0	0	0	0
FB 1/26/24 %	58.82	17.65	5.88	0.00	0.00	5.88	11.76	0.00	0.00	50.00	50.00	0.00	0.00	0.00	0
FB 2/9/24	14	7	1	0	0	0	2	1	2	0	0	0	0	1	0
FB 2/9/24 %	51.85	25.93	3.70	0.00	0.00	0.00	7.41	3.70	7.41	0.00	0.00	0.00	0.00	100.00	0

Table 21: Breakdown of shape and size for Field Blanks. All results are per two liters (Source: Created by Author).

Site/Date	FB MMP	FR MMP	FI MMP	FB MP
FB 9/27/23	30	4	1	6
FB 9/27/23 %	85.71	11.43	2.86	100.00
FB 10/20/23	17	0	1	7
FB 10/20/23 %	94.44	0.00	5.56	100.00
FB 10/23/23	9	1	0	3
FB 10/23/23 %	90.00	10.00	0.00	100.00
FB 11/29/23	22	3	0	6
FB 11/29/23 %	88.00	12.00	0.00	100.00
FB 12/12/23	9	1	0	1
FB 12/12/23 %	90.00	10.00	0.00	100.00
FB 1/26/24	15	2	0	2
FB 1/26/24 %	88.24	11.76	0.00	100.00
FB 2/9/24	20	1	0	7
FB 2/9/24 %	95.24	4.76	0.00	100.00

Table 22: Breakdown of color and size for Field Blanks. All results are per two liters (Source: Created by Author).

Site/Date	CL MMP	MC MMP	BL MMP	PK MMP	BK MMP	RD MMP	GY MMP	GN MMP	PR MMP	CL MP	MC MP	BL MP	GY MP	PK MP	RD MP	PR MP
FB 9/27/23	14	4	10	0	4	1	1	1	0	5	1	0	0	0	0	0
FB 9/27/23 %	40.00	11.43	28.57	0.00	11.43	2.86	2.86	2.86	0.00	83.33	16.67	0.00	0.00	0.00	0.00	0.00
FB 10/20/23	12	2	2	0	1	0	1	0	0	2	0	5	0	0	0	0
FB 10/20/23 %	66.67	11.11	11.11	0.00	5.56	0.00	5.56	0.00	0.00	28.57	0.00	71.43	0.00	0.00	0.00	0.00
FB 10/23/23	1	1	4	1	1	2	0	0	0	1	0	2	0	0	0	0
FB 10/23/23 %	10.00	10.00	40.00	10.00	10.00	20.00	0.00	0.00	0.00	33.33	0.00	66.67	0.00	0.00	0.00	0.00
FB 11/29/23	8	2	11	1	1	1	0	0	1	1	0	4	1	0	0	0
FB 11/29/23 %	32.00	8.00	44.00	4.00	4.00	4.00	0.00	0.00	4.00	16.67	0.00	66.67	16.67	0.00	0.00	0.00
FB 12/12/23	2	2	3	2	0	1	0	0	0	0	0	1	0	0	0	0
FB 12/12/23 %	20.00	20.00	30.00	20.00	0.00	10.00	0.00	0.00	0.00	0.00	0.00	100.00	0.00	0.00	0.00	0.00
FB 1/26/24	9	1	4	1	1	1	0	0	0	1	0	0	0	1	0	0
FB 1/26/24 %	52.94	5.88	23.53	5.88	5.88	5.88	0.00	0.00	0.00	50.00	0.00	0.00	0.00	50.00	0.00	0.00
FB 2/9/24	13	0	3	2	1	0	0	1	1	1	0	4	0	0	1	1

FB 2/9/24 %	61.90	0.00	14.29	9.52	4.76	0.00	0.00	4.76	4.76	14.29	0.00	57.14	0.00	0.00	14.29	14.29

5.6 Combined Results

Total MPs concentrations detected for all sites are provided in Tables 23-26. Shapes identified included: fibers, films, fragments, and pellets. Colors identified: clear, blue, pink, red, green, brown, grey, black, purple, orange, and multi-color. MPs identified fell within the MMP and MP size range. Monthly differences are displayed in Figure 26 based on shape, color, and size.

In total, across all sites, there were a total of 824 particles identified, composed of 733 fibers, 9 films, 79 fragments, and 3 pellets. The predominant color observed was clear (63.23%), followed by blue (22.21%), multi-color (3.88%), black (3.16%), pink (2.67%), green (2.06%), red (1.46%), grey (0.85%), purple (0.24%), brown (0.12%), and orange (0.12%). Of the 824 particles identified, 90.53% fell within the MMP size range and 9.47% fell within the MP size range. Among all the fibers identified, the most identified color was clear (68.76%), followed by blue (17.87%), multi-color (3.68%), black (3.55%), pink (2.86%), green (1.09%), red (0.95%), grey (0.82%), brown (0.14%), purple (0.14%), and orange (0.14%). Of all the fragments detected, the predominant color seen was blue (65.82%), followed by green (11.39%), clear (7.59%), red (6.33%), multi-color (5.06%), pink (1.27%), grey (1.27%), and purple (1.27%). Of the films identified, 88.89% were clear and 11.11% were multi-color. All pellets seen were clear.

Of the particles identified within the MMP size range, the predominant shape seen was fibers (87.94%), followed by fragments (10.46%), films (1.21%), and pellets (0.40%). All particles within the MP size range were fibers. The predominant color documented within the MMP size range was clear (63.67%), followed by blue (22.12%), multi-color (3.35%), black (3.22%), pink (2.55%), green (2.28%), red (1.34%), grey (0.94%), purple (0.27%), brown

(0.13%), and orange (0.13%). Among particles identified within the MP size range, the most frequently identified color was clear (60.26%), followed by blue (23.08%), multi-color (7.69%), pink (5.13%), black (2.56%), and red (1.28%).

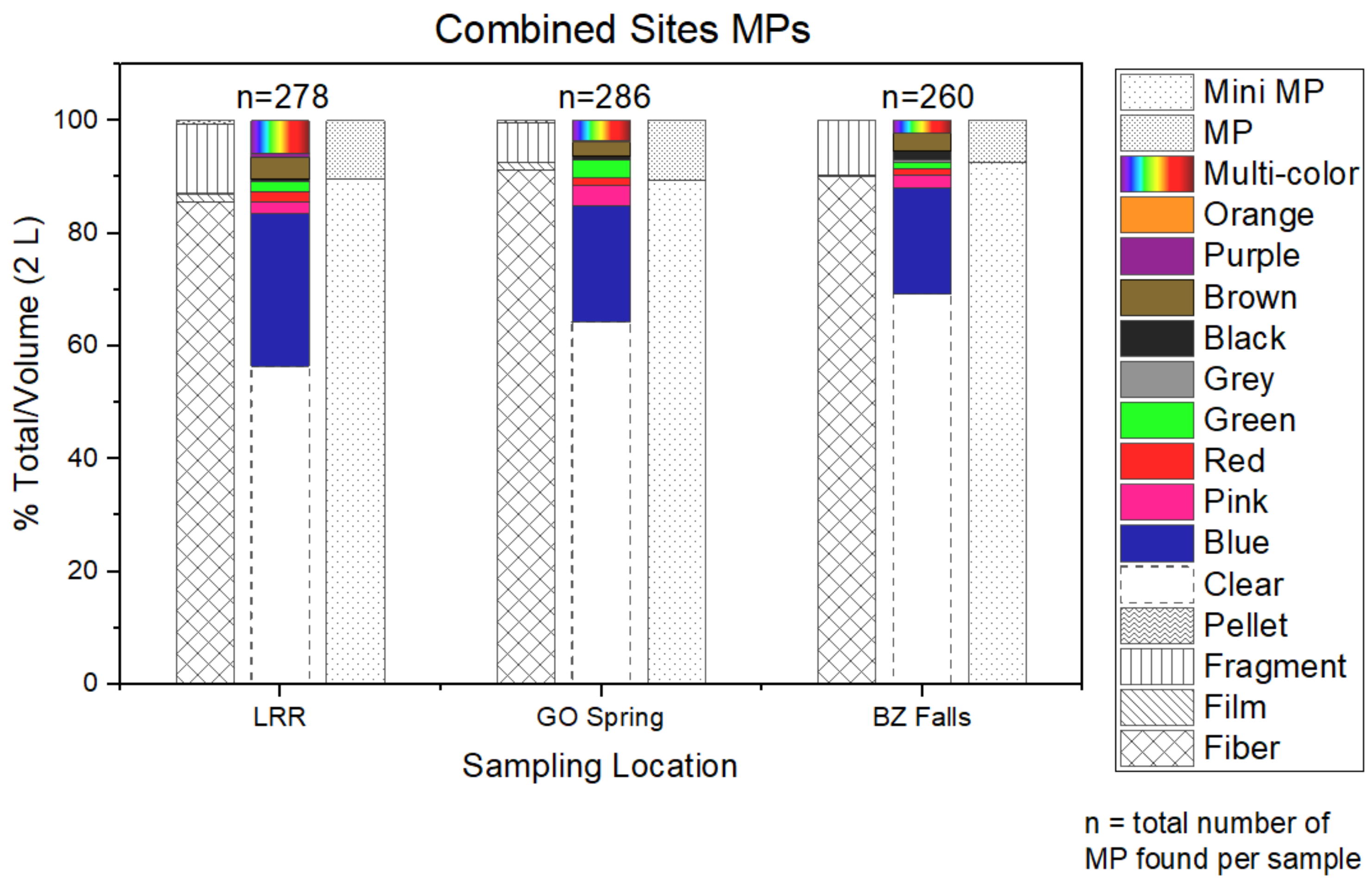

Figure 30: Total combined MPs concentrations characteristics differences grouped by shape, color, and size (Source: created by Author).

Table 23: Total MP results combined from all sites. All results are per two liters (Source: Created by Author).

Site	FB	FI	FR	PT	CL	BL	PK	RD	GN	BN	GY	BK	PR	OR	MC	MMP	MP	Total
LRR	238.00	4.00	34.00	2.00	157.00	75.00	6.00	5.00	5.00	0.00	1.00	11.00	2.00	0.00	16.00	249.00	29.00	278.00
	85.61	1.44	12.23	0.72	56.47	26.98	2.16	1.80	1.80	0.00	0.36	3.96	0.72	0.00	5.76	89.57	10.43	
GO Spr	261.00	4.00	20.00	1.00	184.00	59.00	10.00	4.00	9.00	0.00	2.00	7.00	0.00	1.00	10.00	256.00	30.00	286.00
	91.26	1.40	6.99	0.35	64.34	20.63	3.50	1.40	3.15	0.00	0.70	2.45	0.00	0.35	3.50	89.51	10.49	
Bz Falls	234.00	1.00	25.00	0.00	180.00	49.00	6.00	3.00	3.00	1.00	4.00	8.00	0.00	0.00	6.00	241.00	19.00	260.00
	90.00	0.38	9.62	0.00	69.23	18.85	2.31	1.15	1.15	0.38	1.54	3.08	0.00	0.00	2.31	92.69	7.31	
Totals	733.00	9.00	79.00	3.00	521.00	183.00	22.00	12.00	17.00	1.00	7.00	26.00	2.00	1.00	32.00	746.00	78.00	824.00
Total %	88.96	1.09	9.59	0.36	63.23	22.21	2.67	1.46	2.06	0.12	0.85	3.16	0.24	0.12	3.88	90.53	9.47	

Table 24: Breakdown of color and fibers for combined results. All results are per two liters (Source: Created by Author).

Site	CL FB	BL FB	BK FB	PK FB	RD FB	GN FB	BN FB	GY FB	PR FB	OR FB	MC FB	Total
LRR	151.00	50.00	11.00	6.00	4.00	0.00	0.00	1.00	1.00	0.00	14.00	278.00
	63.45	21.01	4.62	2.52	1.68	0.00	0.00	0.42	0.42	0.00	5.88	
GO Spr	177.00	44.00	7.00	10.00	3.00	7.00	0.00	2.00	0.00	1.00	10.00	286.00
	67.82	16.86	2.68	3.83	1.15	2.68	0.00	0.77	0.00	0.38	3.83	
Bz Falls	176.00	37.00	8.00	5.00	0.00	1.00	1.00	3.00	0.00	0.00	3.00	260.00
	75.21	15.81	3.42	2.14	0.00	0.43	0.43	1.28	0.00	0.00	1.28	
Totals	504.00	131.00	26.00	21.00	7.00	8.00	1.00	6.00	1.00	1.00	27.00	824.00
Total %	68.76	17.87	3.55	2.86	0.95	1.09	0.14	0.82	0.14	0.14	3.68	

Table 25: Breakdown of color and fragments, pellets, and films for combined results. All results are per two liters (Source: Created by Author).

Site	CL FR	BL FR	PK FR	RD FR	GN FR	GY FR	PR FR	MC FR	CL FI	MC FI	CL PT	Total
LRR	0.00	25.00	0.00	1.00	5.00	0.00	1.00	2.00	4.00	0.00	2.00	278.00
	0.00	73.53	0.00	2.94	14.71	0.00	2.94	5.88	100.00	0.00	100.00	
GO Spr	2.00	15.00	0.00	1.00	2.00	0.00	0.00	0.00	4.00	0.00	1.00	286.00
	10.00	75.00	0.00	5.00	10.00	0.00	0.00	0.00	100.00	0.00	100.00	
Bz Falls	4.00	12.00	1.00	3.00	2.00	1.00	0.00	2.00	0.00	1.00	0.00	260.00
	16.00	48.00	4.00	12.00	8.00	4.00	0.00	8.00	0.00	100.00	0.00	
Totals	6.00	52.00	1.00	5.00	9.00	1.00	1.00	4.00	8.00	1.00	3.00	824.00
Total %	7.59	65.82	1.27	6.33	11.39	1.27	1.27	5.06	88.89	11.11	100.00	

Table 26: Breakdown of shape and size for combined results. All results are per two liters (Source: Created by Author).

Site	FB MMP	FR MMP	FI MMP	PT MMP	FB MP	Total
LRR	209.00	34.00	4.00	2.00	29.00	278.00
	83.94	13.65	1.61	0.80	100.00	
GO Spr	232.00	19.00	4.00	1.00	30.00	286.00
	90.63	7.42	1.56	0.39	100.00	
Bz Falls	215.00	25.00	1.00	0.00	19.00	260.00
	89.21	10.37	0.41	0.00	100.00	
Totals	656.00	78.00	9.00	3.00	78.00	824.00
Total %	87.94	10.46	1.21	0.40	100.00	

Table 27: Breakdown of color and size for combined results. All results are per two liters (Source: Created by Author).

Site	CL MMP	BL MMP	BK MMP	PK MMP	RD MMP	GN MMP	BN MMP	GY MMP	PR MMP	OR MMP	MC MMP	CL MP	BL MP	BK MP	PK MP	RD MP	MC MP	Total
LRR	136.00	69.00	11.00	6.00	5.00	5.00	0.00	1.00	2.00	0.00	14.00	20.00	6.00	0.00	0.00	0.00	3.00	278.00
	54.62	27.71	4.42	2.41	2.01	2.01	0.00	0.40	0.80	0.00	5.62	68.97	20.69	0.00	0.00	0.00	10.34	
GO Spr	172.00	49.00	5.00	8.00	3.00	9.00	0.00	2.00	0.00	1.00	7.00	13.00	10.00	2.00	2.00	1.00	2.00	286.00
	67.19	19.14	1.95	3.13	1.17	3.52	0.00	0.78	0.00	0.39	2.73	43.33	33.33	6.67	6.67	3.33	6.67	
Bz Falls	167.00	47.00	8.00	5.00	2.00	3.00	1.00	4.00	0.00	0.00	4.00	14.00	2.00	0.00	2.00	0.00	1.00	260.00
	69.29	19.50	3.32	2.07	0.83	1.24	0.41	1.66	0.00	0.00	1.66	73.68	10.53	0.00	10.53	0.00	5.26	
Totals	475.00	165.00	24.00	19.00	10.00	17.00	1.00	7.00	2.00	1.00	25.00	47.00	18.00	2.00	4.00	1.00	6.00	824.00
Total %	63.67	22.12	3.22	2.55	1.34	2.28	0.13	0.94	0.27	0.13	3.35	60.26	23.08	2.56	5.13	1.28	7.69	

5.7 Air QA/QC

When sampling in the field, filters were left out to capture any potential air contamination. Any contamination was then subtracted out from the corresponding sample date. All three sampling locations had contamination on one or more sampling dates.

Lost River Rise air QA/QC concentrations are provided in Tables 28-331. October 20th, 2023, sampling event had a total of seven fibers identified, of which four were blue, one clear, one pink, and one red. All seven fibers identified fell within the MMP size range. October 23rd 2023, sampling event had a total of three particles identified, of which two were fibers and one was a fragment. One of the fibers was blue while the other was clear. The fragment identified was blue. All three particles fell within the MMP size range. November 29th, 2023, had a one fiber identified, that was clear falling within the MMP size range. February 9th, 2024, had a total of two fibers identified, one being clear and the other multi-color. The clear fiber fell within the MMP size range, while the multi-color fiber fell within the MP size range.

Table 28: Total MP Results from LRR air contamination. All results are per two liters (Source: Created by Author).

Site/Date	Fiber	Fragment	Clear	Blue	Pink	Red	Multi-color	MMP	MP	Totals
LRR 10.20	7.00	0.00	1.00	4.00	1.00	1.00	0.00	7.00	0.00	7.00
LRR 10.20 %	100.00	0.00	14.29	57.14	14.29	14.29	0.00	100.00	0.00	
LRR 10.23	2.00	1.00	1.00	2.00	0.00	0.00	0.00	3.00	0.00	3.00
LRR 10.23 %	66.67	33.33	33.33	66.67	0.00	0.00	0.00	100.00	0.00	
LRR 11.29	1.00	0.00	1.00	0.00	0.00	0.00	0.00	1.00	0.00	1.00
LRR 11.29 %	100.00	0.00	100.00	0.00	0.00	0.00	0.00	100.00	0.00	
LRR 2.9	2.00	0.00	1.00	0.00	0.00	0.00	1.00	1.00	1.00	2.00
LRR 2.9%	100.00	0.00	50.00	0.00	0.00	0.00	50.00	50.00	50.00	
LRR TOTAL	12.00	1.00	4.00	6.00	1.00	1.00	1.00	12.00	1.00	13.00
LRR TOTAL %	92.31	7.69	30.77	46.15	7.69	7.69	7.69	92.31	7.69	

Table 29: Breakdown of color and shape for LRR air contamination. All results are per two liters (Source: Created by Author).

Site/Date	CL FB	BL FB	PK FB	RD FB	MC FB	BL FR
LRR 10.20	1.00	4.00	1.00	1.00	0.00	0.00
LRR 10.20 %	14.29	57.14	14.29	14.29	0.00	0.00
LRR 10.23	1.00	1.00	0.00	0.00	0.00	0.00
LRR 10.23 %	50.00	50.00	0.00	0.00	0.00	0.00
LRR 11.29	1.00	0.00	0.00	0.00	0.00	0.00
LRR 11.29 %	100.00	0.00	0.00	0.00	0.00	0.00
LRR 2.9	1.00	0.00	0.00	0.00	0.00	0.00
LRR 2.9%	50.00	0.00	0.00	0.00	0.00	0.00
LRR TOTAL	4.00	5.00	1.00	1.00	0.00	1.00
LRR TOTAL %	33.33	41.67	8.33	8.33	8.33	100.00

Table 30: Breakdown of shape and size for LRR air contamination. All results are per two liters (Source: Created by Author).

Site/Date	FB MMP	FR MMP	FB MP
LRR 10.20	7.00	0.00	0.00
LRR 10.20 %	100.00	0.00	0.00
LRR 10.23	2.00	1.00	0.00
LRR 10.23 %	66.67	33.33	0.00
LRR 11.29	1.00	0.00	0.00
LRR 11.29 %	100.00	0.00	0.00
LRR 2.9	1.00	0.00	1.00
LRR 2.9%	100.00	0.00	100.00
LRR TOTAL	11.00	1.00	1.00
LRR TOTAL %	91.67	8.33	100.00

Table 31: Breakdown of color and size for LRR air contamination. All results are per two liters (Source: Created by Author).

Site/Date	CL MMP	BL MMP	PK MMP	RD MMP	MC MP	CL MP	RD MP
LRR 10.20	1.00	4.00	1.00	1.00	0.00	0.00	0.00
LRR 10.20 %	14.29	57.14	14.29	14.29	0.00	0.00	0.00
LRR 10.23	1.00	0.00	2.00	0.00	0.00	0.00	0.00
LRR 10.23 %	33.33	0.00	66.67	0.00	0.00	0.00	0.00
LRR 11.29	1.00	0.00	0.00	0.00	0.00	0.00	0.00
LRR 11.29 %	100.00	0.00	0.00	0.00	0.00	0.00	0.00
LRR 2.9	1.00	0.00	0.00	0.00	1.00	0.00	0.00
LRR 2.9%	100.00	0.00	0.00	0.00	100.00	0.00	0.00
LRR TOTAL	4.00	4.00	3.00	1.00	1.00	0.00	0.00
LRR TOTAL %	33.33	33.33	25.00	8.33	100.00	0.00	0.00

GO Spring air QA/QC concentrations are provided in Tables 32-35. September 27th, 2023 had a total of three fibers identified, all being blue, and all being in the MMP size range. November 29th, 2023, had a total of three fibers identified, two of which were pink and one was clear. All three fibers were in the MMP size range. December 12th, 2023 had a total of two fibers identified, of which one was clear and the other was red, both in the MP size range.

Table 32: Total MP Results from GO Spring air contamination. All results are per two liters (Source: Created by Author).

Site/Date	Fiber	Fragment	Clear	Blue	Pink	Red	Multi-color	MMP	MP	Totals
GO SPR 9.27	3.00	0.00	0.00	3.00	0.00	0.00	0.00	3.00	0.00	3.00
GO SPR 9.27%	100.00	0.00	0.00	100.00	0.00	0.00	0.00	100.00	0.00	
GO SPR 11.29	3.00	0.00	1.00	0.00	2.00	0.00	0.00	3.00	0.00	3.00
GO SPR 11.29 %	100.00	0.00	33.33	0.00	66.67	0.00	0.00	100.00	0.00	
GO SPR 12.12	2.00	0.00	1.00	0.00	0.00	1.00	0.00	0.00	2.00	2.00
GO SPR 12.12 %	100.00	0.00	50.00	0.00	0.00	50.00	0.00	0.00	100.00	
GO SPR TOTAL	8.00	0.00	2.00	3.00	2.00	1.00	0.00	6.00	2.00	8.00
GO SPR TOTAL %	100.00	0.00	25.00	37.50	25.00	12.50	0.00	75.00	25.00	

Table 33: Breakdown of color and shape for GO Spring air contamination. All results are per two liters (Source: Created by Author).

Site/Date	CL FB	BL FB	PK FB	RD FB	MC FB	BL FR
GO SPR 9.27	0.00	3.00	0.00	0.00	0.00	0.00
GO SPR 9.27%	0.00	100.00	0.00	0.00	0.00	0.00
GO SPR 11.29	1.00	0.00	2.00	0.00	0.00	0.00
GO SPR 11.29 %	33.33	0.00	66.67	0.00	0.00	0.00
GO SPR 12.12	1.00	0.00	0.00	1.00	0.00	0.00
GO SPR 12.12 %	50.00	0.00	0.00	50.00	0.00	0.00
GO SPR TOTAL	2.00	3.00	2.00	1.00	0.00	0.00
GO SPR TOTAL %	25.00	37.50	25.00	12.50	0.00	0.00

Table 34: Breakdown of shape and size for GO Spring air contamination. All results are per two liters (Source: Created by Author).

Site/Date	FB MMP	FR MMP	FB MP
GO SPR 9.27	3.00	0.00	0.00
GO SPR 9.27%	100.00	0.00	0.00
GO SPR 11.29	3.00	0.00	0.00
GO SPR 11.29 %	100.00	0.00	0.00
GO SPR 12.12	0.00	0.00	2.00
GO SPR 12.12 %	0.00	0.00	100.00
GO SPR TOTAL	6.00	0.00	2.00
GO SPR TOTAL %	100.00	0.00	100.00

Table 35: Breakdown of color and size for GO Spring air contamination. All results are per two liters (Source: Created by Author).

Site/Date	CL MMP	BL MMP	PK MMP	CL MP	RD MP
GO SPR 9.27	0.00	3.00	0.00	0.00	0.00
GO SPR 9.27%	0.00	100.00	0.00	0.00	0.00
GO SPR 11.29	1.00	0.00	2.00	0.00	0.00
GO SPR 11.29 %	33.33	0.00	66.67	0.00	0.00
GO SPR 12.12	0.00	0.00	0.00	1.00	1.00
GO SPR 12.12 %	0.00	0.00	0.00	50.00	50.00
GO SPR TOTAL	1.00	3.00	3.00	1.00	1.00
GO SPR TOTAL %	16.67	50.00	50.00	50.00	50.00

Biz Falls air QA/QC concentrations are provided in Tables 36-39. September 27th, 2023, had a total of two fibers identified, one being clear and the other being multi-colored. Both fibers fell within the MMP size range. October 23rd, 2023, had one fiber identified, that was clear and fell within the MMP size range. November 29th, had a total of six fibers identified, of which two were clear, one was blue, two were pink, and one was red. All six fibers fell within the MMP size range. December 12th, 2023, had one fiber identified, which was clear, falling within the MMP size range. January 26th, 2024, had one fiber was identified, which was clear and falling within the MMP size range.

Table 36: Total MP Results from Biz Falls air contamination. All results are per two liters (Source: Created by Author).

Site/Date	Fiber	Fragment	Clear	Blue	Pink	Red	Multi-color	MMP	MP	Totals
BZ FALLS 9.27	2.00	0.00	1.00	0.00	0.00	0.00	1.00	2.00	0.00	2.00
BZ FALLS 9.27 %	100.00	0.00	50.00	0.00	0.00	0.00	50.00	100.00	0.00	
BZ FALLS 10.23	1.00	0.00	1.00	0.00	0.00	0.00	0.00	1.00	0.00	1.00
BZ FALLS 10.23 %	100.00	0.00	100.00	0.00	0.00	0.00	0.00	100.00	0.00	
BZ FALLS 11.29	6.00	0.00	2.00	1.00	2.00	1.00	0.00	6.00	0.00	8.00
BZ FALLS 11.29 %	100.00	0.00	33.33	16.67	16.67	33.33	0.00	100.00	0.00	
BZ FALLS 12.12	1.00	0.00	1.00	0.00	0.00	0.00	0.00	1.00	0.00	1.00
BZ FALLS 12.12 %	100.00	0.00	100.00	0.00	0.00	0.00	0.00	100.00	0.00	
BZ FALLS 1.26	1.00	0.00	1.00	0.00	0.00	0.00	0.00	1.00	0.00	1.00
BZ FALLS 1.26 %	100.00	0.00	100.00	0.00	0.00	0.00	0.00	100.00	0.00	
BZ FALLS TOTAL	11.00	0.00	6.00	1.00	2.00	1.00	1.00	11.00	0.00	11.00
BZ FALLS TOTAL %	100.00	0.00	54.55	9.09	18.18	9.09	9.09	100.00	0.00	

Table 37: Breakdown of color and shape for Biz Falls air contamination. All results are per two liters (Source: Created by Author).

Site/Date	CL FB	BL FB	PK FB	RD FB	MC FB	BL FR
BZ FALLS 9.27	1.00	0.00	0.00	0.00	1.00	0.00
BZ FALLS 9.27 %	50.00	0.00	0.00	0.00	50.00	0.00
BZ FALLS 10.23	1.00	0.00	0.00	0.00	0.00	0.00
BZ FALLS 10.23 %	100.00	0.00	0.00	0.00	0.00	0.00
BZ FALLS 11.29	2.00	1.00	2.00	1.00	0.00	0.00
BZ FALLS 11.29 %	33.33	16.67	33.33	16.67	0.00	0.00
BZ FALLS 12.12	1.00	0.00	0.00	0.00	0.00	0.00
BZ FALLS 12.12 %	100.00	0.00	0.00	0.00	0.00	0.00
BZ FALLS 1.26	1.00	0.00	0.00	0.00	0.00	0.00
BZ FALLS 1.26 %	100.00	0.00	0.00	0.00	0.00	0.00
BZ FALLS TOTAL	6.00	1.00	2.00	1.00	1.00	0.00
BZ FALLS TOTAL %	54.55	9.09	18.18	9.09	9.09	0.00

Table 38: Breakdown of shape and size for Biz Falls air contamination. All results are per two liters (Source: Created by Author).

Site/Date	FB MMP	FR MMP	FB MP
BZ FALLS 9.27	2.00	0.00	0.00
BZ FALLS 9.27 %	100.00	0.00	0.00
BZ FALLS 10.23	1.00	0.00	0.00
BZ FALLS 10.23 %	100.00	0.00	0.00
BZ FALLS 11.29	6.00	0.00	0.00
BZ FALLS 11.29 %	100.00	0.00	0.00
BZ FALLS 12.12	1.00	0.00	0.00
BZ FALLS 12.12 %	100.00	0.00	0.00
BZ FALLS 1.26	1.00	0.00	0.00
BZ FALLS 1.26 %	100.00	0.00	0.00
BZ FALLS TOTAL	11.00	0.00	0.00
BZ FALLS TOTAL %	100.00	0.00	0.00

Table 39: Breakdown of color and size for Biz Falls air contamination. All results are per two liters (Source: Created by Author).

Site/Date	CL MMP	BL MMP	PK MMP	RD MMP	MC MP	CL MP	RD MP
BZ FALLS 9.27	1.00	0.00	0.00	0.00	1.00	0.00	0.00
BZ FALLS 9.27 %	50.00	0.00	0.00	0.00	50.00	0.00	0.00
BZ FALLS 10.23	1.00	0.00	0.00	0.00	0.00	0.00	0.00
BZ FALLS 10.23 %	100.00	0.00	0.00	0.00	0.00	0.00	0.00
BZ FALLS 11.29	2.00	1.00	2.00	1.00	0.00	0.00	0.00
BZ FALLS 11.29 %	33.33	16.67	33.33	16.67	0.00	0.00	0.00
BZ FALLS 12.12	1.00	0.00	0.00	0.00	0.00	0.00	0.00
BZ FALLS 12.12 %	100.00	0.00	0.00	0.00	0.00	0.00	0.00
BZ FALLS 1.26	1.00	0.00	0.00	0.00	0.00	0.00	0.00
BZ FALLS 1.26 %	100.00	0.00	0.00	0.00	0.00	0.00	0.00
BZ FALLS TOTAL	6.00	1.00	2.00	1.00	1.00	0.00	0.00
BZ FALLS TOTAL %	54.55	9.09	18.18	9.09	9.09	0.00	0.00

Chapter 6: Discussion and Conclusion

6.1 Discussion

Microplastics were documented monthly at every site indicating that they are a pervasive, ubiquitous contaminant in karst groundwater. Table 40 represents a summary of results found. It is important for monitoring to be maintained to understand how these concentrations fluctuate.

Table 40: Summary of results found (Source: Created by Author).

	Lost River Rise	**GO Spring**	**Biz Falls**
Predominant Color	Clear	Clear	Clear
Predominant Shape	Fibers	Fibers	Fibers
Predominant Size	MMP	MMP	MMP
Highest Month	September	January	September
Lowest Month	November	December	December
Total Detected	278	286	260

It is evident that certain MMP characteristics are dominant across all sampling locations. These characteristics are important when evaluating potential sources of MP contamination. When examining Lost River Rise, the area is heavily impacted by urban land use. Sources of MPs in urban areas include surface runoff (Werbowski et al., 2021), wastewater discharge (Sun et al., 2018), personal care products (Bråte et al., 2014), tire wear (Werbowski et al., 2021), and microfibers from textiles (Thompson et al., 2004; Browne et al., 2007), to name a few. Fibers found within Lost River Rise could be attributed to surface runoff, wastewater discharge, or textiles. An example of fibers entering via wastewater discharge is a result of washing clothing. There are also several clothing manufacturing plants that could potentially contribute to fibers entering the waterway. Fragments, especially blue, could be a result of various personal care products, such as scrubbers used in face wash. Fibers could also be more prevalent since there are often not large pieces of plastic (small scale plastic islands) accumulating in this waterway. This means that there are likely not as many secondary MPs breaking down and entering the waterway.

Great Onyx Groundwater Basin lies within an undeveloped portion of Mammoth Cave National Park. GO Spring runs downstream of the tour that takes place within GO Cave. The tour likely contributes to fibers detected within GO Groundwater Basin. It is interesting to note that main color observed was clear. Clear fibers are typically made from materials such as polyester, nylon, and acrylic. In additional to chemical analysis of the fibers, a short survey regarding clothing worn could be conducted prior to the tours occurring. The small fiber sizes also point to fibers shed from clothing that travel through the cave system then into the spring. Fragments found in the spring could result from shoe wear or other accessories made from plastic that enter the cave.

Biz Falls lies upstream of the tour route and the above ground surface is remote, void of human use. Theoretically, this should be the most likely sampling location to have very low, if any, microplastic contamination. However, this was not the case, as Biz Falls had very similar results to GO Spring. A couple potential sources of MP contamination could be 1) through air currents in the cave 2) from rainwater that enters the system as groundwater. MPs can transport through the atmosphere (Shao et al., 2022). Additional studies should be conducted at Biz Falls, both in-cave and above ground, to determine to what extent MPs are being transported airborne. A way to examine potential impact of the tour would be to set up various filters along both avenues of the cave to examine atmospheric transport. Additional sampling should be taken both in and out of the cave during various rain events to examine potential MP contamination.

Identifying sources of microplastics is key in effective prevention and mitigation. Once MPs are in the environment, it is extremely hard to remove them due to their size. Rather than removing MPs once present, researchers and policy makers should focus on prevention. Knowing the source allows for targeted strategies and specific regulations for large corporations and industries to reduce MP elimination. For instance, locally, if it is observed that wastewater treatment is a main contributor to MP pollution, new regulations could perhaps be created to enhance wastewater-treatment processing. Identifying the source can also provide knowledge regarding degradation times and toxicity. Not all MPs degrade the same and different types of MPs can leach different types of toxic chemicals. A main key to identifying source of MPs is to be able to hold industries and large corporations accountable. Large corporations and industries produce MP pollution to a much higher degree compared to household sources. People often do not have the choice or financial means to choose the most environmentally friendly product. Identifying sources of MPs raises public awareness and addresses the need for change.

MPs were found in karst groundwater regardless of land use. This is important because 9.2% of the global population relies on aquifers for drinking water (Stevanović, 2019). There are many communities near these study areas that use karst aquifers for drinking water. It is likely that MPs are widespread throughout karst aquifers, as MPs were seen in an undeveloped groundwater basin. As MP pollution has a variety of implications, karst aquifers should be monitored for microplastics.

Sampling was conducted during later summer, fall and winter months. It is interesting to note that for both GO Spring and Biz Falls December had the lowest MPs detected. This could be due to reduced tours in the winter months. Additionally for all sites, November and December could have also been the lowest months due to lack of precipitation resulting in decreased runoff. The highest detection was seen during September for Lost River Rise which could be associated with summer activities and September being the first full month of classes for Western Kentucky University. Lost River Rise rain event had less microplastics identified in comparison to the previous month. This suggests that rain events cause the microplastic concentrations to dilute, most likely due to the high volume of water moving through the system.

6.2 Limitations

Overall, the main limitation faced in this study was the unknowns and lack of standardization when it came to designing the methodology. Standardization of methodology would make it easier for studies to be recreated or mimicked in a different environment. While standardization of methodology is beneficial, it is important to also note that not all ecosystems require the same type of methodology. Standardization of methodology should be dependent on sampling conditions/location. The field of microplastics holds a lot of unknowns, and more information is rapidly becoming available. For future studies, it would be beneficial to have a yearlong study to be able to capture flow conditions in all seasons, as well as additional rain events. While some studies collect discharge to then extrapolate to get an MP load, MP distribution is not uniform. To calculate a more representative MP load, samples should be conducted at multiple depths of the water column and widths of the body of water.

6.2.1 Field

One limitation that occurred in the field was not being able to sample at the exact sample point every time due to unsafe flow conditions. Future studies could try to utilize a pole extender to extend the reach when grab sampling. When working in remote field sites, such as Great Onyx

Spring or Biz Falls, another limitation is the transportation of sample bottles. It is not ideal to carry multiple glass bottles down a steep, remote hillside. Future work could utilize pumping and filtering the water at the sampling location. This would take more time, however, there would not be any worry about potentially breaking bottles and would eliminate transporting heavy bottles. Another limitation is potentially contaminating the sample site based on the clothing worn during sampling. To counteract potential contamination, it is important to stand downstream or, if possible, stand out of water. It is important to make note of the clothing that is worn and try to wear clothing that would have identifiable colors if looked at under the microscope (i.e. neon green or purple) or wear all cotton.

6.2.2 Lab Processing

A major limitation when processing samples in the laboratory is that there is no standard methodology. Methodology varies by study; the inconsistencies make it difficult to compare between studies. In the future, standardization of methodology could provide a framework that can be used, which would increase reliability and comparability between research findings. It would also make troubleshooting easier as there would be steps to follow. Another limitation faced was equipment breaking. During filtration, the vacuum pump created a vibration that over time caused the beaker to slide into the lab sink (hole in the table that functions as a sink) and break. There were about 50 ml of sample that was lost due to this accident. Once the equipment was replaced, placing a couple of heavy textbooks behind the vacuum pump stabilized the pump eliminating the vibrations.

A major limitation when processing samples in the laboratory was the potential atmospheric exposure. Both rooms (sample processing room and microscope analysis room) had other uses resulting in people coming in and out. To overcome this, a petri dish was placed on top of the funnel to eliminate any atmospheric exposure during filtering. Additionally, a filter was left uncovered during filtering and analysis to capture any atmospheric contamination. Future studies should always have a filter out while processing samples, and if possible, work in a room that has little foot traffic or under a fume hood. Ideally, a room that has restricted access and is not attached to the main HVAC system would be optimal for sample processing and microscopy.

6.2.3 Chemical Analysis

An additional direction of work that could provide useful information that was beyond the scope of the current effort would be determining the chemical composition of the microplastics identified. Chemical composition provides information pertaining to the source of microplastics. Chemical composition also confirms that the particles being identified are in fact microplastics. This issue was addressed by using the hot needle (Figure 31) test to determine if a particle is a microplastics based off its reaction to heat. Additionally, any particle that was not subjected to the hot needle test and still questionable was not counted in this study. There were several particles that looked like Quartz (Figure 32), therefore not included in counts, chemical composition would be able to identify these particles. In future studies, if accessible, an FTIR or Raman spectroscopy should be used to identify microplastics. Another limitation is the size to which microplastics can degrade to. In this study specifically, using a 100x microscope, it became challenging to identify particles smaller than 15-20 μm. To look at smaller microplastics or nanoplastics, a microscope with higher magnification would be needed.

Figure 31: Example of a fiber shrinking as a result of the hot needle test (Source: Created by Author).

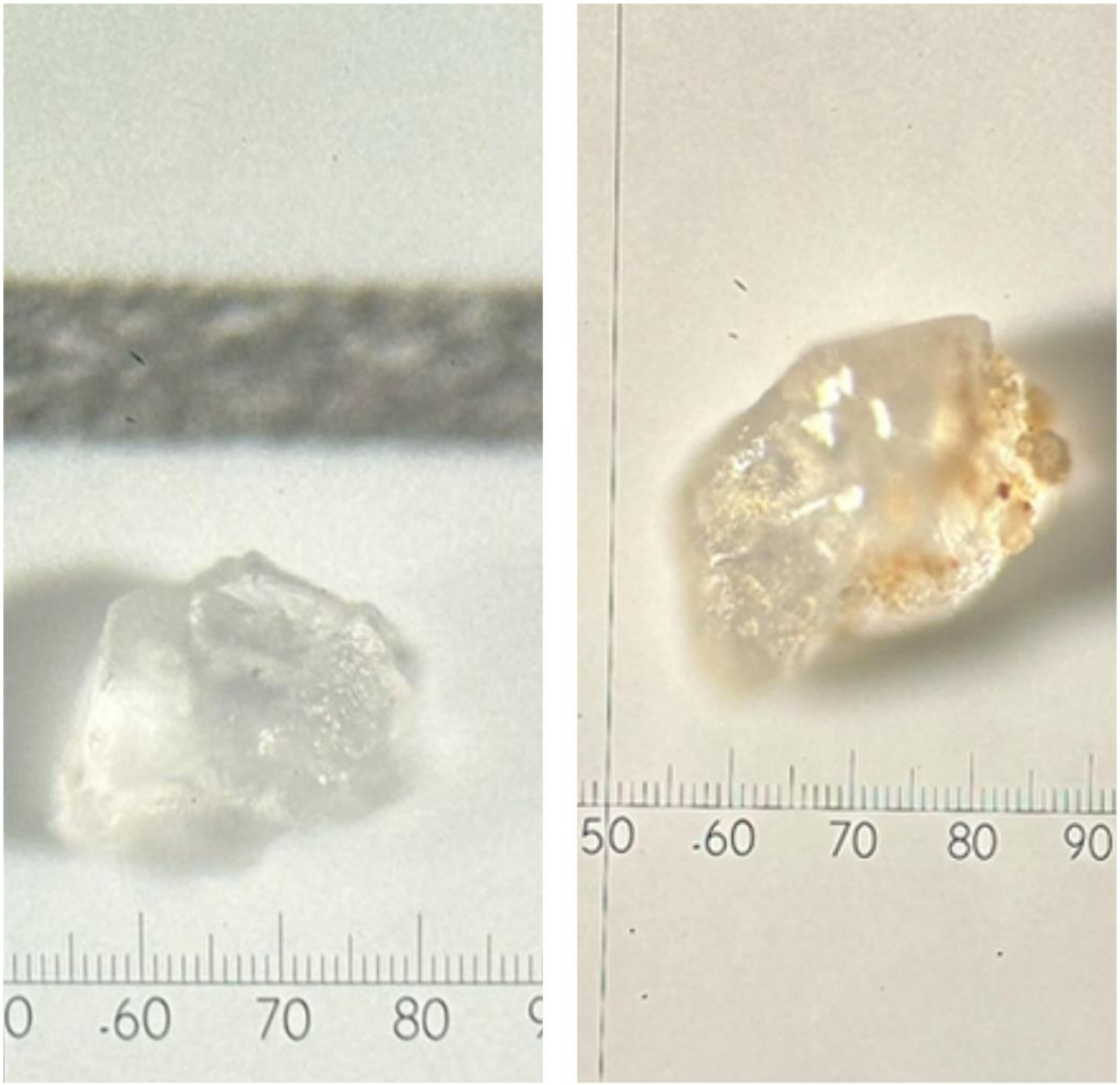

Figure 32: Examples of Quartz particles (Source: Created by Author).

6.3 Summary

In conclusion, the purpose of this study was to examine and characterize microplastic concentrations in the Lost River Groundwater basin and Great Onyx Groundwater Basin. Every month, at every site, microplastic concentrations were observed by collecting 2 L of groundwater. Overall, across all sites, there were a total of 824 particles identified, composed of 733 fibers, 9 films, 79 fragments, and 3 pellets. The predominant color seen was clear (63.23%), followed by blue (22.21%). For fibers specifically, the most frequent color observed was clear, while the most frequent color seen for fragments was blue. Of the 824 particles identified, 90.53% fell within the MMP size range and 9.47% fell within the MP size range. These results suggest that microplastic pollution is ubiquitous to the karst groundwater of southcentral Kentucky regardless of the surrounding land use. These results suggest that the main source for these particles is coming from textiles rather than degradation of a larger plastic or originating from a primary microplastic.

These results emphasize the importance of monitoring groundwater for microplastic contamination. Karst aquifers are an important source of drinking water that is impacted by microplastic contamination. Long-term monitoring should be conducted not only to see how concentrations vary over time, flow conditions, seasonality, but also to examine the implications contamination has on the ecosystem. This study is important also for undeveloped areas, such as National Parks, to monitor for microplastics as these particles can be transported to remote areas.

6.4 Future Work

Overall, knowledge pertaining to microplastics is still limited, with more unknowns regarding microplastics than known facts. On a broader scale more research needs to be done in a variety of topics including but not limited to 1) MPs long-term effects on ecosystems 2) how ingestion of MPs impacts health 3) transportation mechanisms of MPs 4) MPs abilities to leach chemicals 5) standardizing methodology 6) MP distribution within the water column and body of water 7) sources of MPs in developed vs undeveloped areas 8) how to regulate MP pollution. Examining sediments could serve as a marker for the Anthropocene, as theoretically there should be a layer that does not have MP pollution. Examining different types of sediments, such as clay, could provide insights into how MPs move within suspended loads.

On a more local level, more research needs to be done to understand how microplastics impact karst systems. Studies could 1) examine how MPs move through groundwater, especially during various rain events 2) long-term impact on karst regions, with an emphasis on karst aquifers 3) transportation of MPs in undeveloped karst groundwater. In relation to Great Onyx Groundwater basin, more specifically Biz Falls, monitoring should be continued to examine how anthropogenic and recreational use affects undeveloped karst regions. Monitoring should be continued at all sites to continue to understand microplastic distribution and abundance.

References

Andrady, A.L., 2011. Microplastics in the marine environment. *Marine Pollution Bulletin*, 62(8), pp.1596-1605. https://doi.org/10.1016/j.marpolbul.2011.05.030

Aragaw, T.A., 2020. Surgical face masks as a potential source for microplastic pollution in the COVID-19 scenario. *Marine Pollution Bulletin*, 159, p.111517. https://doi.org/10.1016/j.marpolbul.2020.111517

Aragaw, T.A. and Mekonnen, B.A., 2021. Current plastics pollution threats due to COVID-19 and its possible mitigation techniques: a waste-to-energy conversion via Pyrolysis. *Environmental Systems Research*, 10(1), p.8. https://doi.org/10.1186/s40068-020-00217-x

Arif, A., Malik, M.F., Liaqat, S., Aslam, A., Mumtaz, K., Afzal, A., Mahmood, D., Nisa, K., Khurshid, F., Arif, F., Khalid, M.S.Z. and Javed, R., 2020. Water pollution and industries. *Pure and Applied Biology*, 9(4), pp.2214-2224. http://dx.doi.org/10.19045/bspab.2020.90237

Arthur, C., Baker, J. and Bamford, H. (eds), 2009. *Proceedings of the International Research Workshop on the Occurrence, Effects and Fate of Microplastic Marine Debris, September 9-11, 2008*. NOAA Technical Memorandum NOS-OR&R-30.

Azzarello, M.Y. and Van Vleet, E.S., 1987. Marine birds and plastic pollution. *Marine Ecology Progress Series*, 37, pp.295-303.

Balestra, V. and Bellopede, R., 2022. Microplastic pollution in show cave sediments: First evidence and detection technique. *Environmental Pollution*, 292(A), p.118261. https://doi.org/10.1016/j.envpol.2021.118261

Barboza, L.G.A., Vethaak, A.D., Lavorante, B.R.B.O., Lundebye, A.K. and Guilhermino, L., 2018. Marine microplastic debris: An emerging issue for food security, food safety and human health. *Marine Pollution Bulletin*, 133, pp.336-348. https://doi.org/10.1016/j.marpolbul.2018.05.047

Barnes, D.K.A., Galgani, F., Thompson, R.C. and Barlaz, M., 2009. Accumulation and fragmentation of plastic debris in global environments. *Philosophical Transactions: Biological Sciences*, 364(1526), pp.1985-1998.

Barrows, A.P.W., Neumann, C.A., Berger, M.L. and Shaw, S.D., 2017. Grab vs. neuston tow net: A microplastic sampling performance comparison and possible advances in the field. *Analytical Methods*, 9(9), pp.1416-1427.

Benson, N.U., Bassey, D.E. and Palanisami, T., 2021. COVID pollution: impact of COVID-19 pandemic on global plastic waste footprint. *Heliyon*, 7(2), p.e06343. https://doi.org/10.1016/j.heliyon.2021.e06343

Betts, K., 2008. Why small plastic particles may pose a big problem in the oceans. *Environmental Science & Technology*, 42(9), pp.2595-2596.

Bledsoe, L. A., Groves, C., & Toomey, R. (2021). The Mammoth Cave National Park World Heritage Site. Zeitschrift für Geomorphologie, 62(3), 145-193.

Bledsoe, L. A. (2023). Great Onyx groundwater basin. [Unpublished ArcGIS Map]. Crawford Hydrology Lab, Western Kentucky University.

Boerger, C.M., Lattin, G.L., Moore, S. and Moore, C.J., 2010. Plastic ingestion by planktivorous fishes in the North Pacific Central Gyre. *Marine Pollution Bulletin*, 60(12), pp.2275-2278.

Boyd, C.E., 2005. *Water quality in aquaculture* [Book]. Springer, Netherlands

Bråte, I.L.N., Halsband, C., Allan, I.J. and Thomas, K.V., 2014. *Microplastics in marine environments: Occurrence, distribution and effects*. Norwegian Institute for Water Research and Akvaplan-niva. Report number: M-319 (miljødir no.) and 6754-2014 (NIVA no.),

Browne, M.A., Galloway, T. and Thompson, R., 2007. Microplastic—An emerging contaminant of potential concern? *Integrated Environmental Assessment and Management*, 3(4), pp.559-561.

Browne, M.A., Galloway, T.S., and Thompson, R.C., 2010. Spatial patterns of plastic debris along estuarine shorelines. *Environmental Science & Technology*, 44(9), pp.3404-3409.

Browne, M.A., Crump, P., Niven, S.J., Teuten, E.L., Tonkin, A., Galloway, T.S. and Thompson, R.C., 2011. Accumulation of microplastic on shorelines woldwide: sources and sinks. *Environmental Science & Technology*, 45(21), pp.9175-9179.

Carpenter, E.J. and Smith, K.L., 1972. Plastics on the Sargasso Sea surface. *Science*, 175(4027), pp.1240-1241.

U.S. Census Bureau, n.d. *QuickFacts: Bowling Green city, Kentucky* [online]. Available at: https://www.census.gov/quickfacts/bowlinggreencitykentucky

Chamas, A., Moon, H., Zheng, J., Qiu, Y., Tabassum, T., Jang, J.H., Abu-Omar, M., Scott, S.L. and Suh, S., 2020. Degradation rates of plastics in the environment. *ACS Sustainable Chemistry & Engineering*, 8(9), pp.3494-3511. https://doi.org/10.1021/acssuschemeng.9b06635

Chaudhry, F.N. and Malik, M.F., 2017. Factors affecting water pollution: a review. *Journal of Ecosystem & Ecography*, 7(1), p.225.

Climate-Data.org. (n.d.). Climate: Mammoth Cave National Park. https://en.climate-data.org/north-america/united-states-of-america/mammoth-cave-national-park-10179/

Cole, M., Lindeque, P., Halsband, C. and Galloway, T.S., 2011. Microplastics as contaminants in the marine environment: A review. *Marine Pollution Bulletin*, 62(12), pp.2588-2597. https://doi.org/10.1016/j.marpolbul.2011.09.025

Crawford, C.B. and Quinn, B., 2017. *Microplastic Pollutants*. Elsevier, Amsterdam.

Crawford, C.B., 1989. *Geology of the Lost River Basin*. University of Kentucky Press, Lexington.

Creech, Zachary Dalton, "Lithological Character and Sequence Stratigraphy of the Ste. Genevieve Limestone in Western Kentucky" (2019). *Masters Theses & Specialist Projects.* Paper 3469. https://digitalcommons.wku.edu/theses/3469Dantas et al., 2012

de Sá, L.C., Oliveira, M., Ribeiro, F. and Lopes Rocha, T., 2018. Studies of the effects of microplastics on aquatic organisms: What do we know and where should we focus our efforts in the future? *Science of The Total Environment*, 645, pp.1029-1039. https://doi.org/10.1016/j.scitotenv.2018.07.207

Derraik, J.G.B., 2002. The pollution of the marine environment by plastic debris: A review. *Marine Pollution Bulletin*, 44(9), pp.842-852.

Duckeck, J. (2021). Great Onyx Cave: Show caves of the world. https://www.showcaves.com/english/usa/showcaves/GreatOnyx.htmlDuis and Coors, 2016

Engler, R.E., 2012. The complex interaction between marine debris and toxic chemicals in the ocean. *Environmental Science & Technology*, 46(22), pp.12302-12312.

EPA (U.S. Environmental Protection Agency), 2003. *National Water Quality Inventory: Report to Congress*. [online]

EPA (U.S. Environmental Protection Agency), 2023. *Urban runoff pollutants*. [online]

European Commission, 2022. *How EU Policy can Tackle Microplastic Pollution*. [online] https://seas-at-risk.org/publications/how-eu-policy-can-tackle-microplastic-pollution/

Fendall, L.S. and Sewell, M.A., 2009. Contributing to marine pollution by washing your face: Microplastics in facial cleansers. *Marine Pollution Bulletin*, 58(8), pp.1225-1232. https://doi.org/10.1016/j.marpolbul.2009.04.025

Florescu, L., Toma, C. and Popa, M., 2010. Water quality and its relation to environmental factors. *Journal of Environmental Management*, 91(11), pp.2345-2356.

Ford, D., & Williams, P. (2007). Karst hydrogeology and geomorphology. John Wiley & Sons Ltd. https://doi.org/10.1002/9781118684986

Gall, S.C., Thompson, R.C., 2015. The impact of debris on marine life. *Marine Pollution Bulletin*, 92(1-2), pp.170-179. http://dx.doi.org/10.1016/j.marpolbul.2014.12.041

Galloway, T.S., Cole, M. and Lewis, C., 2017. Interactions of microplastic debris throughout the marine ecosystem. *Nature Ecology & Evolution*, 1(5), pp.116-125. http://dx.doi.org/10.1038/s41559-017-0116

GESAMP Working Group 40, 2016. *Sources, fate and effects of microplastics in the marine environment: Part two of a global assessment*. A report to inform the Second United Nations Environment Assembly. [online] Available at: https://www.gesamp.org/sites/g/files/jcwhs0amul/files/gesamp-publications/gesamp-reports-and-studies/gesamp-reports-and-studies-2016-sources-fate-and-effects-of-microplastics-in-the-marine-environment.pdf

Geyer, R., Jambeck, J.R. and Law, K.L., 2017. Production, use, and fate of all plastics ever made. *Science*, Recycling special issue, 27(2), pp.766-771. Available at: https://doi.org/10.1126/science.aas9800

Giacovelli, C., De Liguoro, M. and Comi, G., 2018. Polypropylene and polyethylene polymers in disposable products: Usage, impact, and alternatives. *Journal of Plastic Research*, 9(3), pp.321-334.

Goldscheider, N., Chen, Z., Auler, A.S., Bakalowicz, M., Broda, S., Drew, D., Hartmann, J., Jiang, G., Moosdorf, N., Stevanovic, Z. and Veni, G., 2020. Global distribution of carbonate rocks and karst water resources. *Hydrology and Earth System Sciences*, 24(4), pp.1527-1558. https://doi.org/10.5194/hess-24-1527-2020

Gregory, M.R., 1996. Plastic 'scrubbers' for cleaning ship hulls and their role in marine pollution. *Marine Pollution Bulletin*, 32(12), pp.835-840.

Groves, C., Singer, A., Bledsoe, L. A., Toomey III, R. S., Algeo, K., & Webb, C. J. (2021). Natural resource condition assessment: Mammoth Cave National Park. Natural Resource Report NPS/MACA/NRR—2021/2258. National Park Service, Fort Collins, Colorado. https://doi.org/10.36967/nrr-2286525

Guzzetti, E., Sureda, A., Tejada, S. and Faggio, C., 2018. Microplastic in marine organisms: Environmental and toxicological effects. *Environmental Toxicology and Pharmacology*, 68, pp.1-11. https://doi.org/10.1016/j.etap.2018.10.009

Hawach Scientific, n.d. *Vacuum filtration process*. [online] Available at: https://www.vacuumfiltrations.com/main-steps-of-vacuum-filtration/Hidalgo-Ruiz et al., 2012

Ivar do Sul, J.A. and Costa, M.F., 2014. The role of plastics in the transport and fate of persistent organic pollutants (POPs) in the marine environment. *Environmental Science & Technology*, 48(16), pp.8802-8812.

Jackson, Leah, "Epikarst Hydrogeochemical Changes in Telogenetic Karst Systems in South-central Kentucky" (2017). *Masters Theses & Specialist Projects.* Paper 2018. https://digitalcommons.wku.edu/theses/2018

Jambeck, J.R., Geyer, R., Wilcox, C., Siegler, T.R., Perryman, M., Andrady, A., Narayan, R. and Law, K.L., 2015. Plastic waste inputs from land into the ocean. *Science*, 347(6223), pp.768-771. https://doi.org/10.1126/science.1260352

Jantz, L.A., Morishige, C.L., Bruland, G.L. and Lepczyk, C.C.A., 2013. Ingestion of plastic marine debris by longnose lancetfish (*Alepisaurus ferox*) in the North Pacific Ocean. *Marine Pollution Bulletin*, 69(1-2), pp.97-104.

Karbalaei, S., Hanachi, P., Walker, T.R. and Cole, M., 2018. Occurrence, sources, human health impacts and mitigation of microplastic pollution. *Environmental Science & Pollution Research*, 25(36), pp.35771-35784. https://doi.org/10.1007/s11356-018-3508-7

Karst Water Institute, 2016. *Karst Water and Its Importance: An Overview*. [online] Available at: https://www.karstwaterinstitute.org/resources

Koelmans, A.A., Bakir, A., Burton, G.A. and Janssen, C.R., 2016. Microplastic as a vector for chemicals in the aquatic environment: Critical review and model-supported re-interpretation of empirical studies. *Environmental Science & Technology*, 50(7), pp.3315-3326. https://doi.org/10.1021/acs.est.5b06069

Koelmans, A.A., Redondo-Hasselerharm, P.E., Mohamed Nor, N.H., de Ruijter, V.N., Mintenig, S.M. and Kooi, M., 2022. Risk assessment of microplastic particles. *Nature Reviews Materials*, 7, pp.138-152. https://doi.org/10.1038/s41578-021-00411-y

Law, K.L., 2017. Plastics in the marine environment. *Annual Review of Marine Science*, 9, pp.205-229. https://doi.org/10.1146/annurev-marine-010816-060409

Lawler, Trayson, "A Predictive Flood Model for Urban Karst Groundwater Systems" (2023). *Masters Theses & Specialist Projects.* Paper 3672. https://digitalcommons.wku.edu/theses/3672

Lebreton, L., Slat, B., Ferrari, F., Sainte-Rose, B., Aitken, J., Marthouse, R., Hajbane, S., Cunsolo, S., Schwarz, A., Levivier, A., Noble, K., Debeljak, P., Maral, H., Schoeneich-Argent, R., Brambini, R. and Reisser, J., 2018. Evidence that the Great Pacific Garbage Patch is rapidly accumulating plastic. *Nature*, 559(7715), pp. 230-234. DOI:10.1038/s41598-018-22939-w

Li, W.C., Tse, H.F. and Fok, L., 2016. Plastic waste in the marine environment: A review of sources, occurrence and effects. *Science of the Total Environment*, 566-567, pp.333-349. https://doi.org/10.1016/j.scitotenv.2016.05.084

Lithner, D., Larsson, Å. and Dave, G., 2011. Environmental and health hazard ranking and assessment of plastic polymers based on chemical composition. *Science of the Total Environment*, 409(18), pp.3309-3324. https://doi.org/10.1016/j.scitotenv.2011.04.038

Lu, Y., Zhang, Y., Deng, Y., Jiang, W., Zhao, Y., Geng, J., Ding, L. and Ren, H.-q., 2016. Uptake and accumulation of polystyrene microplastics in zebrafish (*Danio rerio*) and toxic effects in liver. *Environmental Science & Technology*. https://doi.org/10.1021/acs.est.6b00183

Lusher, A.L., McHugh, M. and Thompson, R.C., 2015. Microplastics in the Arctic: Evidence for their presence and potential impact. *Science of the Total Environment*, 514, pp. 174-183.

Mai, L., Bao, L.-J., Shi, L., Wong, C.S. and Zeng, E.Y., 2018. A review of methods for measuring microplastics in aquatic environments. *Environmental Science and Pollution Research*, 25(6), pp. 4390-4402. https://doi.org/10.1007/s11356-018-1692-0

Masura, J., Baker, J., Foster, G., Arthur, C., Herring, C. and Morrison, P., 2015. *Laboratory methods for the analysis of microplastics in the marine environment: Recommendations for quantifying synthetic particles in waters and sediments*. NOAA Technical Memorandum NOS-OR&R-48.

McCauley, S.J. and Bjorndal, K.A., 1999. The effect of plastic ingestion on the behavior of marine turtles. *Marine Pollution Bulletin*, 38(12), pp. 1184-1187.

Meredith, J. 2024. Great Onyx Cave Tour Numbers. [Personal Communication].

Millet, H., Vangheluwe, P., Block, C., Sevenster, A., Garcia, L. and Antonopoulos, R., 2020. The nature of plastics and their societal usage. *Journal of Environmental Management*, 261, p.110217.

Molecular Corporation, 2019. *Membrane Filtration for Concentration of Bacteria*. [online]

Moore, C.J., 2008. Synthetic polymers in the marine environment: A rapidly increasing, long-term threat. *Environmental Research*, 108(2), pp. 131-139.

Muirhead, E.K., Skillman, A.D., Hook, S.E., Schulz, I.R., 2006. Oral exposure of PBDE-47 in Fish: toxicokentics and reproductive effects in Japanese medaka (Oryzias latipes) and fat-head minnows (Pimephales promelas). Environ Sci Technol 40 (2), 523–528.

NOAA (National Oceanic and Atmospheric Administration), n.d. *Industrial pollutants and atmospheric deposition*. National Oceanic and Atmospheric Administration..

National Park Service, n.d. *Cave Tours*. [online] https://www.nps.gov/maca/planyourvisit/cave-tours.htm

Obbard, R.W., Sadri, S., Hurley, R.R., C. H. A. P. and C. J. M., 2014. Arctic sea ice: A review of the presence and impacts of microplastics. *Marine Pollution Bulletin*, 79(1-2), pp. 113-119.

Oehlmann, J., Schulte-Oehlmann, U., Kloas, W., Jobling, S., Paull, G.C., Bursztyka, A., Ternes, T.A. and Lang, T., 2009. A critical review of the biological impacts of plasticizers on wildlife. *Philosophical Transactions of the Royal Society B: Biological Sciences*, 364(1526), pp. 2047-2062.

Ongley, E.D., Zhang, X. and Yu, T., 2009. *Current status of agricultural and rural non-point source pollution assessment in China*. *Environmental Pollution*, 157(8), pp. 2304-2314. https://doi.org/10.1016/j.envpol.2009.10.047

Palmer, A. N. (1995). A geological guide to Mammoth Cave National Park. Zephyrus Press.

Palmer, A.N., 2012. *Subsurface karst features include caves and conduits where bedrock has dissolved away*. *In: Introduction to Karst Hydrogeology*.

Palmer, A. N. (2017). In Hobbs III, H. H., Olson, R. A., Winkler, E. G., & Culver, D. C. (Eds.). Mammoth Cave: A human and natural history. Springer, 97-109.

Parise, M., Vacca, A., Rossi, G. and Carrasco, J., 2008. *An overview of karst systems in Italy: Distribution, features, and hydrogeological importance*. *Environmental Geology*, 53(3), pp. 411-421.

Patel, S., Ghosh, S., Vankayala, R. and Lin, C.Y., 2009. *Linking plastic intracellularly with drugs: New approaches in pharmaceutical delivery*. *Journal of Drug Delivery Science and Technology*, 19(2), pp. 157-164.

Plastics Europe, 2017. *Plastics – the Facts 2017: An analysis of European plastics production, demand and waste data*. [pdf] Plastics Europe.

Possatto, F.E., Barletta, M., Costa, M.F. and Silva, A.M., 2011. *Occurrence and distribution of plastic debris in the South Atlantic Ocean*. *Marine Pollution Bulletin*, 62(11), pp. 2364-2371.

Prata, J.C., da Costa, J.P., Duarte, A.C. and Rocha-Santos, T., 2018. *Methods for sampling and detection of microplastics in water and sediment: A critical review*. *Science of The Total Environment*, 645, pp. 203-226.

Prata, J.C., da Costa, J.P., Silva, A.L.P., Duarte, A.C. and Rocha-Santos, T., 2019. *Microplastics in the environment: A review of sources, distribution, and impacts*. *Science of The Total Environment*, 652, pp. 1251-1264.

Ragusa et al., 2020

Raines, Meghan, "Landscape/Atmosphere Interactions and Carbon-Dioxide Dynamics in the Great Onyx Groundwater Basin, Mammoth Cave National Park, Kentucky"

(2023). *Masters Theses & Specialist Projects.* Paper 3686. https://digitalcommons.wku.edu/theses/3686

Rees, E.I.S. and Southward, A.J., 2008. *The influence of plastic debris on the northward extension of the large barnacle Perforatus perforates*. *Marine Pollution Bulletin*, 56(5), pp. 738-746.

Ribeiro, F., Garcia, A.R., Pereira, B.P., et al., 2017. Microplastics in aquatic environments: Occurrence, impacts, and management strategies. *Marine Pollution Bulletin*, 119(1), pp.45-62.

Rillig, M.C., 2012. Microplastic in Terrestrial Ecosystems and the Soil? *Environmental Science & Technology*, 46(12), pp.6453-6454.

Rios, L.M., Moore, C. & Jones, P.R., 2007. Persistent organic pollutants carried by synthetic polymers in the ocean environment. *Marine Pollution Bulletin*, 54(8), pp.1230-1237.

Romeo, T., Pietro, B., Peda, C., Consoli, P., Andaloro, F. & Fossi, M.C., 2015. First evidence of presence of plastic debris in stomach of large pelagic fish in the Mediterranean Sea. *Marine Pollution Bulletin*, 95(1), pp.358-361.

Ryan, P.G., Moore, C.J., van Franeker, J.A. & Moloney, C.L., 2009. Monitoring the abundance of plastic debris in the marine environment. *Philosophical Transactions of the Royal Society B: Biological Sciences*, 364(1526), pp.1999-2012.

Schöpel, B. and Stamminger, R., 2019. *A comprehensive literature study on microfibres from washing machines*. *Tenside Surfactants Detergents*. De Gruyter. https://doi.org/10.3139/113.110610

Schwabl, P., Köppel, S., Koelmel, J., et al., 2019. *Detection of microplastics in human stool*. *Annals of Internal Medicine*, 171(7), pp.453-457.

Schweitzer, L. and Noblet, J., 2018. *Water contamination and pollution*. In: *Green chemistry: An inclusive approach*. Elsevier, pp. 261-290.

Shao, L., Li, Y., Jones, T., Santosh, M., Liu, P., Zhang, M., Xu, L., Li, W., Lu, J., Yang, C.-X., Zhang, D., Feng, X. & BéruBé, K., 2022. Airborne microplastics: A review of current perspectives and environmental implications. *Journal of Cleaner Production*, 347, p.131048. https://doi.org/10.1016/j.jclepro.2022.131048

Shiklomanov, I.A. and Rodda, J.C. (eds), 2003. *World Water Resources at the Beginning of the Twenty-First Century*. Cambridge University Press.

Soto, L., & Pate, D. L. (2016). Cave and Karst Resources Summary, Mammoth Cave National Park, Kentucky. U.S. Department of the Interior. http://npshistory.com/publications/maca/cave-karst-summary-2016.pdf

Spear, L.B., Ainley, D.G., Ribic, C.A., 1995. Incidence of plastic in seabirds from the Tropical Pacific, 1984–91: relation with distribution of species, sex, age, season, year and body weight. Marine Environmental Research 40, 123–146.

Staples, C.A., Peterson, D.R., Parkerton, T.F., Adams, W.J., 1997. The environmental fate of phthalates esters: a literature review. Chemosphere 35, 667–749.

Stevanović, Z., 2019. Karst waters in potable water supply: a global scale overview. *Environmental Earth Sciences*, 78, article 662. https://doi.org/10.1007/s12665-019-8670-9

Stubbins, A., Law, K.L., Muñoz, S.E., Bianchi, T.S. & Zhu, L., 2021. Plastics in the Earth system. *Science*, 373(6550), pp.51-55. https://doi.org/10.1126/science.abb0354

Sun, J., Dai, X., Wang, Q., van Loosdrecht, M.C.M. & Ni, B.-J., 2018. Microplastics in wastewater treatment plants: Detection, occurrence and removal. *Water Research*, 152, pp.21-37. https://doi.org/10.1016/j.watres.2018.12.050

Talsness, C.E., Andrade, A.J.M., Kuriyama, S.N., Taylor, J.A. & vom Saal, F.S., 2009. Components of plastic: Experimental studies and human exposure. *Environmental Health Perspectives*, 117(11), pp.1556-1563.

Teuten, E.L., Saquing, J.M., Knappe, D.R.U., Barlaz, M.A., Jonsson, S., Björn, A., Rowland, S.J., Thompson, R.C., Galloway, T.S., Yamashita, R., Ochi, D., Watanuki, Y., Moore, C., Viet, P.H., Tana, T.S., Prudente, M., Boonyatumanond, R., Zakaria, M.P., Akkhavong, K., Ogata, Y., Hirai, H., Iwasa, S., Mizukawa, K., Hagino, Y., Imamura, A., Saha, M. & Takada, H., 2009. Transport and release of chemicals from plastics to the environment and to wildlife. *Philosophical Transactions of the Royal Society B: Biological Sciences*, 364(1526), pp.2027-2045.

Thompson, R.C., Olsen, Y., Mitchell, R.P., Davis, A., Rowland, S.J., John, A.W.G., McGonigle, D. & Russell, A.E., 2004. Lost at sea: Where is all the plastic? *Science*, 304(5672), pp.838-838.

Thompson, R.C., Moore, C.J., vom Saal, F.S. & Swan, S.H., 2009. Plastics, the environment and human health: current consensus and future trends. *Philosophical Transactions of the Royal Society B: Biological Sciences*, 364(1526), pp.2153-2166. https://doi.org/10.1098/rstb.2009.0053

Tirkey, A. & Upadhyay, L.S.B., 2021. Microplastics: An overview on separation, identification and characterization of microplastics. *Marine Pollution Bulletin*, 170, p.112604. https://doi.org/10.1016/j.marpolbul.2021.112604

U.S. Geological Survey (USGS), 2024. How much water is there on Earth? *U.S. Geological Survey*. https://www.usgs.gov/special-topics/water-science-school/science/how-much-water-there-earth van Sebille, E., Wilcox, C., Lebreton, L.C.M., Maximenko, N., Van Franeker, J.A., & Law, K.L., 2015. A global inventory of small floating plastic debris. *Environmental Research Letters*, 10(12), p.124006.

Veni, G., Duchene, H., Crawford, N.C., Groves, C., Huppert, G. N., Kastning, E. H., Olson, R., & Wheeler, B. J. (2001). Living with karst: a fragile foundation. American Geological Institute.

Watson, R., Revenga, C. & Kura, Y., 2006. Fishing gear associated with global marine catches: I. Database development. *Fisheries Research*, 79(1–2), pp.97-102.

Werbowski, L.M., Gilbreath, A.N., Munno, K., Zhu, X., Grbic, J., Wu, T., Sutton, R., Sedlak, M.D., Deshpande, A.D. & Rochman, C.M., 2021. Urban stormwater runoff: A major pathway for anthropogenic particles, black rubbery fragments, and other types of microplastics to urban receiving waters. *ACS EST Water*, 1, pp.1420-1428. https://doi.org/10.1021/acsestwater.1c00017?rel=cite-as&ref=PDF&jav=VoR

Williams, Jessica, "Atmosphere/Landscape CO2 Interactions in Mammoth Cave National Park: Hydrochemistry of Cascade River, Great Onyx Cave" (2021). *Mahurin Honors College Capstone Experience/Thesis Projects*. Paper 957. https://digitalcommons.wku.edu/stu_hon_theses/957

World Health Organization, 2017. 2.1 billion people lack safe drinking water at home, more than twice as many lack safe sanitation [WWW Document], n.d. URL https://www.who.int/news/item/12-07-2017-2-1-billion-people-lack-safe-drinking-water-at-home-more-than-twice-as-many-lack-safe-sanitation.

Wright, S., Thompson, R.C. & Galloway, T.S., 2013. The physical impacts of microplastics on marine organisms: A review. *Environmental Pollution*, 178, pp.483-492. http://dx.doi.org/10.1016/j.envpol.2013.02.031

Wu, Y. & Chen, J., 2013. Investigating the effects of point source and nonpoint source pollution on the water quality of the East River (Dongjiang) in South China. *Ecological Indicators*, 32, pp.294-304. https://doi.org/10.1016/j.ecolind.2013.04.002

Yang, X., Man, Y.B., Wong, M.H., Owen, R.B. & Chow, K.L., 2022. Environmental health impacts of microplastics exposure on structural organization levels in the human body. *Science of The Total Environment*, 825, p.154025. https://doi.org/10.1016/j.scitotenv.2022.154025

Yogui, G.T., Sericano, J.L., 2009. Polybrominated diphenyl ether flame retardants in the U.S. marine environment: a review. Environ. Int. 35, 655–666.

Zarfl, C. & Matthies, M., 2010. Are marine plastic particles transport vectors for organic pollutants to the Arctic? *Marine Pollution Bulletin*, 60(10), pp.1810-1814. https://doi.org/10.1016/j.marpolbul.2010.05.026

Zektser, I.S. & Everett, L.G., 2004. *Groundwater and Surface Water Interaction*. *Water Resources Publications*, pp. 1-25.

Zitko, V. & Hanlon, S., 1991. *Marine Pollution Bulletin*, 22(12), pp.620-623.

Copyright Permission

Name: Norman, Katie

Email (to receive future readership statistics): katienorman077@gmail.com

Type of document: ['Thesis']

Title: Landuse and Microplastic Transport in Karst Groundwater of South-Central Kentucky

Keywords (3-5 keywords not included in the title that uniquely describe content): pollution, hydrology, plastic, contaminants

Committee Chair: Dr. Chris Groves

Additional Committee Members: Dr. Pat Kambesis Dr. Michael May

Select 3-5 TopSCHOLAR® disciplines for indexing your research topic in TopSCHOLAR®: Earth Sciences Environmental Sciences Hydrology Fresh Water Studies Physical Sciences and Mathematics Environmental Monitoring